UNITED STATES
DEPARTMENT OF THE INTERIOR
GEOLOGICAL SURVEY

National Center for Earthquake Research
345 Middlefield Road
Menlo Park, California 94025

EFFECTS OF LOCAL GEOLOGY ON GROUND MOTION IN THE SAN FRANCISCO BAY REGION, CALIFORNIA--A CONTINUED STUDY

by

James F. Gibbs and Roger D. Borcherdt

Open-File Report 74-222
1974

This report is preliminary and has not been edited or reviewed for conformity with Geological Survey standards and nomenclature.

ABSTRACT

Measurements of ground motion generated by nuclear explosions in Nevada have been completed for 99 locations in the San Francisco Bay region, California. The seismograms, Fourier amplitude spectra, spectral amplification curves for the signal, and the Fourier amplitude spectra of the seismic noise are presented for 60 locations. Analog amplifications, based on the maximum signal amplitude, are computed for an additional 39 locations. The recordings of the nuclear explosions show marked amplitude variations which are consistently related to the local geologic conditions of the recording site. The average spectral amplifications observed for vertical and horizontal ground motions are, respectively: (1, 1) for granite, (1.5, 1.6) for the Franciscan Formation, (2.3, 2.3), for other pre-Tertiary and Tertiary rocks, (3.0, 2.7) for the Santa Clara Formation, (3.3 , 4.4) for older bay sediments, and (3.7, 11.3) for younger bay mud. Spectral amplification curves define predominant ground frequencies for younger bay mud sites and for some older bay sediment sites. The predominant frequencies for most sites were not clearly defined by the amplitude spectra computed from the seismic background noise.

The intensities ascribed to various sites in the San Francisco Bay region for the California earthquake of April 18, 1906, are strongly dependent on distance from the zone of surface faulting and the geological character of the ground. Considering only those sites (approximately one square city block in size) for which there is good evidence for the degree of ascribed intensity, the intensities for 917 sites on Franciscan rocks generally decrease with the logarithm of distance as

$$\text{Intensity} = 2.69 - 1.90 \log(\text{Distance Km}).$$

For sites on other geologic units, intensity increments, derived from this empirical relation, correlate strongly with the Average Horizontal Spectral Amplifications (AHSA) according to the empirical relation

$$\text{Intensity Increment} = 0.27 + 2.70 \log(\text{AHSA}).$$

Average intensity increments predicted for various geologic units are -0.3 for granite, 0.2 for Franciscan Formation, 0.6 for other pre-Tertiary, Tertiary bedrock, 0.8 for Santa Clara Formation, 1.3 for older bay sediments, 2.4 for younger bay mud. These empirical relations, together with detailed geologic maps, delineate areas in the San Francisco Bay region of potentially high intensity from future earthquakes on either the San Andreas fault or the Hayward fault.

1. INTRODUCTION

Local geologic deposits can substantially change the characteristics of incoming seismic waves. In particular, incoming waves of certain frequencies can be amplified considerably by thick sections of unconsolidated near-surface deposits. The San Francisco Bay region includes a wide variety of deposits ranging from sedimentary rocks to semiconsolidated and unconsolidated alluvium to water saturated recent mud deposits. The close proximity of these deposits and high seismicity make the San Francisco Bay Area nearly ideal for studying the in-situ seismic response of various geologic units.

Borcherdt (1970) made a comparative ground-motion study in the San Francisco Bay region. He analyzed the following data:

(1) seismic waves generated by five nuclear explosions in Nevada as recorded at 37 locations in the San Francisco Bay Area,

(2) recordings of the San Francisco earthquake of March 22, 1957,

(3) recordings of seismic background noise, and

(4) intensity data for the California earthquake of April 18, 1906.

For the data considered, his work established that with appropriate analyses it is possible to isolate the effects of local geologic units from those of the source, travel path, and recording instruments. He established the existence of predominant ground frequencies at sites underlain by water-saturated unconsolidated deposits and found that for frequencies of shaking near the predominant, the amplitude of shaking on unconsolidated alluvial deposits can be many times greater than that on nearby bedrock.

Borcherdt (1970) analyzed the recordings obtained at 37 sites in the San Francisco Bay region of ground motion generated by five nuclear explosions in Nevada. As part of a continuing program, an additional 12 nuclear explosions have been recorded to date at 62 additional sites (fig. 1). The first purpose of this report is to present efficiently the entire set of additional data.

Nuclear explosions in Nevada are especially useful for comparative ground-motion studies in the San Francisco Bay region. The distance from the explosions to the recording sites is approximately 550 km. At these distances, the majority of the ground-motion energy is in the frequency band for which the effects of the local geologic deposits are greatest. This coincidence of frequency bands causes the amplification effects of the soil layers to be readily apparent on the analog recordings. In addition, the time, location, and approximate magnitude of the explosions are known in advance so efficient use of manpower and recording equipment is possible.

The intensities ascribed for the California earthquake of April 18, 1906, correlate strongly with the geological character of the ground and generally decrease with increasing distance from the zone of surface faulting. Examination of published 1906 intensity data shows that the quality of evidence for the assigned intensities varies considerably. A second purpose of this report is to derive quantitative estimates of the dependence of the observed intensities on distance and the geological character of the ground, using only the 1906 intensities for which there is good evidence.

2. GEOLOGY OF THE RECORDING AREA

Tectonic movements and sea-level changes have contributed to a complicated geologic history for the San Francisco Bay region. The region is located in the central portion of the Coast Ranges province. Roughly parallel ranges of hills, the Santa Cruz Mountains on the west and the Berkeley Hills on the east, flank the sides of San Francisco Bay. The bay itself is thought to be part of the San Francisco Peninsula block which has been downfaulted or tilted so that it is now below sea level.

The active San Andreas and Hayward fault zones are prominent tectonic features in the Bay Area. The fault zones trend roughly parallel along the western and eastern margins, respectively, of San Francisco Bay. Slippage along the faults is right-lateral strike slip with minor components of vertical movement. The San Andreas fault system is interpreted as part of the boundary between the Pacific Plate on the west and the North American Plate on the east. An average rate of movement for the plates is estimated at about 1 inch per year.

A wide variety of geologic units exists in the San Francisco Bay region. In general, various bedrock units are exposed in the ridge systems and form the irregular floor of a trough containing a more recent sedimentary sequence. The lower part of the sedimentary sequence was designated "older bay sediments" and the upper part "younger bay mud" (Schlocker, 1968, p. 24). More recent alluvial mapping by Lajoie and Helley (1974) has resulted in renaming these units and in the delineation of other sedimentary units within the older bay sediment unit.

A brief description of the various geologic units follows:

(1) bedrock, which includes the Early Pleistocene and Pliocene deposits together with the Tertiary and pre-Tertiary bedrock unit of Lajoie and Helley (1974). These units include: the Santa Clara and Merced Formations, consisting of semiconsolidated and consolidated sandstone, siltstone, and mudstone; marine sandstone and shale of Eocene, Miocene, and Pliocene age; the Franciscan Formation, consisting mostly of sandstone, shale, radiolarian chert, and greenstone (volcanic rocks); Page Mill Basalt, lava flows and pyroclastics of Miocene age; and minor granitic rocks. The thicknesses of these units are variable and shear velocities range from 500-2,000 meters per second,

(2) older bay sediment, which includes the Holocene and Late Pleistocene alluvial units of Lajoie and Helley (1974), consists mostly of greenish-gray silty sandy clay, silty clayey sand, and sand and gravel with less than 40 weight percent water, with thicknesses up to 600 meters and shear velocities approximately 200 meters per second at the surface which increase with depth, and

(3) younger bay mud, which is equivalent to the Holocene bay mud unit described by Lajoie and Helley (1974), consists mostly of recently deposited plastic, organic-rich, soft clay, silt and minor sand with more than 50 weight percent water, with thicknesses up to 40 meters and shear velocities 90-130 meters per second.

3. SEISMIC DATA

Three components of ground motion generated by nuclear explosions (vertical, east-west, horizontal, and north-south horizontal) have been recorded at 99 separate sites in the San Francisco Bay region (fig. 1). One base station and up to nine additional sites were occupied for each explosion. The sites near Black Mountain (BLM), Golden Gate Park (GGP), and Coyote Hills (CHY), which are underlain by rocks of the Franciscan Formation, were chosen as base stations and at least one has been occupied for each of the 17 explosions recorded to date.

The recordings were made using a set of 10 identical mobile seismic-refraction units, each equipped with six vertical and two horizontal 1-Hz EV17 seismometers. For each site, the outputs from at least two vertical and two horizontal seismometers were recorded. The outputs of the seismometers are recorded on both photographic paper and magnetic tape in analog form. The velocity unit impulse response of the recording units is essentially flat from 2 Hz to above 100 Hz. The response is down 3 db at 1 Hz and at the frequency imposed by the high-cut filters, which was chosen to be 37 Hz (see Warrick and others, 1961, for a more detailed description of recording instrumentation).

The analog magnetic tape recordings of the outputs of one vertical seismometer and the two horizontal seismometers were digitized using a U.S. Geological Survey CDC 1700 computer. Two hundred seconds of

the analog recordings starting 22 seconds before the arrival of the nuclear-generated signal were digitized with a 12-bit resolution at 50 samples per second. Prior to digitization, the traces were filtered with a 18-Hz high-cut analog filter to minimize alaising.

4. AMPLIFICATION OF GROUND MOTION BY LOCAL GEOLOGIC UNITS

Local geologic deposits amplify certain frequencies of seismic waves and attenuate other frequencies. However, such effects may or may not be immediately apparent on analog recordings depending on the nature and distance of the source, the travel paths, and the unit-impulse response of the recording instruments.

To compare the analog recordings for each nuclear explosion, the digitized recordings of each explosion were replotted at the same scale. Such plots are useful for comparative analyses, for detection of digitization errors, and for identification of anomalous seismic noise.

For nuclear explosions 7, 8, 9, 11, 16, 17, and 18, the equi-scaled recordings of vertical ground motion are shown in figures 2-8; the equi-scaled recordings of east-west horizontal ground motion are shown in figures 9-15, and the equi-scaled recordings of north-south horizontal ground motion are shown in figures 16-22. The recordings for each nuclear explosion are grouped according to the type of underlying generalized geologic unit. Comparison of the recordings for each individual nuclear explosion shows that the maximum analog amplitudes (especially the horizontal) recorded on older bay sediments and younger bay mud are often several times larger than those recorded on bedrock. In addition, the recordings with high seismic noise levels and spurious signals are quickly discernible.

4.1 Analog Amplification of Vertical and Horizontal Ground Motion

To compare the analog recordings of one nuclear explosion with those of another, the maximum peak-to-trough amplitude on each recording (in microvolts of seismometer output which is proportional to particle velocity for frequencies greater than 2 Hz) was measured. For each explosion, these were normalized by the corresponding maximum observed at Black Mountain. Such ratios will be referred to as analog amplifications with respect to Black Mountain. (For nuclear explosions 6, 7, 8, and 11 no recordings were obtained at the Black Mountain location. For these explosions the maximum analog values were first normalized by the maximum analog value recorded at the bedrock site in Golden Gate Park, then multiplied by a constant factor [0.94 for vertical motion and 0.65 for horizontal motion] to normalize the ratios to Black Mountain.) These amplification ratios were then normalized by the average amplification recorded at five sites (H16, I16, H17, P17, R17) located on granite. The multiplication factors used to convert the analog amplifications with respect to Black Mountain to analog amplifications with respect to granite are 1.81 for vertical motion and 1.99 for horizontal motion. Justification for the normalization to average granite will become apparent with further discussion of results.

The analog amplifications with respect to granite are tabulated (table 1) and plotted on a geologic map for horizontal motion (fig. 23).

Two recordings of vertical ground motion were made at several sites for various nuclear explosions. The two resulting vertical analog amplification values computed for several sites (table 2) show that the maximum measurement error (including variations in recording instruments) is 18 percent and that the mean measurement error is 5.5 percent, and the standard deviation of the measurement error is 4.5.

Table 1

ANALOG AMPLIFICATION WITH RESPECT TO AVERAGE GRANITE†

Location Identification	Vertical	East-West	North-South	Average E-W N-S	Depth to water table (M)	Thickness of surface layer†† (M)	Depth to bedrock (M)
SURFACE LAYER--GRANITE							
H16	1.01	0.92	0.80	0.86	---	---	0
I16	1.16	0.74	0.74	0.74	---	---	0
H17	0.83	1.06	0.82	0.94	---	---	0
P17	1.07	1.30	0.76	1.03	---	---	0
R17	0.92	1.75	1.12	1.44	---	---	0
Mean	1.00	1.15	0.85	1.00			
Standard deviation	0.13	0.39	0.16	0.27			
SURFACE LAYER--FRANCISCAN FORMATION							
CYH*	1.45	0.70	0.70	0.70	---		0
BLM*	1.81	1.99	1.99	1.99	---		0
GGP*	1.70	1.30	1.30	1.30	---		0
J5	1.20	0.92	1.69	1.30	---		0
I7	1.01	1.18	0.88	1.03	---		0
J7	1.20	0.92	1.00	0.96	---		0
I8	1.32	1.27	1.02	1.14	---		0
L11	2.10	1.22	1.20	1.21	---		0
K16	1.34	1.00	1.43	1.22	>6.1		0
L16	2.23	1.22	1.67	1.44	---		0
Q16	1.30	1.69	1.69	1.69	---		0
T16	1.85	---	2.41	2.41	---		0
S17	1.01	1.51	1.29	1.40	---		0
Mean	1.46	1.21	1.43	1.38			
Standard deviation	0.44	0.26	0.46	0.42			
SURFACE LAYER--SERPENTINE AND ULTRAMAFIC ROCKS							
J16	---	1.83	1.37	1.60	---		
H9	---	2.03	---	---	---		

Table 1--Continued

ANALOG AMPLIFICATION WITH RESPECT TO AVERAGE GRANITE†

Location Identification	Vertical	East-West	North-South	Average E-W N-S	Depth to water table (M)	Thickness of surface layer†† (M)	Depth to bedrock (M)
SURFACE LAYER--OTHER ROCKS OF PRE-TERTIARY AND TERTIARY AGE							
Q13	2.86	---	1.93	1.93			
Q14	1.82	1.59	1.17	1.38			
P19	2.97	1.87	2.09	1.98			
R19	2.62	3.88	---	3.88			
T19	2.68	2.21	2.71	2.46			
19B	2.19	1.17	2.53	1.85			
19C	1.32	2.11	3.08	2.59			
19E	2.33	1.75	2.11	1.93			
19W	2.12	3.00	1.75	2.37			
Mean	2.32	2.20	2.17	2.26			
Standard deviation	0.53	0.86	0.60	0.71			
SURFACE LAYER--SANTA CLARA FORMATION							
P1	4.53	2.99	2.59	2.79		7±2	1370±152
P2	5.07	2.59	---	2.59		7±2	1370±152
K9	5.02	3.57	2.47	3.02			
K17	2.99	3.13	2.31	2.72			
L17	1.27	1.67	1.24	1.46			
Q17	3.95	3.73	2.81	3.27			
Mean	3.80	2.95	2.28	2.64			
Standard deviation	1.46	0.75	0.61	0.63			
SURFACE LAYER--PAGE MILL BASALT							
L3	---	3.39	---	---		30±8	1070±152
J4	3.44	2.99	3.19	3.09		7±2	1070±152

Table 1--Continued

ANALOG AMPLIFICATION WITH RESPECT TO AVERAGE GRANITE†

Location Identification	Vertical	East-West	North-South	Average E-W N-S	Depth to water table (M)	Thickness of surface layer†† (M)	Depth to bedrock (M)
SURFACE LAYER--OLDER BAY SEDIMENTS							
J1	2.54	3.59	3.98	3.78	>6.1	221	
H2	5.43	2.59	2.39	2.49	>6.1	458±152	
K2	5.25	2.59	2.79	2.69	1.5-3.0	259±46	
L2	3.80	---	---	---	1.5-3.0	198±76	
Q2	5.98	1.99	2.59	2.29	>6.1	389±15	
T2	5.07	3.19	2.19	2.69	>6.1	38±8	
T3	3.80	---	---	---	1.5-3.0	198±76	
H4	3.62	3.39	3.19	3.29	>6.1	30±8	
I4	3.80	3.59	3.39	3.49		267±69	
K4	4.17	2.59	2.59	2.59	>6.1	244±30	
K5	3.39	2.85	---	2.85	---	33±5	
K7	---	2.29	2.21	2.25	---		
R7	1.12	1.43	---	1.43	---		
H8	3.46	2.67	---	2.67	3.0-6.1		
J8	2.26	1.93	1.47	1.70	3.0-6.1		
K8	6.14	5.02	9.14	7.08	>6.1		
L8	5.38	3.24		3.24			
R8	3.12	1.95	1.81	1.88	>6.1		
T8	8.58	3.61	5.08	4.34	>6.1		
L9	6.50	5.28	4.24	4.76	>6.1		
J11	1.74	1.87	1.89	1.88	---		
K11	1.38	1.14	1.10	1.12	---		
Q11	---	6.87	6.47	6.67	---		
T11	3.35	4.42	6.93	5.68	---		
S12	1.96	1.24	1.50	1.37	1.5-3.0		611±244
15W	5.78	3.98	2.62	3.30	3.0-6.1		
I18	4.89	6.75	4.82	5.78	>6.1		
K18	3.12	7.41	7.89	7.65	3.0-6.1		
L18	5.09	---	3.80	3.80	>6.1		
P18	5.16	5.64	4.70	5.17	3.0-6.1		
S18	3.08	---	3.94	3.94	>6.1		
T18	5.56	8.76	7.95	8.85	3.0-6.1		
L19	3.56	3.78	3.15	3.46	---		
Mean	4.13	3.64	3.85	3.68			
Standard deviation	1.68	1.94	2.17	1.95			

Table 1--Continued

ANALOG AMPLIFICATION WITH RESPECT TO AVERAGE GRANITE†

Location Identification	Vertical	East-West	North-South	Average E-W N-S	Depth to water table (M)	Thickness of surface layer†† (M)	Depth to bedrock (M)
SURFACE LAYER--YOUNGER BAY MUD							
H1	6.34	16.14	19.32	17.73	0-1.5	15.8	122±30
Q1	4.35	11.16	13.15	12.16	0-1.5	19.8	208±4
T1	2.90	8.76	6.37	7.56	0-1.5	6.7	107±15
R2	3.99	6.18	4.78	5.48	0-1.5	24.4	99±23
H3	3.44	9.36	8.96	9.16	0-1.5	7.3	99±23
J3	3.62	---	---	---	0-1.5	8.2	152±8
K3	2.72	7.77	9.16	8.46	0-1.5	3.7	320±46
P3	2.36	---	---	---	0-1.5	5.2	320±46
R3	3.44	---	---	---	0-1.5	6.7	320±15
L4	2.17	4.78	3.78	4.28	0-1.5	5.2	351±76
P4	2.54	3.98	5.18	4.58	0-1.5	12.2	92±8
Q4	3.26	14.94	10.16	12.55	0-1.5	12.2	122±30
R4	3.26	12.95	14.34	13.64	0-1.5	7.9	163±4
I5A	---	17.53	---	17.53	0-1.5	15.2	191±8
I5B	4.08	11.81	15.46	13.64	0-1.5	12.2	176±8
I5C	---	12.21	---	12.21	0-1.5	9.1	107±15
P5	2.72	6.75	10.38	8.56	---	26.2	80
Q5	2.72	7.93	12.21	10.07	---	26.2	80
R5	3.73	8.96	15.32	12.14	0-1.5	9.1	137±15
T5	3.57	12.47	11.43	11.95	---	13.7	46
H7	3.15	3.98	6.81	5.40	---	9.1±3.0	
P7	---	9.52	7.13	8.32	---	16.7±3.0	76±8
T7	4.18	9.06	12.61	10.84	---	21.3	76±3
T9	9.69	7.41	7.83	7.62	0-1.5	0±0.3	672±244
I11	3.37	7.65	6.43	7.04	0-1.5	10.1±0.9	183
Q12	4.20	2.11	3.41	2.76	1.5-3.0	0±0.3	883±244
$L_1$14	2.66	5.23	---	5.23	0-1.5	5.8±0.6	214±15
$L_2$14	3.42	9.56	8.08	8.82	0-1.5	5.5±0.6	214±15
$L_3$14	3.36	4.65	4.46	4.55	0-1.5	4.9±0.6	197±15
$L_4$14	2.71	5.03	6.24	5.63	0-1.5	4.0±0.6	167±15
$L_5$14	2.28	6.35	7.74	5.54	0-1.5	3.4±0.6	183±15
$L_6$14	---	---	4.63	4.63	0-1.5	1.8±0.6	216±15
15H	7.37	5.46	4.48	4.97	0-1.5	4.3±0.6	396±61
H18	2.93	6.37	6.97	6.67	---		
Q18	2.03	5.30	4.08	4.69	---		
R18	3.10	8.71	6.43	7.57	---		
Mean	3.61	8.44	8.58	8.54			
Standard deviation	1.56	3.70	4.07	3.85			

†Average granite is the mean amplification of five sites H16, I16, H17, P17, and R17.
††Includes artificial fill.
*Bedrock values used to normalize amplifications to average granite, not used in computing average or standard deviation.

Table 2

MEASUREMENT ERROR FOR VERTICAL ANALOG AMPLIFICATIONS

Location Identification	Vertical V_1	Vertical V_2	Difference $[V_1-V_2]$	Mean $\overline{V}$	Error percentage $\frac{[V_1-V_2]}{\overline{V}}$ 100
H7	2.43	2.31	0.12	2.37	5.06
I7	1.00	1.04	0.04	1.02	3.92
R7	1.09	1.16	0.07	1.12	6.25
T7	3.83	4.59	0.76	4.23	17.97
I8	1.28	1.39	0.11	1.34	8.21
J8	2.24	2.31	0.07	2.28	3.07
K9	5.13	4.95	0.18	5.04	3.57
L9	6.51	6.53	0.02	6.52	0.31
T9	9.79	9.64	0.15	9.72	1.54
S12	1.93	2.00	0.07	1.96	3.57
Q14	1.73	1.91	0.18	1.82	9.89
H16	0.98	1.05	0.07	1.02	6.86
I16	1.18	1.16	0.02	1.17	1.71
K16	1.25	1.41	0.16	1.33	12.03
L16	2.36	2.12	0.24	2.24	10.71
Q16	1.32	1.29	0.03	1.30	2.31
T16	1.76	1.95	0.19	1.86	10.22
H17	0.80	0.87	0.07	0.84	8.33
K17	2.77	3.22	0.45	3.00	15.00
L17	1.27	1.27	0.00	1.27	0.00
P17	1.07	1.07	0.00	1.07	0.00
R17	0.90	0.94	0.04	0.92	4.35
S17	1.01	1.01	0.00	1.01	0.00
H18	2.93	2.95	0.02	2.94	0.68
I18	4.98	4.80	0.19	4.89	3.89
K18	3.00	3.24	0.24	3.12	7.69
L18	5.05	5.12	0.07	5.08	1.38
P18	5.43	4.91	0.52	5.17	10.06
Q18	1.97	2.06	0.09	2.02	4.46
R18	3.04	3.17	0.13	3.10	4.19
S18	3.02	3.13	0.11	3.08	3.57
T18	5.24	5.55	0.31	5.40	5.74
Mean					5.52
Standard deviation					4.49

Histograms constructed to compare the analog amplification values observed on three bedrock units (fig. 24, table 1) (granite, Franciscan Formation and Santa Clara Formation) show:

(1) for vertical ground motion, the mean maximum analog amplitudes recorded on the Santa Clara and Franciscan Formations were, respectively, 3.80 and 1.46 times larger than that recorded on granite,

(2) for horizontal ground motion, the mean maximum analog amplitudes recorded on the Santa Clara and Franciscan Formations were, respectively, 2.64 and 1.38 times larger than that recorded on granite, each of which is smaller than the corresponding value observed for vertical motion, and

(3) the range and standard deviation of the analog amplification samples for granite (both horizontal and vertical) are distinctly smaller than those for the Franciscan Formation or the Santa Clara Formation. (The Franciscan and Santa Clara Formations each include a variety of rock types. Also, each formation is distributed over a wider geographic area than is the granite.)

Histograms constructed to compare the analog amplifications of alluvial sites with those of sites on granitic rocks and rocks of the Franciscan Formation (figs. 25 and 26, table 1) show:

(1) for horizontal ground motion, the mean analog amplification of the younger bay mud unit (8.54) is substantially larger than that of the older bay sediment unit (3.68), which in turn is larger than that of the combined bedrock sample (1.25),

(2) for vertical motion, the mean analog amplification of the younger bay mud unit (3.61) is slightly smaller than that of the older bay sediment unit (4.13) and both are significantly larger than that of the combined bedrock sample (1.30),

(3) for the younger bay mud unit, the mean analog amplification of vertical motion (3.61) is considerably smaller than that for horizontal motion (8.54),

(4) the standard deviation for each of the alluvial samples is substantially larger than those for the combined bedrock sample, and

(5) for vertical motion, the standard deviation of the younger bay mud sample is approximately the same as that of the older bay sediment sample (1.56, 1.68, respectively); however, for horizontal motion the standard deviation of the younger bay mud sample (3.85) is considerably larger than that of the older bay sediment sample (1.95) (the magnitudes of the standard deviations are indicative of variations in amplification due mainly to variations in thicknesses of the corresponding alluvial units).

Maximum amplitude of the analog recordings (figs. 2-22) and the analog amplifications with respect to granite (table 1) show strong correlations with the types of geologic units. However, in general, analog amplifications are dependent upon the nature and distance of the source, the seismic wave travel paths, and the response of the recording instruments. For the nuclear explosion data, concentration of the majority of the ground motion energy in the frequency band for which the amplification effects of many of the local geologic deposits are greatest and the frequency response of the

recording instruments give rise to maximum amplitudes on the analog recordings which clearly show the amplification effects of the local geologic deposits. However, Borcherdt (1970), in analyzing the strong-motion analog recordings of the San Francisco earthquake of March 22, 1957, showed that this is not true for analog recordings from every seismic event and to isolate the effects of local geologic units one must consider the spectral characteristics of the ground motion.

4.2 Spectral Amplification of Vertical and Horizontal Ground Motion

The seismic amplitude response characteristics of local geologic units can be estimated by considering the ratio of the absolute value of the Fourier transform of a seismogram recorded on an alluvial layer to that computed from a seismogram recorded from the same source on identical instruments at a nearby bedrock location. Borcherdt (1970) established that this ratio over the frequency band for which there is a good signal-to-noise ratio approximates the seismic amplitude response of the alluvial layer with the effects of the source, travel path, and recording instruments removed. These spectral ratios are a measure of the ground motion amplification at each frequency. This type of amplification, as distinguished from that measured on the analog records, will be referred to as spectral amplification.

4.2.1 Fourier Amplitude Spectra

As a first step toward computing spectral amplification curves, Fourier amplitude spectra were computed from the digitized seismic recordings of vertical ground motion (figs. 27-30), of east-west horizontal ground motion (figs. 31-34), and of north-south horizontal ground motion (figs. 35-38). The minimum spectral value is plotted at those frequencies for which the

signal-to-noise ratio is less than two (see Appendix 1 for a detailed discussion of computational techniques). The amplitude spectra have been arranged according to the type of associated geologic unit. Comparison of the amplitude spectra shows:

(1) the majority of the ground motion energy is concentrated in the frequency band 0.5 Hz to 1.5 or 2 Hz with the peak for bedrock sites occurring between .75 Hz and 1 Hz,

(2) the frequency bands for which the signal-to-noise ratio is greater than two varies considerably from site to site, but in general they are broadest for sites on bedrock and narrowest for sites on younger bay mud (the seismic noise level is generally significantly higher at alluvial sites than at bedrock sites), and

(3) amplification effects of local geologic deposits are not easily discernible by visual inspection of the amplitude spectra.

4.2.2 Spectral Ratios

For each nuclear explosion the Fourier amplitude spectrum for each component of recorded ground motion has been normalized by the corresponding amplitude spectrum computed for the bedrock site near Black Mountain (BLM). The spectral amplification curves are shown: in figures 39-41 for vertical ground motion, in figures 42-44 for east-west horizontal ground motion, and in figures 45-47 for north-south horizontal ground motion. The ratios of the amplitude spectra are plotted only for those frequencies for which the signal-to-noise ratio for each spectra is greater than two. The spectral ratios are grouped according to the type of underlying generalized geologic

unit. For nuclear explosions 6, 7, 8, and 11, no recordings were obtained at the Black Mountain location. For these explosions the amplitude spectra were first normalized by that obtained at the bedrock site in Golden Gate Park (GGP), then multiplied by a constant factor (0.94 for vertical motion and 0.65 for horizontal motion) to normalize the ratios to Black Mountain.

The spectral amplification curves with respect to Black Mountain (figs. 39-47) show the following correlations with the generalized geologic units:

(1) for bedrock sites the amplification curves are approximately constant as a function of frequency, suggesting that the major distinction between the seismic amplitude response (both horizontal and vertical) of the various bedrock units is a constant factor independent of frequency,

(2) for sites on younger bay mud, pronounced peaks are apparent in the horizontal spectral amplifications (e.g., H7, P7, T7, Q6, figs. 42 and 45), and the maximum horizontal spectral amplification is generally considerably larger than the maximum vertical,

(3) for sites on older bay sediments, both the horizontal and vertical spectral amplifications are irregular as a function of frequency, generally greater than unity for all frequencies, and in some cases have several peaks, and

(4) for the alluvial units, the frequencies of the pronounced peaks differ considerably from one site to another (these variations appear to be due principally to variations in thicknesses of the alluvial units).

To summarize on a regional basis the seismic amplitude response of the various geologic units, the average of each spectral amplification curve was computed over the frequency band for which the corresponding signal-to-noise ratios were greater than two. (For bedrock sites, these average values characterize the spectral amplification curves reasonably well. For alluvial sites, the average values indicate the general level of amplification but do not provide a complete characterization of the spectral amplification curves, especially those with pronounced peaks.)

To reduce the data to a common-rock type, the computed average spectral amplifications were normalized to the average value obtained on granite (0.78 for vertical motion and 0.51 for horizontal motion). The average spectral amplification with respect to granite for each site is tabulated (table 3) and plotted on a geologic map for horizontal motion (fig. 48).

Comparison of the horizontal spectral amplification curves for east-west ground motion with those for north-south ground motion shows they differ in detail but their overall gross features are the same. A plot of the average horizontal spectral amplifications for east-west motion versus that for north-south motion (fig. 49) shows the average values computed for the two directions are approximately the same. As a result, the average of the east-west and north-south average horizontal spectral amplifications have been tabulated (table 3) and plotted (fig. 48).

Histograms constructed to compare the amplitude response of three bedrock units (fig. 50, table 3) show:

Table 3

SPECTRAL AMPLIFICATION WITH RESPECT TO AVERAGE GRANITE

Location Identification	Vertical	East-West	North-South	Average E-W N-S
SURFACE LAYER--GRANITE				
H16	0.99	0.95	0.97	0.96
I16	0.98	0.79	0.81	0.80
H17	0.94	1.21	1.09	1.15
P17	1.04	0.91	0.83	0.87
R17	1.04	1.34	1.11	1.22
Mean	1.00	1.04	0.96	1.00
Standard deviation	0.04	0.23	0.14	0.18
SURFACE LAYER--FRANCISCAN FORMATION				
CYH*	0.93	0.79	0.79	0.79
BLM*	1.29	1.98	1.98	1.98
GGP*	1.21	1.29	1.29	1.29
I7	1.10	1.34	1.25	1.30
J7	1.19	0.99	1.09	1.04
I8	1.02	1.44	1.26	1.35
L11	1.44	1.23	1.32	1.28
K16	1.46	1.13	1.28	1.20
L16	2.01	1.88	2.06	1.97
Q16	1.71	2.09	2.33	2.21
T16	2.13	---	2.51	2.51
S17	1.61	2.33	2.33	2.33
Mean	1.52	1.55	1.71	1.60
Standard deviation	0.39	0.49	0.58	0.56
SURFACE LAYER--SERPENTINE AND ULTRAMAFIC ROCKS				
H9	---	2.49	---	2.49
J16	---	1.21	0.89	1.05

*Bedrock values used to normalize spectral amplification to average granite, not used in computing average or standard deviation.

Table 3--Continued

SPECTRAL AMPLIFICATION WITH RESPECT TO AVERAGE GRANITE

Location Identification	Vertical	East-West	North-South	Average E-W N-S
SURFACE LAYER--SANTA CLARA FORMATION				
P1	2.84	2.18	2.57	2.38
P2	2.58	1.78	---	1.78
K9	3.75	3.52	3.14	3.33
K17	4.28	3.79	3.14	3.46
L17	1.30	1.42	1.36	1.39
Q17	3.11	4.07	3.83	3.95
Mean	2.98	2.79	2.81	2.72
Standard deviation	1.03	1.13	0.92	1.02
SURFACE LAYER--OLDER BAY SEDIMENTS				
K2	2.32	2.17	2.57	2.37
Q2	1.93	1.58	1.98	1.78
K5	3.51	4.40	---	4.40
K7	---	3.32	3.79	3.56
R7	1.39	2.06	---	2.06
H8	3.16	4.94	---	4.94
J8	1.78	2.59	3.34	2.96
K8	3.39	6.11	3.89	5.00
L8	4.02	6.64	---	6.64
T8	5.28	6.64	8.24	7.44
L9	6.66	5.97	6.50	6.24
J11	1.48	1.94	1.88	1.91
K11	1.71	1.31	---	1.31
Q11	---	5.79	5.69	5.74
T11	3.25	4.94	5.53	5.24
I18	4.42	3.77	4.92	4.34
K18	4.11	5.69	5.87	5.78
L18	3.21	---	3.70	3.70
P18	3.65	3.95	5.10	4.52
S18	2.76	---	5.16	5.16
T18	5.32	7.27	8.75	8.01
Mean	3.33	4.27	4.81	4.43
Standard deviation	1.43	1.92	1.99	1.89

Table 3--Continued

SPECTRAL AMPLIFICATION WITH RESPECT TO AVERAGE GRANITE

Location Identification	Vertical	East-West	North-South	Average E-W N-S
		SURFACE LAYER--YOUNGER BAY MUD		
H1	5.67	6.13	9.29	7.71
Q1	5.54	7.11	10.47	8.79
T1	2.96	4.94	5.93	5.44
Q4	2.58	---	8.30	8.30
I5a	---	25.89	---	25.89
I5b	4.10	23.32	20.47	21.90
I5c	---	19.58	---	19.58
P5	3.26	9.15	11.34	10.24
Q5	3.62	12.23	10.55	11.39
R5	3.74	14.55	14.55	14.55
H7	2.22	5.42	7.39	6.40
P7	2.05	8.87	8.50	8.68
T7	3.72	10.81	12.73	11.77
T9	8.61	9.90	11.62	10.76
I11	3.39	8.02	12.45	10.24
Q18	2.16	3.58	4.53	4.06
R18	2.36	6.32	5.61	5.96
Mean	3.73	10.99	10.25	11.27
Standard deviation	1.75	6.65	4.02	6.03

(1) the average amplitude responses (vertical and horizontal, respectively) of the Santa Clara Formation (2.98, 2.72) are significantly larger than those for the Franciscan Formation (1.52, 1.60) which in turn are larger than those for granite (1.0, 1.0),

(2) the amplitude responses computed at five different sites on granite are very similar (the standard deviation (S.D.) for the vertical responses is 0.04 and that for the horizontal response is 0.18),

(3) the range and standard deviations of both the vertical and horizontal average spectral amplifications observed on the Santa Clara and Franciscan Formations are substantially larger than those observed on granite (Both the Franciscan and Santa Clara Formations include a variety of rock types. Also, outcrops of the formations are distributed over a wider geographic area than are the outcrops of granitic rocks.), and

(4) for each of the three bedrock units, the vertical amplitude response is similar to the horizontal amplitude response.

Histograms constructed to compare the amplitude response (as measured by the average spectral amplification values) of the alluvial units with the amplitude response of two combined bedrock units (granitic rocks and rocks of the Franciscan Formation) (figs. 51 and 52, table 3) show:

(1) the mean amplitude response (both vertical and horizontal) of each of the alluvial units is larger than that of the combined bedrock unit, especially the mean horizontal amplitude response of the younger bay mud unit (11.27),

(2) the mean vertical amplitude response of the younger bay mud unit (3.73) is only slightly larger than that of the older bay sediment unit (3.33), however, the mean horizontal amplitude response of the younger bay unit 11.27 is substantially larger than that of the older bay sediment unit (4.43) (compare figs. 51 and 52), and

(3) the range and standard deviations of each alluvial sample (table 3) are larger than those for the combined bedrock sample, with those for horizontal motion being substantially larger (the variations in amplitude response observed for the two alluvial units are due in large part to variations in thickness of the units).

4.3 Analog Amplification Versus Average Spectral Amplification

Analog amplifications are easier to determine than average spectral amplifications, however, in general they are dependent on the nature and distance of the source, the travel paths of the seismic waves, and the amplitude response of the recording units as well as the amplitude response of local geologic units. To evaluate their usefulness for the nuclear explosion data, analog amplifications are compared to the average spectral amplification values which are to a first approximation dependent on only the average amplitude response of the local geologic deposits. The analog amplification is plotted versus the corresponding average spectral amplification at each site for vertical motion (fig. 53), for east-west horizontal motion (fig. 54), and for north-south horizontal motion (fig. 55).

For the bedrock recording locations, the analog amplifications determined from the nuclear explosions are approximately equivalent to the average spectral amplifications. This correspondence is consistent with the amplitude response of the bedrock units being approximately constant independent of frequency.

For the older bay sediment locations and the younger bay mud locations, the correspondence between the analog amplifications and the average spectral amplifications becomes increasingly poor with increasing magnitude of amplification. A decrease in the correspondence with increasing amplification is consistent with the larger amplifications being associated with sites having predominant ground frequencies. For such sites to characterize completely the amplitude response, a spectral amplification curve is required rather than a single amplification value.

In brief, for the nuclear explosion data the preceding comparison suggests that the analog amplifications are an approximate measure of the average amplitude response of the various geologic units with those observed on bedrock being the most reliable. However, this conclusion cannot be generalized to analog amplifications that might be measured from other seismic events at substantially different distances. The nuclear explosions are at an appropriate distance range such that the majority of the ground motion energy is concentrated in a frequency band for which the amplification effects of many of the local geologic deposits are greatest. Hence, the maximum analog amplitudes as measured by the particular recording instruments are indicative of the average amplification effects of the local geologic deposits. For other seismic events recorded at different distances on different recording units, this coincidence of frequency bands may not occur.

5. SEISMIC NOISE ANALYSES

Seismic noise has been used extensively in Japan to estimate predominant ground frequencies (e.g., Kanai and others, 1966). Borcherdt (1970) analyzed seismic noise recorded at six locations chosen to avoid nearby cultural noise sources and hence noise signals which had not propagated through the underlying soil. These analyses suggested that predominant frequencies were more clearly defined by the spectral-amplification curves computed from the recordings of the nuclear explosions than by the amplitude spectra computed for the seismic noise.

The following seismic noise analyses differ from those presented previously by Borcherdt in that here no attempt is made to analyze sections of noise which have not traveled through the underlying soil. The Fourier amplitude spectrum was computed of 20.48 seconds of noise immediately prior to the arrival of the nuclear generated signal for each component of ground motion recorded at each location (fig. 1). (The principal reason for choosing this section of noise was to determine those frequency bands for which the nuclear-generated signal-to-seismic noise ratio was greater than two.)

The amplitude spectra for the seismic noise corresponding to nuclear explosions 7-18 are shown for vertical motion (figs. 56-59), for east-west horizontal motion (figs. 60-63), and for north-south horizontal motion (figs. 64-67). Comparisons of these spectra suggest that:

(1) no predominant frequencies are apparent on the seismic-noise spectra computed for the younger bay mud sites,

(2) the average seismic noise level over the frequency band 0.25-5 Hz for sites on younger bay mud is in general higher than that for older bay sediments which in turn is higher than that for bedrock, which is partially due to the fact that the main sources of noise for the bedrock sites are not the same as those for the alluvial sites,

(3) the general shapes of the amplitude spectra for the two components of horizontal motions are essentially the same for each site,

(4) also, the general shapes of many of the vertical amplitude spectra are similar to the horizontal amplitude spectra, with an interesting distinction--ratios of horizontal to vertical amplitude spectra for younger bay mud sites (not shown) suggest pronounced peaks which in several cases coincide with those defined by the spectral amplification curves (no such peaks in these ratios have been observed for sites on older bay sediments),

(5) for bedrock sites and for some of the older bay sediment sites, the noise level is approximately constant over the frequency band 0.25-5 Hz.

6. COMPARISON OF THE NUCLEAR DATA WITH THE INTENSITY DATA FOR THE 1906 EARTHQUAKE

The amounts of damage resulting from the 1906 earthquake varied greatly for different areas in the San Francisco Bay region. The degree of intensity ascribed to various areas correlates strongly with the geological character of the ground and generally decreases with increasing distance from the zone of surface faulting. To quantify these observations, the 1906 intensity data were reconsidered on a site-by-site basis. Only those sites (approximately one square city block in size) for which there was good evidence for the degree of ascribed intensity were considered. (In the city of San Francisco [Map no. 19; Lawson, 1908], intensity data only from those areas for which there was "unequivocal evidence" were used and for the area south of the city [Maps nos. 21 and 22, Lawson, 1908], only those data for which the site was intersected by an "examined route" were used.)

The 1906 intensity data plotted as a function of distance for sites underlain by rocks of the Franciscan Formation is shown (fig. 68). The empirical relation, determined by the method of least squares, suggests that the ascribed intensity values for sites on the Franciscan Formation generally decrease as the logarithm of increasing distance. The empirical relation shows that the intensity values decrease very rapidly with distance, with sites 3 km from the fault having observed intensities more than two intensity units smaller than those at the fault.

The sites with the highest ascribed intensities ("A", 1906 San Francisco scale) are located within 0.7 km of the center of the zone of surface rupture. For most of these sites the unit of intensity was assigned on the basis of

evidence for some form of ground failure much of which was associated with surface faulting. Since the degree of intensity assigned to most of the other sites at greater distances from the fault was based on damage resulting from ground shaking, either directly or indirectly through shaking induced ground failures, the sites with assigned intensities of A (based mostly on surface faulting evidence) were eliminated from the data set. The resulting empirical relation determined from the reduced data set is

$$\text{Intensity} = 2.73 - 1.96 \log(\underset{(\text{Km})}{\text{Distance}}).$$

This relation is essentially the same as the one determined from the complete data set. Intensities predicted from either relation differ by less than 0.2 over the entire distance interval of 0-15 km. For explicitness only the relation determined from the complete data set will be referred to hereafter.

The intensity values assigned for the 1906 earthquake in general correlate with the type of the underlying geologic unit. To quantify this correlation, intensity increments were defined for each of the sites as the difference between the observed intensity at the site and that predicted by the empirical relation for sites on the Franciscan Formation at the same distance. These intensity increments are plotted as a function of the AHSA values determined at the same sites (fig. 69). (The AHSA values plotted have been normalized by the average AHSA value determined for sites on the Franciscan Formation.) Empirical relations were determined using the method of least squares from the complete data set (".") and from only the data ("•") for sites in the city of San Francisco for which there was "unequivocal evidence" for the degree of ascribed 1906 intensity. The two empirical relations are similar with intensity increments predicted by either relation differing by less than

two-tenths. The empirical relation ($\delta I = 0.27 + 2.70 \log(AHSA)$) based on only the good intensity data in the city of San Francisco is preferred.

The correlation coefficient of 0.95 computed for the preferred empirical relation ($\delta I = 0.27 + 2.70 \log(AHSA)$) shows that a strong correlation exists between the computed intensity increments and the amplifications observed at low-strain levels. The physical meaning of this empirical correlation is complex and does not necessarily mean that amplifications observed at low-strain levels can be extrapolated directly to high-strain levels. However, there are two possible reasons for this correlation:

(1) for levels of ground shaking that did <u>not</u> cause ground failure, the higher amplifications indicate those sites that experienced the higher levels of ground shaking, and

(2) for levels of ground shaking that did cause ground failure, the higher amplifications indicate those sites that were most susceptible to ground failure.

In either case the sites of higher amplification would have experienced greater amounts of damage and be assigned higher degrees of intensity.

On the basis of the two preferred empirical relations, intensity increments and absolute intensities have been predicted for each of the 99 sites at which amplification values have been measured from the nuclear explosions (table 4). The average intensity increment for the various geologic units ranges from -0.29 for granite to 2.43 for younger bay mud.

Table 4

PREDICTED INTENSITY INCREMENTS AND ABSOLUTE INTENSITIES FOR LARGE EARTHQUAKES ON THE SAN ANDREAS FAULT AND THE HAYWARD FAULT

Location Identification	Distance from San Andreas km	Distance from Hayward km	Horizontal amplification†	Intensity increment	Predicted intensity (San Andreas)	Predicted intensity (Hayward)
			SURFACE LAYER--GRANITE			
H16	2.90	32.83	0.60	-0.32	1.49	-0.51
I16	7.89	37.66	0.50	-0.53	0.45	-0.83
H17	4.83	34.92	0.72	-0.11	1.28	-0.35
P17	7.89	37.66	0.55	-0.44	0.55	-0.74
R17	7.08	36.21	0.77	-0.04	1.04	-0.31
Mean (Spectral)			0.63	-0.29		
Standard deviation			0.11	0.21		
			SURFACE LAYER--FRANCISCAN FORMATION			
K1	21.40	8.69	0.46	-0.63	-0.46	0.28
J5*	14.65	15.93	0.82	0.03	0.51	0.44
I7	14.65	15.61	0.82	0.03	0.51	0.46
J7	14.65	15.93	0.65	-0.23	0.25	0.18
I8	14.65	15.61	0.85	0.08	0.56	0.50
L11	8.21	22.21	0.80	0.02	0.97	0.15
K16	4.18	25.43	0.75	-0.06	1.45	-0.04
L16	2.41	27.20	1.24	0.52	2.48	0.49
Q16	1.77	27.68	1.39	0.66	2.87	0.61
T16	1.93	31.70	1.58	0.81	2.95	0.65
S17	31.70	1.77	1.46	0.72	0.56	2.94
Mean (Spectral)			1.00	0.19		
Standard deviation			0.38	0.47		

Table 4--Continued

PREDICTED INTENSITY INCREMENTS AND ABSOLUTE INTENSITIES FOR LARGE EARTHQUAKES ON THE SAN ANDREAS FAULT AND THE HAYWARD FAULT

Location Identification	Distance from San Andreas km	Distance from Hayward km	Horizontal amplification†	Intensity increment	Predicted intensity (San Andreas)	Predicted intensity (Hayward)
SURFACE LAYER--SERPENTINE AND ULTRAMAFIC ROCKS						
H9	2.09	28.00	1.56	0.80	2.88	0.74
J16	0.16	29.61	0.66	-0.22	3.98	-0.32
Mean (Spectral)			1.11	0.29		
Standard deviation			0.64	0.72		
SURFACE LAYER--OTHER PRE-TERTIARY, TERTIARY ROCKS						
Q13*	31.38	4.35	1.21	0.50	0.35	1.98
Q14*	32.99	4.83	0.87	0.10	-0.09	1.50
P19*	36.05	6.12	1.25	0.53	0.27	1.73
R19*	34.44	5.15	2.44	1.32	1.09	2.66
T19*	33.96	4.51	1.55	0.79	0.57	2.24
19B*	5.63	35.89	1.16	0.45	1.71	0.19
19C*	2.90	32.83	1.63	0.84	2.66	0.66
19E*	4.99	34.44	1.21	0.50	1.86	0.27
19W*	7.56	37.34	1.49	0.74	1.76	0.45
Mean (Analog)			1.42	0.64		
Standard deviation			0.45	0.34		
SURFACE LAYER--SANTA CLARA FORMATION						
P1	4.83	24.94	1.49	0.74	2.14	0.78
P2	4.83	24.94	1.12	0.40	1.79	0.44
K9	4.18	23.17	2.09	1.14	2.65	1.24
K17	4.51	22.05	2.17	1.18	2.63	1.32
L17	0.48	30.26	0.87	0.11	3.40	-0.01
Q17	6.76	21.24	2.48	1.34	2.45	1.51
Mean (Spectral)			1.70	0.82		
Standard deviation			0.64	0.49		

Table 4--Continued

PREDICTED INTENSITY INCREMENTS AND ABSOLUTE INTENSITIES FOR LARGE EARTHQUAKES ON THE SAN ANDREAS FAULT AND THE HAYWARD FAULT

Location Identification	Distance from San Andreas km	Distance from Hayward km	Horizontal amplification†	Intensity increment	Predicted intensity (San Andreas)	Predicted intensity (Hayward)
			SURFACE LAYER--PAGE MILL BASALT			
L3*	5.63	24.14	2.13	1.16	2.42	1.23
J4*	6.12	23.66	1.94	1.05	2.25	1.13
Mean (Spectral)			2.04	1.11		
Standard deviation			0.13	0.08		

Table 4--Continued

PREDICTED INTENSITY INCREMENTS AND ABSOLUTE INTENSITIES FOR LARGE EARTHQUAKES ON THE SAN ANDREAS FAULT AND THE HAYWARD FAULT

Location Identification	Distance from San Andreas km	Distance from Hayward km	Horizontal amplification†	Intensity increment	Predicted intensity (San Andreas)	Predicted intensity (Hayward)
SURFACE LAYER--OLDER BAY SEDIMENTS						
J1*	8.85	20.92	2.37	1.29	2.18	1.47
H2*	11.10	18.51	1.56	0.80	1.50	1.08
K2	13.20	16.25	1.49	0.74	1.30	1.13
Q2	9.17	20.44	1.12	0.40	1.27	0.61
T2*	4.51	25.43	1.69	0.89	2.34	0.91
H4*	5.95	23.66	2.07	1.12	2.34	1.21
I4*	24.46	5.79	2.19	1.19	1.25	2.43
K4*	9.33	18.99	1.63	0.84	1.69	1.11
K5	12.39	17.86	2.76	1.46	2.08	1.78
K7	12.39	17.86	2.23	1.22	1.83	1.53
R7	14.16	16.09	1.29	0.57	1.08	0.97
H8	10.94	18.67	3.10	1.60	2.32	1.88
J8	5.47	24.62	1.86	1.00	2.29	1.05
K8	7.56	22.21	3.14	1.61	2.64	1.75
L8	7.08	20.60	3.47	1.73	2.81	1.93
R8*	19.47	7.24	1.18	0.47	0.71	1.53
T8	14.32	13.68	4.67	2.08	2.58	2.61
L9	8.85	17.86	3.92	1.87	2.77	2.19
J11	5.63	24.78	1.20	0.49	1.75	0.53
K11	10.46	20.12	0.82	0.04	0.80	0.26
Q11	1.61	28.81	3.60	1.78	4.07	1.70
T11	4.51	25.75	3.29	1.67	3.12	1.68
S12*	17.06	11.59	0.86	0.10	0.45	0.77
W15*	27.84	2.74	2.07	1.13	1.08	2.99
I18	13.36	13.52	2.72	1.45	2.00	1.99
K18	23.17	4.83	3.63	1.78	1.88	3.18
L18	16.25	10.14	2.32	1.26	1.65	2.04
P18	18.83	7.56	2.84	1.50	1.77	2.52
S18	17.06	9.50	3.24	1.65	2.00	2.49
T18	21.40	4.99	5.03	2.17	2.33	3.53
L19*	2.74	27.84	2.17	1.18	3.04	1.13
Mean (spectral)			2.44	1.34		
Standard deviation			1.08	0.58		

Table 4--Continued

PREDICTED INTENSITY INCREMENTS AND ABSOLUTE INTENSITIES FOR LARGE EARTHQUAKES ON THE SAN ANDREAS FAULT AND THE HAYWARD FAULT

Location Identification	Distance from San Andreas km	Distance from Hayward km	Horizontal amplification†	Intensity increment	Predicted intensity (San Andreas)	Predicted intensity (Hayward)
			SURFACE LAYER--YOUNGER BAY MUD			
H1	14.48	15.61	4.84	2.12	2.61	2.55
Q1	11.27	18.67	5.52	2.28	2.97	2.55
T1	19.96	10.30	3.41	1.71	1.94	2.48
R2*	10.78	18.83	3.44	1.72	2.45	1.99
H3*	13.20	16.74	5.75	2.33	2.89	2.69
K3*	13.84	15.93	5.31	2.23	2.76	2.64
L4*	13.84	15.77	2.69	1.43	1.96	1.85
P4*	7.89	21.89	2.88	1.51	2.50	1.66
Q4	9.66	20.60	5.21	2.21	3.03	2.41
R4*	18.99	11.43	8.56	2.79	3.06	3.47
I5A	10.14	20.12	16.25	3.54	4.32	3.76
I5B	9.66	20.60	13.75	3.35	4.17	3.54
I5C	8.69	21.57	12.29	3.22	4.12	3.38
P5	14.81	15.45	6.43	2.46	2.92	2.89
Q5	14.97	15.29	7.15	2.58	3.04	3.02
R5	10.46	19.96	9.13	2.87	3.62	3.09
T5*	14.16	16.42	7.50	2.64	3.14	3.02
H7	14.32	15.77	4.02	1.90	2.40	2.32
P7	14.81	15.45	5.45	2.26	2.73	2.70
T7	13.04	17.54	7.39	2.62	3.19	2.95
T9	21.56	6.76	6.75	2.51	2.67	3.63
I11	14.48	15.61	6.43	2.46	2.94	2.88
Q12*	26.55	3.06	1.73	0.92	0.91	2.69
$L_1$14*	20.28	9.01	3.28	1.67	1.88	2.55
$L_2$14*	19.96	9.33	5.54	2.28	2.50	3.13
$L_3$14*	19.63	9.66	2.86	1.50	1.74	2.32
$L_4$14*	19.31	9.98	3.53	1.75	2.00	2.55
$L_5$14*	18.99	10.30	3.48	1.74	2.00	2.50
$L_6$14*	18.67	10.62	2.91	1.52	1.79	2.19
H15*	22.21	7.56	3.12	1.61	1.74	2.63
H18*	24.78	5.63	4.19	1.95	2.00	3.22
Q18	24.62	5.79	2.55	1.37	1.42	2.61
R18	23.50	6.76	3.74	1.82	1.91	2.94
Mean (spectral)			7.08	2.43		
Standard deviation			3.78	0.58		

†With respect to average Franciscan.

*Predicted intensities determined from analog amplifications.

Average intensity increments have been estimated (table 5) by a group of six U.S. Geological Survey scientists familiar with the geology of the San Francisco Bay region (Wentworth, written commun., 1970). The intensity increments were estimated, based on degree of consolidation and lithology of the geologic units following a summary by Popov, 1959. The estimated intensity increments were used as the basis for the seismic susceptibility map by Gibbs and Eaton, 1971. A comparison of these intensity increments with those obtained from the empirical relationship (equation 2) follows:

Table 5

Intensity Increments

	This report (Normalized to granite)	Gibbs and Eaton, 1971
Granite	0	0
Franciscan	0.48	0.5
Tertiary	0.93	1.0
Santa Clara	1.11	1.5
Older bay sediments	1.63	2.0
Younger bay mud	2.72[1/]	2.5-4.0[2/]

[1/] Average thickness of mud approximately 30'.

[2/] Increments increase with thickness of mud, <15' = 2.5, 15-30' = 3.0, >30' = 4.0.

The estimates of the intensity increments for the Santa Clara, older bay sediments, and younger bay mud may be slightly high. In particular, the increase in intensity with thickness of mud may not be as rapid as estimated. However, the trend and overall agreement between the derived and estimated intensity increments is very good.

Utilizing the computed average intensity increments for the various geologic units, the empirical relation between intensity and distance, and a geologic map (compiled by K. R. Lajoie, personal commun., 1974), Borcherdt and Gibbs (1974) predicted absolute intensities on a regional basis for the San Francisco Bay region. The resulting predicted intensity map (Borcherdt and Gibbs, 1974) shows the maximum intensity predicted for a site that might result from an earthquake in the San Francisco Bay region on either the San Andreas fault or the Hayward fault. Such a map is useful for delineating general earthquake problem areas in the San Francisco Bay region and for evaluating the earthquake hazard in areas not developed at the time of the 1906 earthquake. In addition, the map is useful for evaluating the hazard due to another large earthquake on the Hayward fault. The map shows that earthquake hazards are not uniformly distributed throughout the San Francisco Bay region.

CONCLUSIONS

Three components of ground motion generated by 17 nuclear explosions in Nevada have been recorded at 99 sites in the San Francisco Bay region. Analyses of these recordings have shown that there are significant differences in the seismic amplitude response of various geologic units. The data collected since that reported by Borcherdt (1970) have confirmed the earlier conclusions (Borcherdt, 1970, p. 58-59) and provided estimates of the seismic amplitude response of additional geologic units. The complete data set, appropriately interpreted, is useful for preparing various types of seismic-zonation maps.

The spectral amplification curves showed several characteristics unique to particular types of geologic units:

(1) surface layer 2-24 meters of younger bay mud,

(a) the horizontal spectral amplification curves defined predominant frequencies in the range 0.5-2.5 Hz for sites with a surface layer thicker than 10 meters,

(b) with few exceptions the vertical spectral amplification curves did not define predominant frequencies in the range 0.5-2.5 Hz,

(c) the means for sites on younger bay mud of the average spectral amplifications for vertical and horizontal ground motion were, respectively, 3.7 and11.3, with corresponding standard deviations of 1.8 and 6.0 ,

(d) the ratio of the average spectral amplification for horizontal ground motion to that for vertical motion is substantially larger for sites on younger bay mud than for sites on the other geologic units,

(e) the spectral amplifications computed for the nuclear data defined predominant frequencies for various sites more accurately than did the amplitude spectra computed from recordings of seismic background noise.

(2) surface layer, older bay sediments,

(a) the horizontal and vertical spectral amplification curves were irregular as a function of frequency and often had several peaks, none of which were generally as distinct as those for younger bay mud sites,

(b) the means for sites on older bay sediments of the average spectral amplification for vertical and horizontal ground motion were, respectively, 3.3 and 4.4, with corresponding standard deviations 1.4 and 1.9,

(3) surface layer, bedrock,

(a) the horizontal and vertical spectral amplification curves were constant as a function of frequency over the approximate range of 0.25-3.5 Hz,

(b) the average spectral amplifications observed for various bedrock units were identifiably distinct with average values for vertical and horizontal ground motion being (1, 1) for granite, (1.5, 1.6) for the Franciscan Formation, and (3.8, 2.6) for Santa Clara bedrock units with corresponding standard deviations (0.04, 0.2), (0.4, 0.6), and (1.0, 1.0).

Additional analyses of the recorded data and geologic data may permit further refinement of seismically identifiable geologic units. A program currently underway in the U.S. Geological Survey to measure seismic shear velocities on a regional basis is expected to help in these further refinements.

Analyses of the 1906 earthquake intensity data in the San Francisco Bay region for which there was good evidence showed that an empirical relation between intensity and distance from the zone of surface faulting for sites on rocks of the Franciscan Formation was

$$\text{Intensity} = 2.69 - 1.90 \log(\text{Distance Km}).$$

Intensity increments defined with respect to this relation for sites on other geologic units were observed to correlate with the Average Horizontal Spectral Amplification values as

$$\text{Intensity Increment} = 0.27 + 2.70 \log(\text{AHSA}).$$

Average intensity increments predicted with the AHSA values were -0.3 for granite, 0.2 for Franciscan Formation, 0.8 for Santa Clara Formation, 1.3 for older bay sediments, and [illegible] for younger bay mud. These mean intensity

increments, together with the intensity versus distance relation, are useful for delineating areas of potentially high intensity in future earthquakes occurring on either the San Andreas fault or the Hayward fault.

ACKNOWLEDGMENTS

To the many co-workers who assisted in the recording and processing of this large data set we are most grateful. Among these who were called on repeatedly to operate recording instruments were John Roller, Edward Roth, Richard Warrick, David Warren, and Wayne Jackson. We also wish to acknowledge Sam Stewart, whose CDC 1700 program for digitizing the analog magnetic tape was used repeatedly. Don Nichols and Julius Schlocker provided geologic and thickness information on the bay mud. Ken Lajoie was most helpful with his knowledge of the Bay Area geology and for his compilation of the geology of the Bay Area at a scale of 1:125,000.

REFERENCES

Borcherdt, R. D., 1970, Effects of local geology on ground motion near San Francisco Bay: Seismol. Soc. America Bull., v. 60, p. 29-61.

Borcherdt, R. D., and Gibbs, J. F., 1974, Prediction of maximum earthquake intensities for the San Francisco Bay region, San Francisco Bay region environment and resources planning study. (In press)

Gibbs, J. F., and Eaton, J. P., 1971, A digitized map of seismic ground response of the San Francisco Bay region, California: U.S. Geol. Survey open-file map.

Kanai, K., Tanaka, T., Morishita, T., and Osada, K., 1966, Observation of microtremors, XI (Matsushiro earthquake swarm area): Earthquake Res. Inst. Bull. 44, p. 1297-1333.

Lajoie, K. R., and Helley, E. J., 1974, Differentiation of sedimentary deposits for seismic-zonation purposes, Chap. III, in A preliminary analysis of seismic zonation in the San Francisco Bay region: U.S. Geol. Survey Prof. Paper ____. (In press)

Lawson, A. C. (chairman), 1908, The California earthquake of April 18, 1906, Report of the State Earthquake Commission: Carnegie Inst. Washington, Atlas maps 21 and 22.

Popov, V. V., 1959, Engineering-geologic criteria of detailed seismic regionalization, in Problems of engineering seismology, v. 2, p. 81-93: Trudy of the Institute of Earth Physics No. 5 (172), Academy of Science Press, Moscow. Translated by J. P. Eaton.

Schlocker, Julius, 1968, The geology of the San Francisco Bay Area and its significance in land use planning: Association of Bay Area Governments Supplemental Report 1S-3, Regional Geology, 47.

Warrick, R. E., Hoover, D. B., Jackson, W. H., Pakiser, L. C., and Roller, J. C., 1961, The specification and testing of a seismic-refraction system for crustal studies: Geophysics, v. 26, p. 820-824.

Wood, H. O., 1908, Distribution of apparent intensity in San Francisco, in The California earthquake of April 18, 1906, Report of the State Earthquake Investigation Commission: Carnegie Inst. Washington, Publ. 87, p. 220-245.

APPENDIX 1

This section describes the computational procedure for computing the spectral amplification curves described in section 4.2.1.

The digital representations of the seismograms (see section 3) were first corrected for "leakage" (Bingham and others, 1967) by tapering one-tenth of each end of each time series with a half cosine function.

The Fourier coefficients of each corrected time series were then computed using a standard Fast Fourier transform algorithm for real data. For the recordings of the nuclear explosions, the Fourier coefficients were obtained from 163.84 seconds of data, starting approximately 2 seconds before the arrival of the first energy at the recording site. This interval includes the majority of the apparent energy on the respective seismograms. For the recordings of seismic noise, the Fourier coefficients were computed from 20.48 seconds of noise recorded immediately prior to the arrival of the nuclear generated signals.

The discrete power spectral density functions, defined in terms of the Fourier coefficients, were smoothed with a symmetric triangular window. A 15-point window was used for the recordings of the nuclear explosions and a 3-point window was used for the seismic noise recordings. The discrete Fourier amplitude spectra (square root of the smoothed power spectral density function) were computed at those frequencies for which signal-to-noise ratio was greater than two. (The signal-to-noise ratio was defined as the ratio of the respective smoothed power spectral density functions.)

The spectral amplification curves were determined by computing ratios of appropriate Fourier amplitude spectra at those frequencies for which the signal-to-noise ratio was greater than two.

APPENDIX 2

The following grades of apparent intensity were ascribed by H. O. Wood (1908, p. 224-225) in the city of San Francisco to describe damage which resulted from the California earthquake of April 18, 1906.

Grade A. Very violent - Comprizes the rending and shearing of rock masses, earth, turf, and all structures along the line of faulting; the fall of rock from mountain sides; numerous landslips of great magnitude; consistent, deep, and extended fissuring in natural earth; some structures totally destroyed.

Grade B. Violent - Comprizes fairly general collapse of brick and frame buildings when not unusually strong; serious cracking of brick work and masonry in excellent structures; the formation of fissures, step faults, sharp compression anticlines, and broad, wave-like folds in paved and asphalt-coated streets, accompanied by the ragged fissuring of asphalt; the destruction of foundation walls and underpinning structures by the undulation of the ground; the breaking of sewers and water-mains; the lateral displacement of streets; and the compression, distension, and lateral waving or displacement of well-ballasted street-car tracks.

Grade C. Very strong - Comprizes brick work and masonry badly cracked, with occasional collapse; some brick and masonry gables thrown down; frame buildings lurched or listed on fair or weak underpinning structures, with occasional falling from underpinning or collapse; general destruction of chimneys

and of masonry, brick or cement veneers; considerable cracking or crushing of foundation walls.

Grade D. Strong - Comprizes general but not universal fall of chimneys; cracks in masonry and brick work; cracks in foundation walls, retaining walls, and curbing; a few isolated cases of lurching or listing of frame buildings built upon weak underpinning structures.

Grade E. Weak - Comprizes occasional fall of chimneys and damage to plaster, partitions, plumbing, and the like.

Illustrations

Page

Figure 1. Location of sites where three components of ground motion were recorded from nuclear explosions. The locations are identified by a letter of the alphabet to designate the recording unit and a number to indicate the nuclear explosion for which the recording unit occupied the location. Sites repeatedly occupied for normalization purposes were BLM (Black Mountain, S16, J17, J18, S19), CYH (Coyote Hill, K12, S13, S14, S15), and GGP (Golden Gate Park, L5, Q7, Q8, Q9, H11). Data recorded from sites indicated by "▲" were reported previously (Borcherdt, 1970) ---------- 57

2a-8b. Analog recordings of 163.84 seconds of vertical ground motion generated by a single nuclear explosion (the first approximately 80 seconds is shown in figure a and the second in figure b). The recordings are identified by location (see fig. 1), arranged according to the type of generalized geologic unit underlying the site, and plotted at the same scale ---------- 58-71

9a-15b. Analog recordings of 163.84 seconds of east-west ground motion generated by a single nuclear explosion (the first approximately 80 seconds is shown in figure a and the second in figure b). The recordings are identified by location (see fig. 1), arranged according to the type of generalized geologic unit underlying the site, and plotted at the same scale ---------- 72-85

Figure | Page

16a-22b. Analog recordings of 163.84 seconds of north-south ground motion generated by a single nuclear explosion (the first approximately 80 seconds is shown in figure a and the second in figure b). The recordings are identified by location (see fig. 1), arranged according to the type of generalized geologic unit underlying the site, and plotted at the same scale ---------- 86-99

23. Horizontal analog amplifications determined with respect to average granite and a generalized geologic map for a portion of the San Francisco Bay region (geologic map compiled by K. R. Lajoie, personal commun.). (The plotted amplification value is an average of the values determined from the east-west and the north-south components of recorded horizontal motion.) ---------- 100

24. Histograms for vertical analog amplification values (a) and horizontal analog amplification (average east-west, north-south) values (b) measured at sites with surface layers of granite, Franciscan Formation, and Santa Clara Formation ---------- 101

25. Histograms for vertical analog amplification values measured at sites with surface layers of granite and Franciscan Formation, older bay sediment, and younger bay mud ---------- 102

Page

Figure 26. Histograms for horizontal analog amplification values (average east-west, north-south) measured at sites with surface layers of granite and Franciscan Formation, older bay sediment, and younger bay mud ---------- 103

27-30. Fourier amplitude spectra computed from recordings of vertical ground motion generated by nuclear explosions. The spectra are identified by location (see fig. 1) and arranged according to type of generalized geologic unit underlying the site. For frequencies with a signal to noise ratio less than two (see Appendix), the minimum spectral value is plotted ---------- 104-107

31-34. Fourier amplitude spectra computed from recordings of the east-west component of horizontal ground motion generated by nuclear explosions. The spectra are identified by location (see fig. 1) and arranged according to type of generalized geologic unit underlying the site. For frequencies with a signal to noise ratio less than two (see Appendix), the minimum spectral value is plotted ---------- 108-111

Figure Page

35-38. Fourier amplitude spectra computed from recordings of the north-south component of horizontal ground motion generated by nuclear explosions. The spectra are identified by location (see fig. 1) and arranged according to type of generalized geologic unit underlying the site. For frequencies with a signal to noise ratio less than two (see Appendix), the minimum spectral value is plotted ---------- 112-115

39-41. Spectral amplification curves determined with respect to Black Mountain for recordings of vertical ground motion. The spectral amplifications are plotted only for those frequencies for which the signal to noise ratio is greater than two (see Appendix 1). The spectral amplification curves are identified by location (see fig. 1) and arranged according to the type of generalized geologic unit underlying the site ---------- 116-118

42-44. Spectral amplification curves determined with respect to Black Mountain for recordings of the east-west component of horizontal ground motion. The spectral amplifications are plotted only for those frequencies for which the signal to noise ratio is greater than two (see Appendix 1). The spectral amplification curves are identified by location (see fig. 1) and arranged according to the type of generalized geologic unit underlying the site ------- 119-121

Figure | Page

45-47. Spectral amplification curves determined with respect to Black Mountain for recordings of the north-south component or horizontal ground motion. The spectral amplifications are plotted only for those frequencies for which the signal to noise ratio is greater than two (see Appendix 1). The spectral amplification curves are identified by location (see fig. 1) and arranged according to the type of generalized geologic unit underlying the site ---------- 122-124

48. Average horizontal spectral amplification values determined with respect to average granite and a generalized geologic map for a portion of the San Francisco Bay region (geologic map compiled by K. R. Lajoie, personal commun.). (The value plotted in an average of the values determined from the east-west and north-south components of recorded horizontal ground motion ---------- 125

49. East-west versus north-south average horizontal spectral amplification ---------- 126

50. Histograms for average vertical spectral amplification values (a) and average horizontal spectral amplification (average east-west, north-south) values (b) measured at sites with surface layers of granite, Franciscan Formation, and Santa Clara Formation ---------- 127

Page

Figure 51. Histograms for average vertical spectral amplification values measured at sites with surface layers of granite and Franciscan Formation, older bay sediment, and younger bay mud ---------- 128

52. Histograms for average horizontal spectral amplification values (average east-west, north-south) measured at sites with surface layers of granite and Franciscan Formation, older bay sediment, and younger bay mud ----- 129

53. Vertical analog amplification versus average vertical spectral amplification for sites with surface layers of granite and Franciscan Formation, Santa Clara Formation, older bay sediment, and younger bay mud ---------- 130

54. East-west analog amplification versus average east-west spectral amplification for sites with surface layers of granite and Franciscan Formation, Santa Clara Formation, older bay sediment, and younger bay mud ---------- 131

55. North-south analog amplification versus average north-south spectral amplification for sites with surface layers of granite and Franciscan Formation, Santa Clara Formation, older bay sediment, and younger bay mud ---------- 132

56-59. Fourier amplitude spectra computed from recordings (20.48 seconds in length) of the vertical component of seismic background noise. The spectra are identified by location and [illegible] according to the type of generalized geol[illegible] unit underlying the site ---------- 133-136

Figure Page

60-63. Fourier amplitude spectra computed from recordings (20.48 seconds in length) of the east-west component of seismic background noise. The spectra are identified by location and arranged according to the type of generalized geologic unit underlying the site ---------- 137-140

64-67. Fourier amplitude spectra computed from recordings (20.48 seconds in length) of the north-south component of seismic background noise. The spectra are identified by location and arranged according to the type of generalized geologic unit underlying the site ---------- 141-144

68. Observed 1906 intensities for sites (one square city block in size) underlain by rocks of the Franciscan Formation versus perpendicular distance from the zone of surface rupture during the 1906 earthquake. For sites with "unequivocal evidence" in the city of San Francisco (Map No. 19, Lawson, 1908), the number of observed intensity values is shown below the corresponding distance interval. For sites intersected by an "examined route" south of the city of San Francisco (Maps Nos. 21 and 22, Lawson, 1908), the number of observed intensities is shown above the corresponding distance interval. The observed 1906 intensities are expressed in terms of the 1906 San Francisco intensity scale with the letters A-E corresponding respectively to the numbers 4-0 (see Appendix 2 for detailed description of intensity scale) ---------- 145

Page

Figure 69. Increments in 1906 intensities versus average horizontal spectral amplification computed at corresponding sites from recordings of nuclear explosions. Both the intensity increment values and the average horizontal spectral amplification values were computed with respect to the corresponding average value determined for sites underlain by rocks of the Franciscan Formation. The empirical relation ($\delta I = 0.19 + 2.97 \log(AHSA)$) is based on the data (".") from all of the recording sites for which there was an observed 1906 intensity value. The empirical relation ($\delta I = 0.27 + 2.70 \log(AHSA)$) is based on only the data ("•") from sites in the city of San Francisco for which there was unequivocal evidence for the degree of ascribed 1906 intensity. (The second empirical relation is preferred, however, intensity increments predicted from either relation will differ by less than two-tenths of an intensity increment.) ---------- 146

Figure 1

Recording Site Locations

(in map pouch)

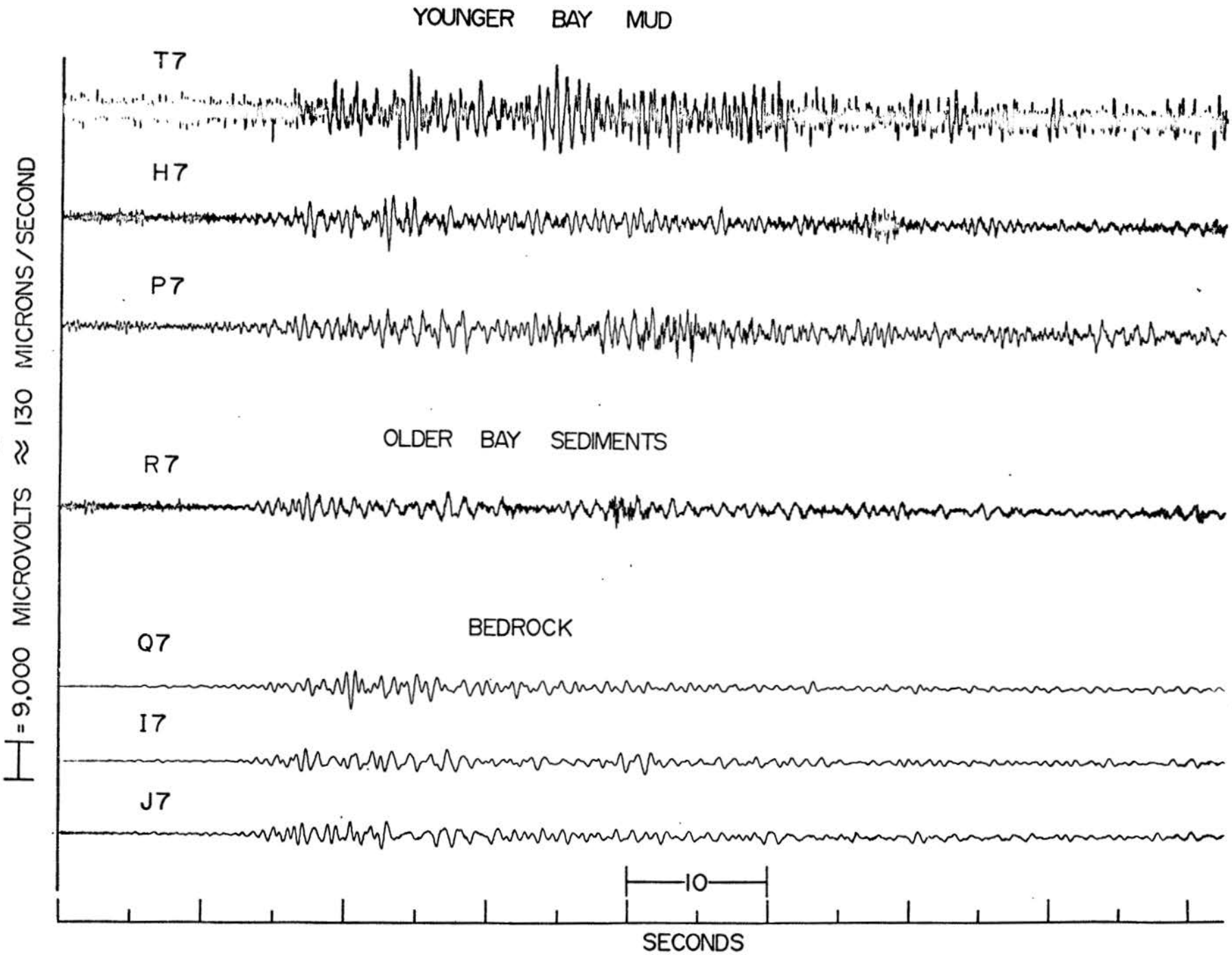
YOUNGER BAY MUD
T7
H7
P7
OLDER BAY SEDIMENTS
R7
BEDROCK
Q7
I7
J7
= 9,000 MICROVOLTS ≈ 130 MICRONS/SECOND
10
SECONDS

Figure 2a

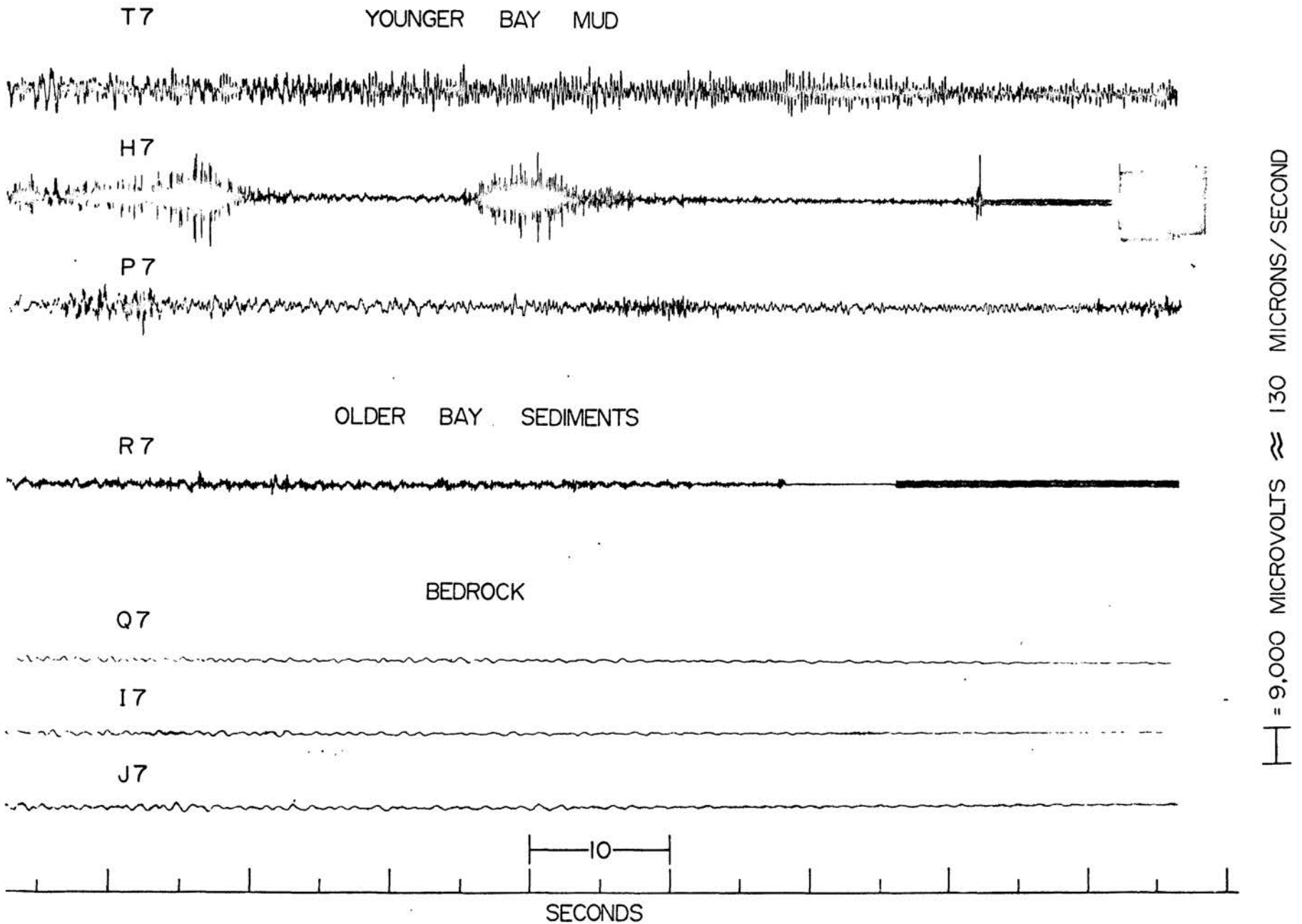
T7
YOUNGER BAY MUD
H7
P7
OLDER BAY SEDIMENTS
R7
BEDROCK
Q7
I7
J7
10
SECONDS
= 9,000 MICROVOLTS ≈ 130 MICRONS/SECOND

Figure 2b

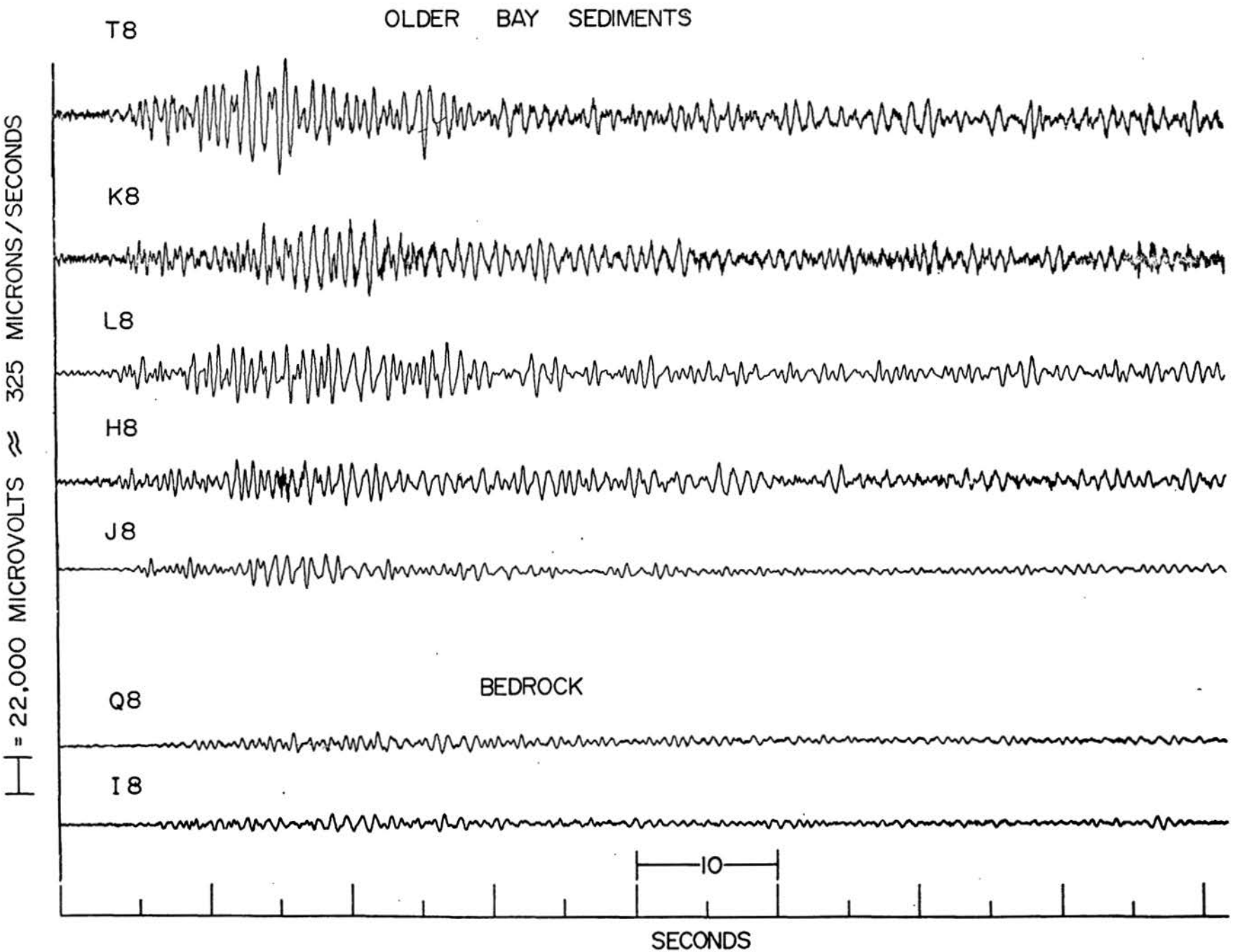
OLDER BAY SEDIMENTS
T8
K8
L8
H8
J8
BEDROCK
Q8
I8
= 22,000 MICROVOLTS ≈ 325 MICRONS/SECONDS
10
SECONDS

Figure 3a

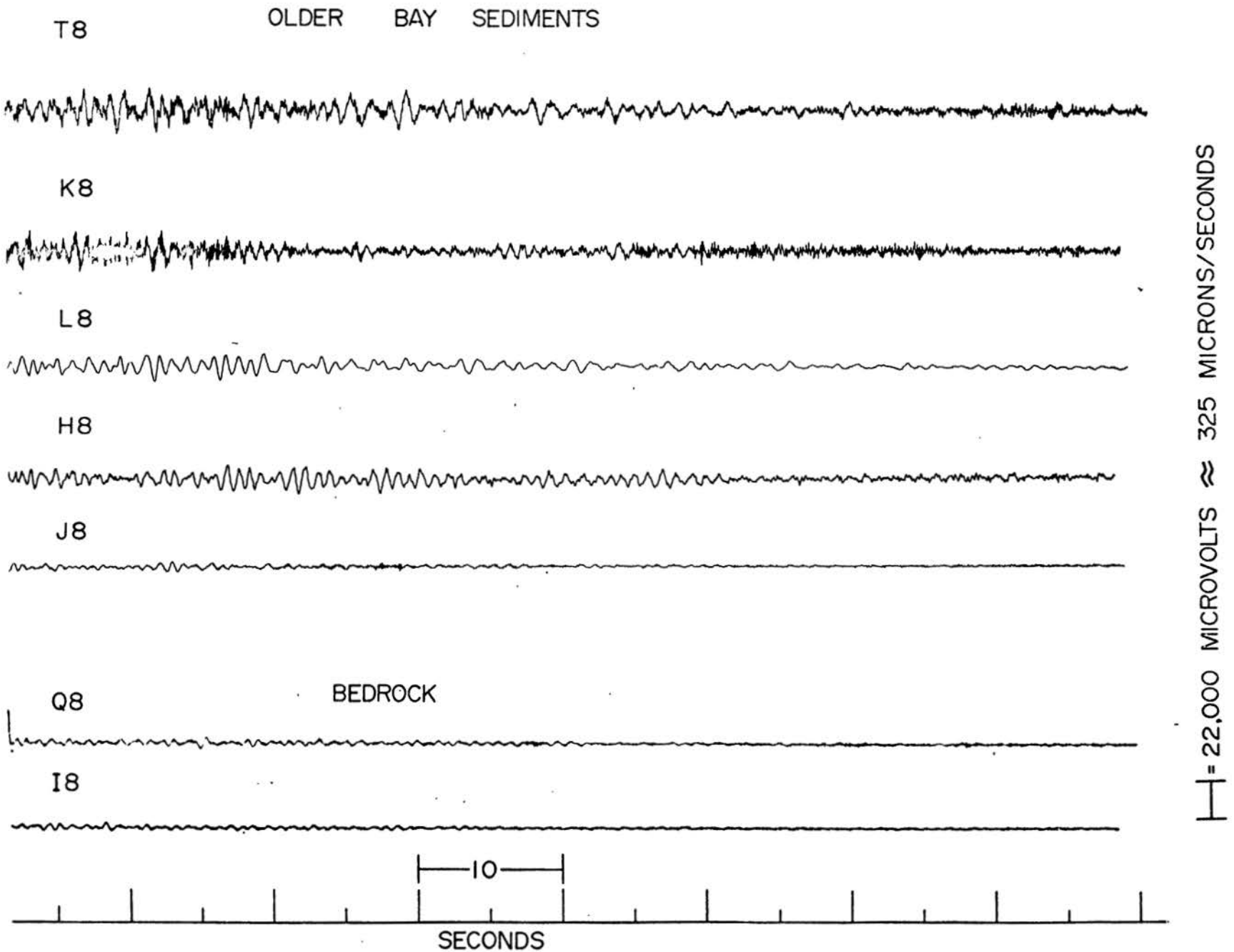
T8
OLDER BAY SEDIMENTS
K8
L8
H8
J8
Q8
BEDROCK
I8
10
SECONDS
= 22,000 MICROVOLTS ≈ 325 MICRONS/SECONDS

Figure 3b

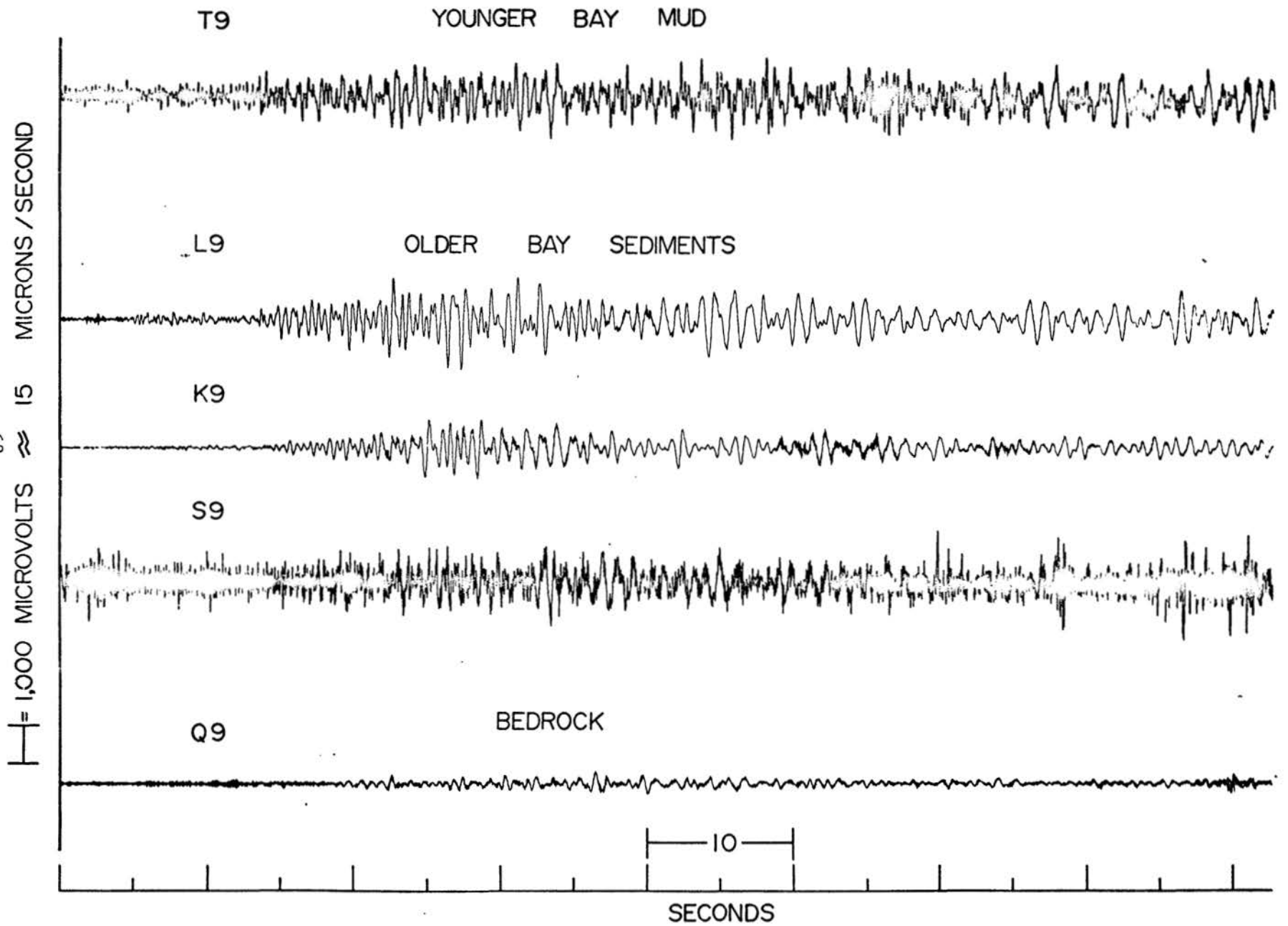
T9
YOUNGER BAY MUD
L9
OLDER BAY SEDIMENTS
K9
S9
Q9
BEDROCK
= 1,000 MICROVOLTS ≈ 15 MICRONS / SECOND
10
SECONDS

Figure 4a

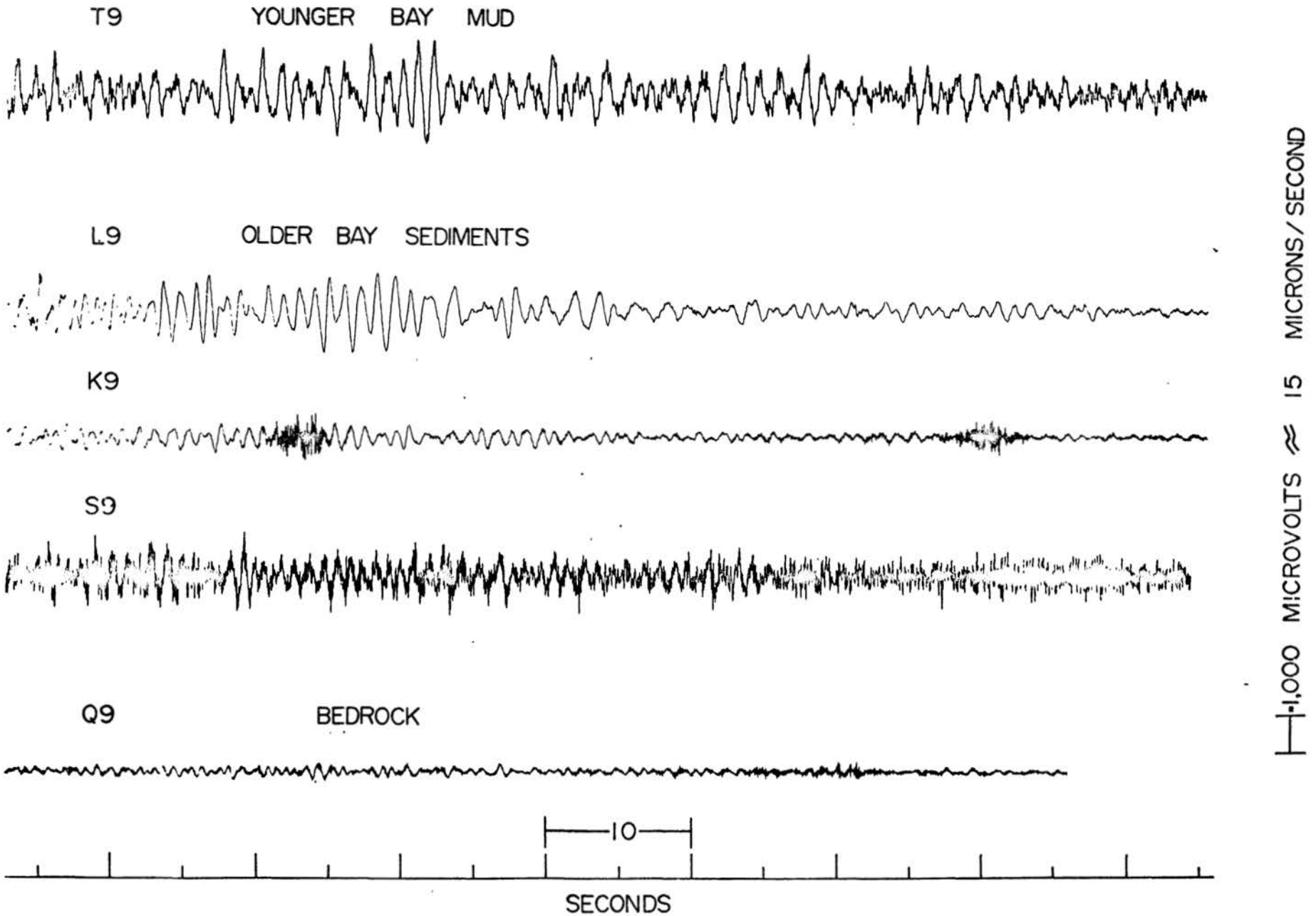
T9
YOUNGER BAY MUD
L9
OLDER BAY SEDIMENTS
K9
S9
Q9
BEDROCK
10
SECONDS
1,000 MICROVOLTS ≈ 15 MICRONS/SECOND

Figure 4b

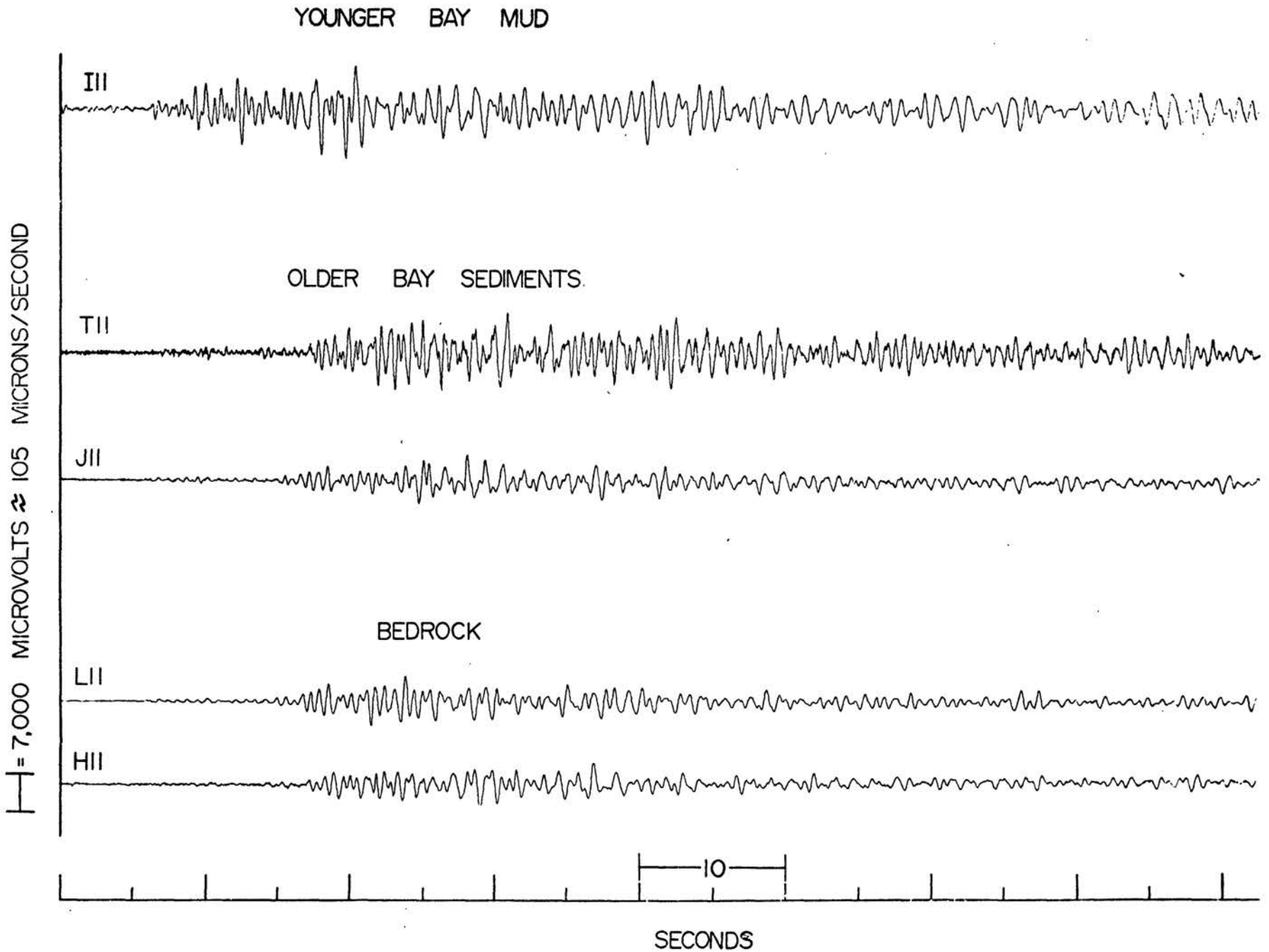
YOUNGER BAY MUD
III
OLDER BAY SEDIMENTS
TII
JII
BEDROCK
LII
HII
= 7,000 MICROVOLTS ≈ 105 MICRONS/SECOND
10
SECONDS

Figure 5a

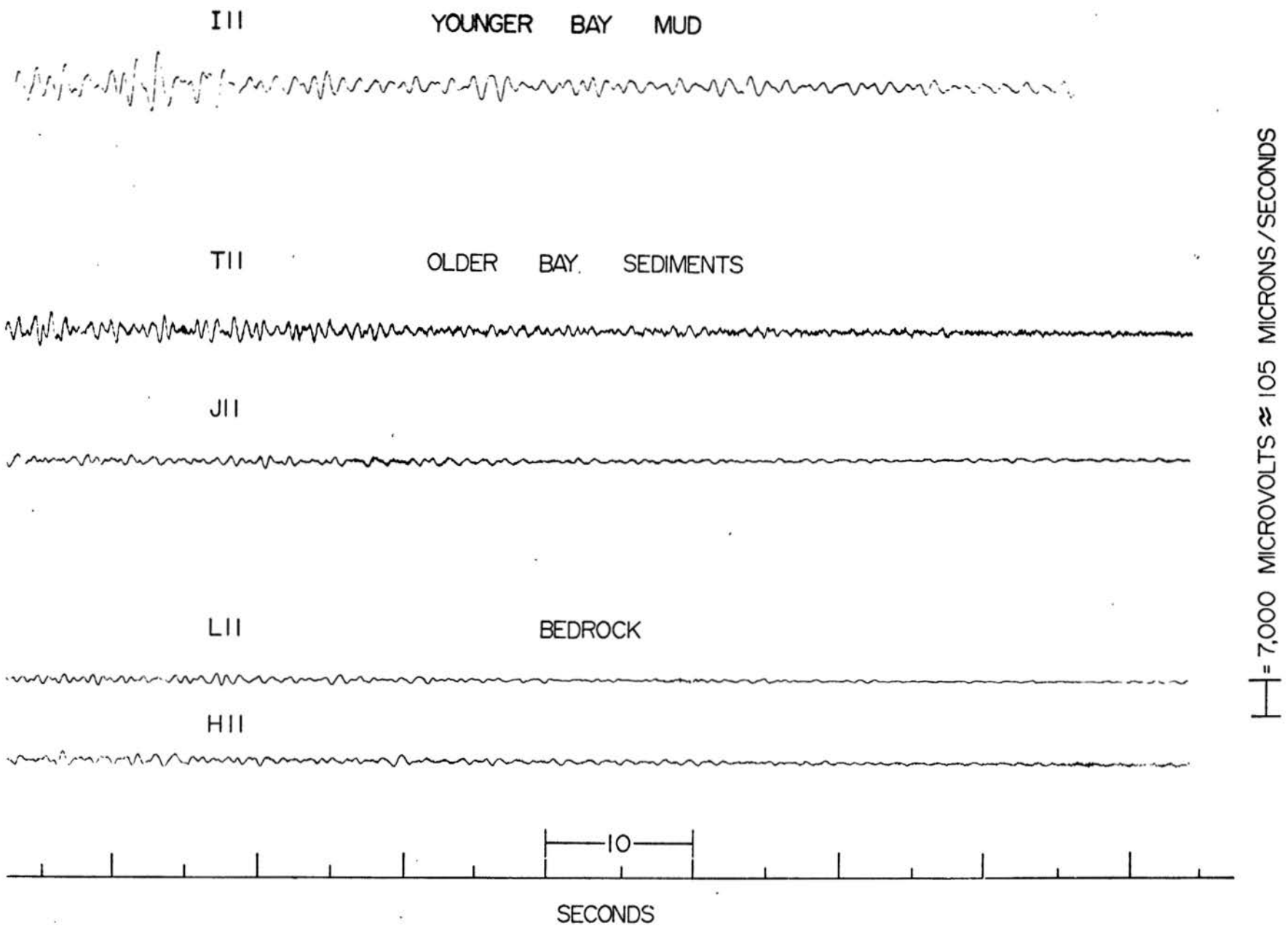
I11
YOUNGER BAY MUD
T11
OLDER BAY SEDIMENTS
J11
L11
BEDROCK
H11
10
SECONDS
= 7,000 MICROVOLTS ≈ 105 MICRONS/SECONDS

Figure 5b

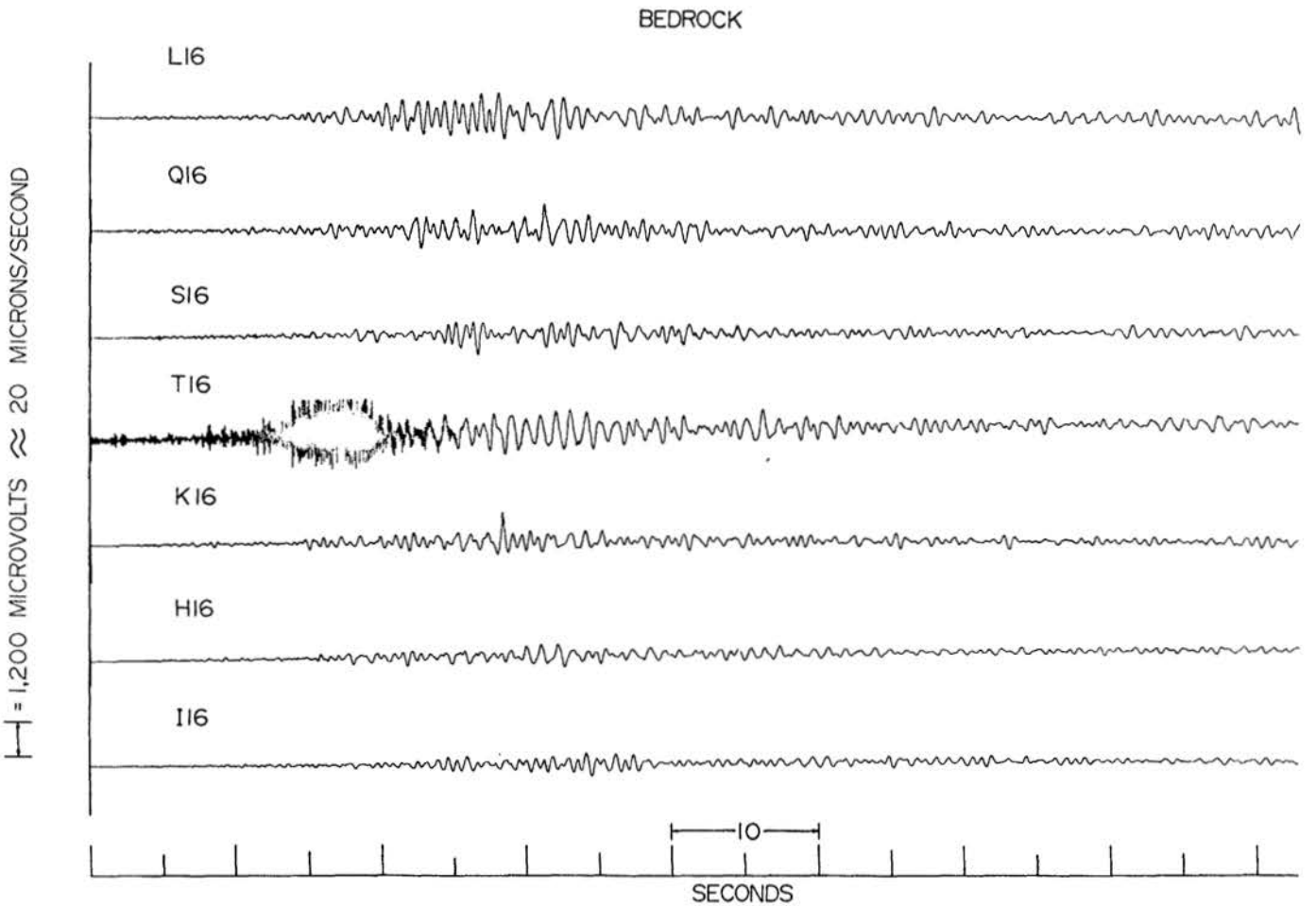
BEDROCK
L16
Q16
S16
T16
K16
H16
I16
= 1,200 MICROVOLTS ≈ 20 MICRONS/SECOND
10
SECONDS

Figure 6a

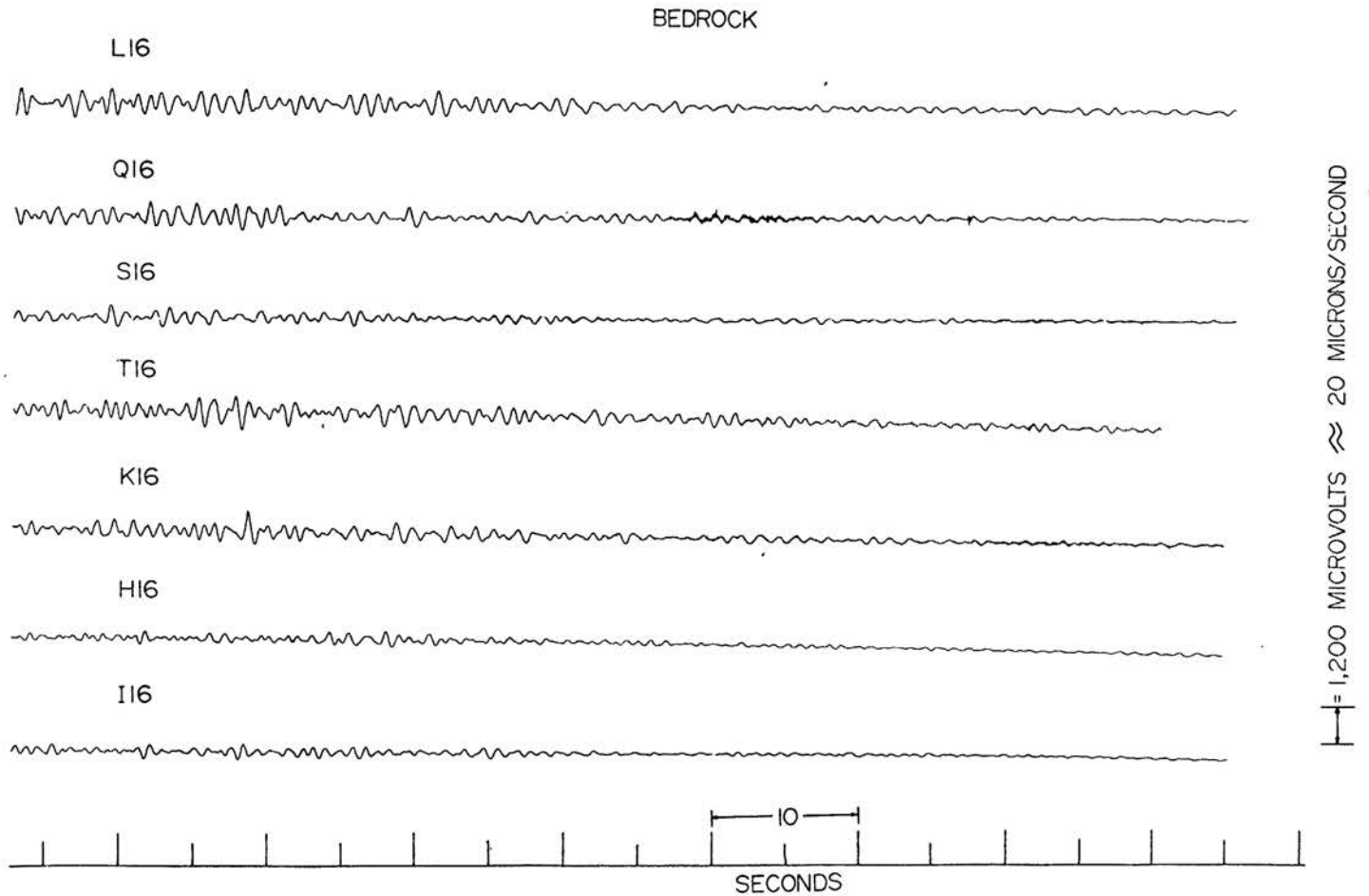
BEDROCK
L16
Q16
S16
T16
K16
H16
I16
10
SECONDS
1,200 MICROVOLTS ≈ 20 MICRONS/SECOND

Figure 6b

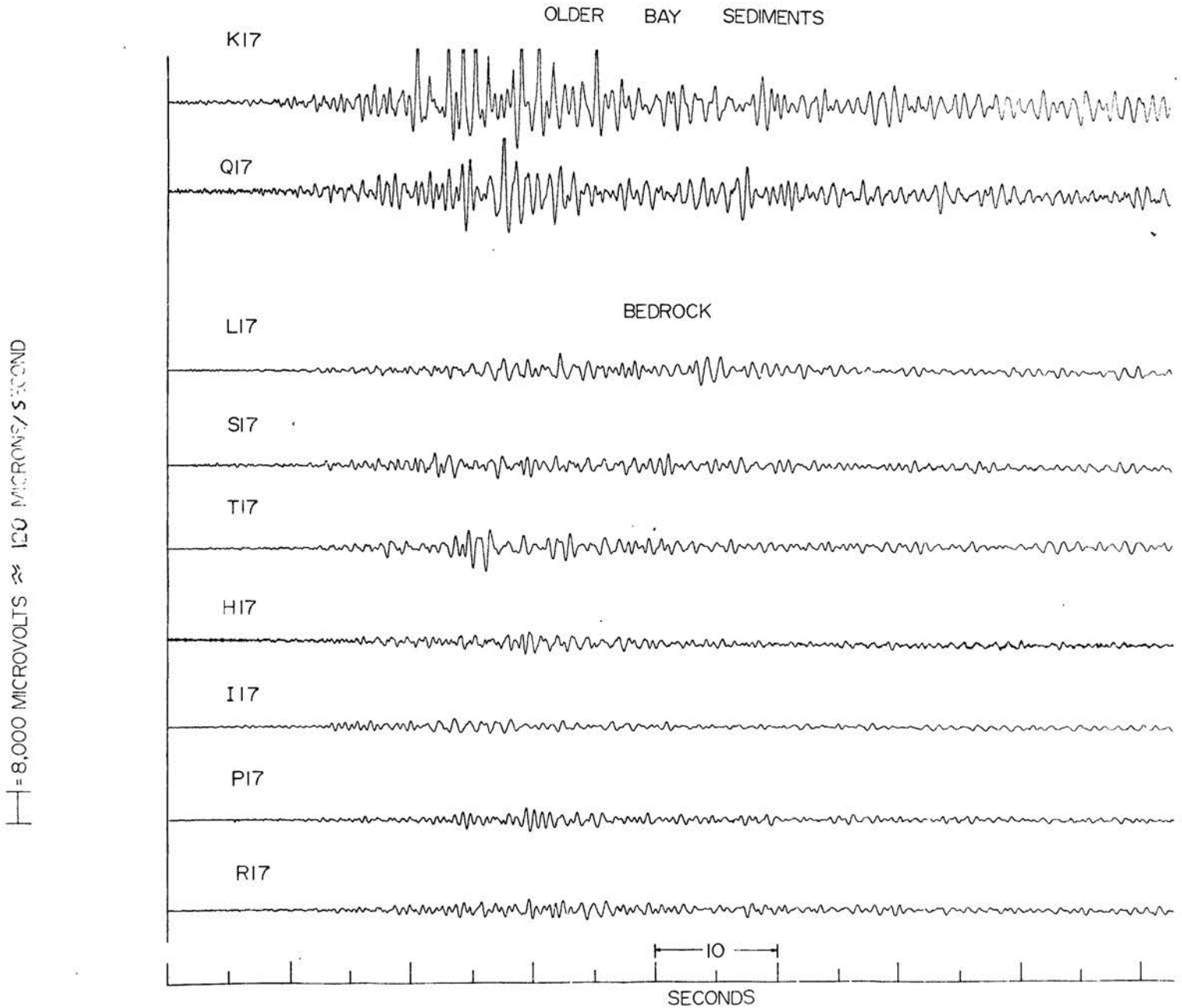
OLDER BAY SEDIMENTS
K17
Q17
BEDROCK
L17
S17
T17
H17
I17
P17
R17
10
SECONDS
= 8,000 MICROVOLTS ≈ 120 MICRONS/SECOND

Figure 7a

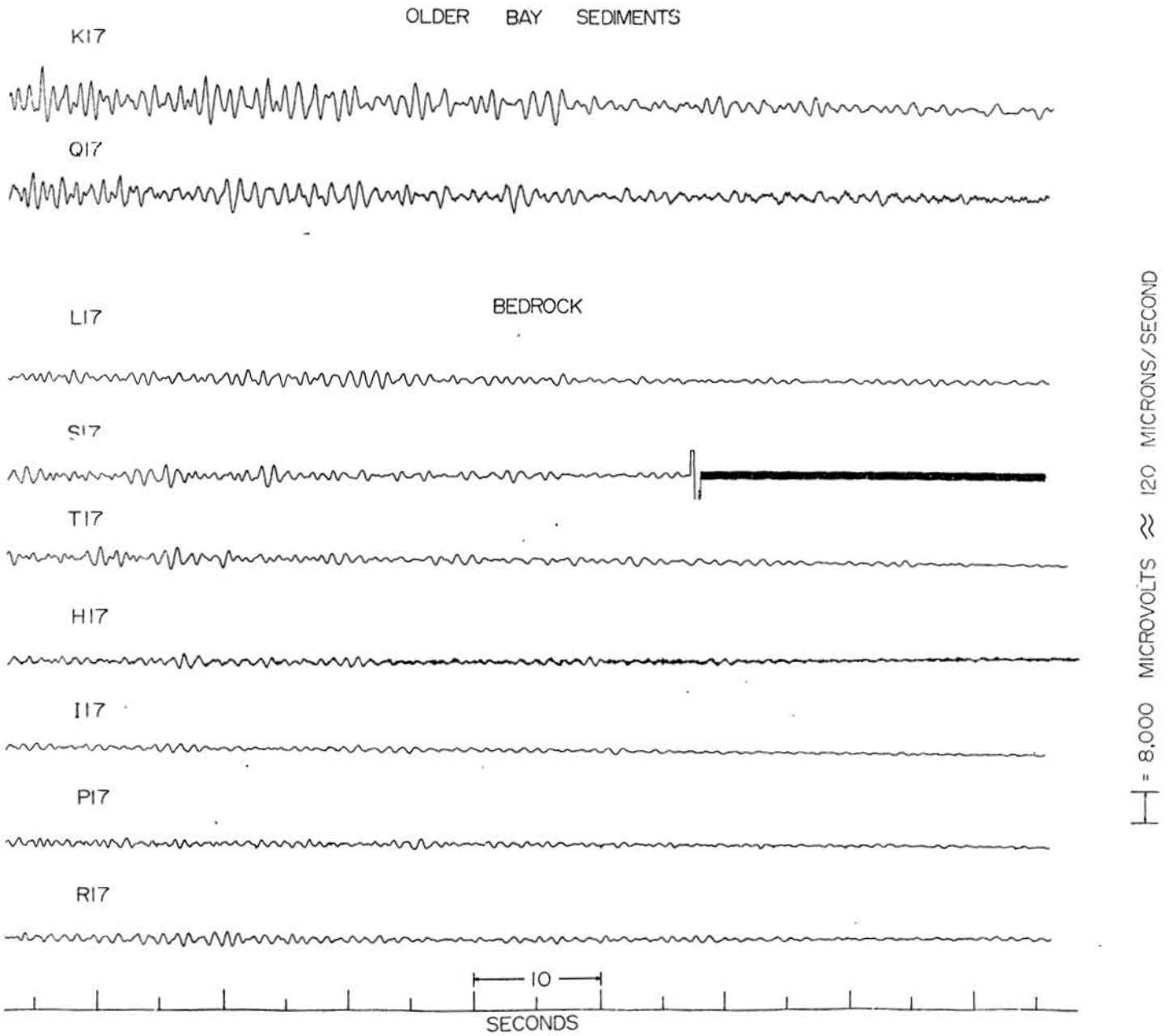
OLDER BAY SEDIMENTS
K17
Q17
BEDROCK
L17
S17
T17
H17
I17
P17
R17
10
SECONDS
= 8,000 MICROVOLTS ≈ 120 MICRONS/SECOND

Figure 7b

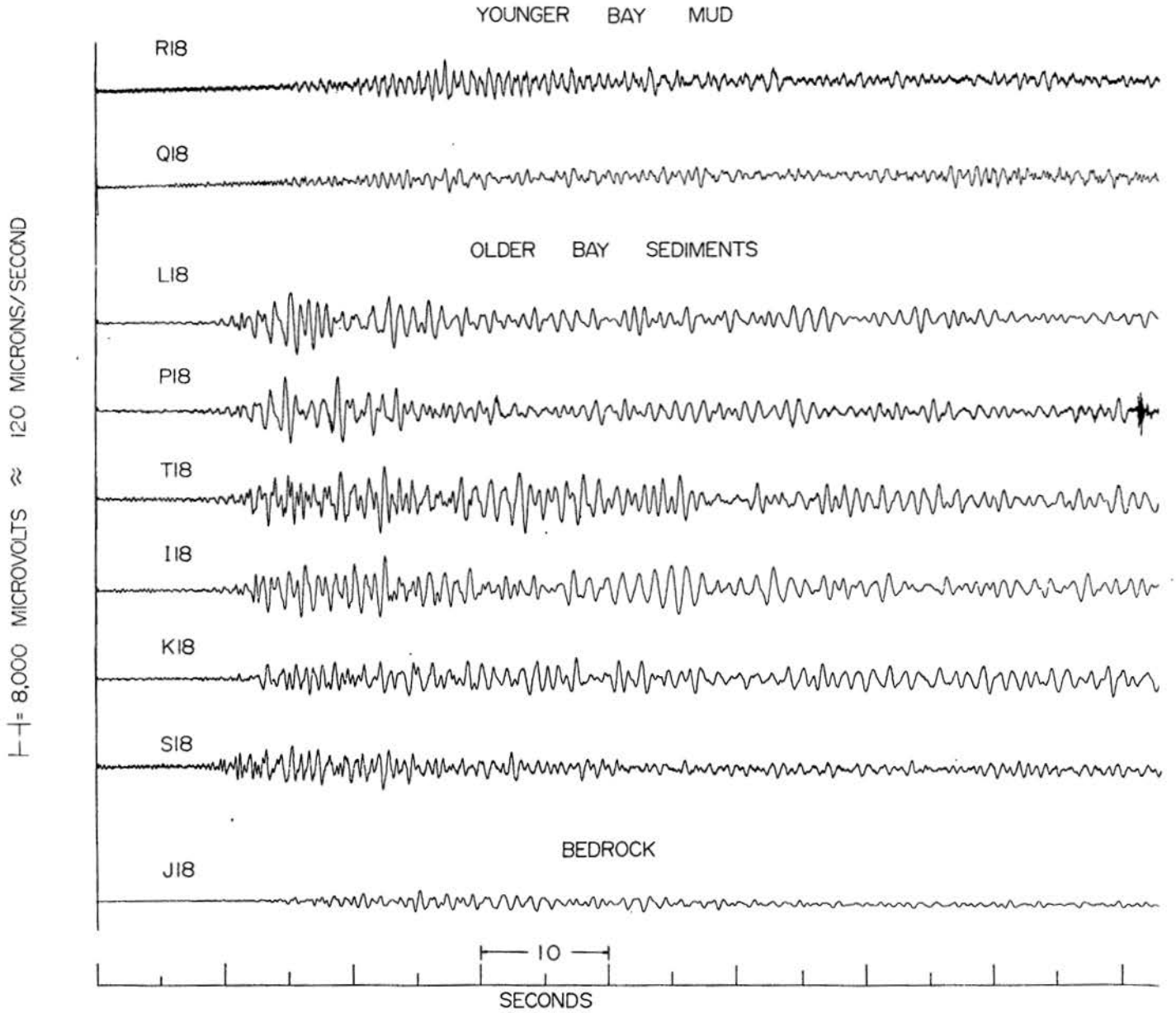
YOUNGER BAY MUD
R18
Q18
OLDER BAY SEDIMENTS
L18
P18
T18
I18
K18
S18
BEDROCK
J18
10
SECONDS
= 8,000 MICROVOLTS ≈ 120 MICRONS/SECOND

Figure 8a

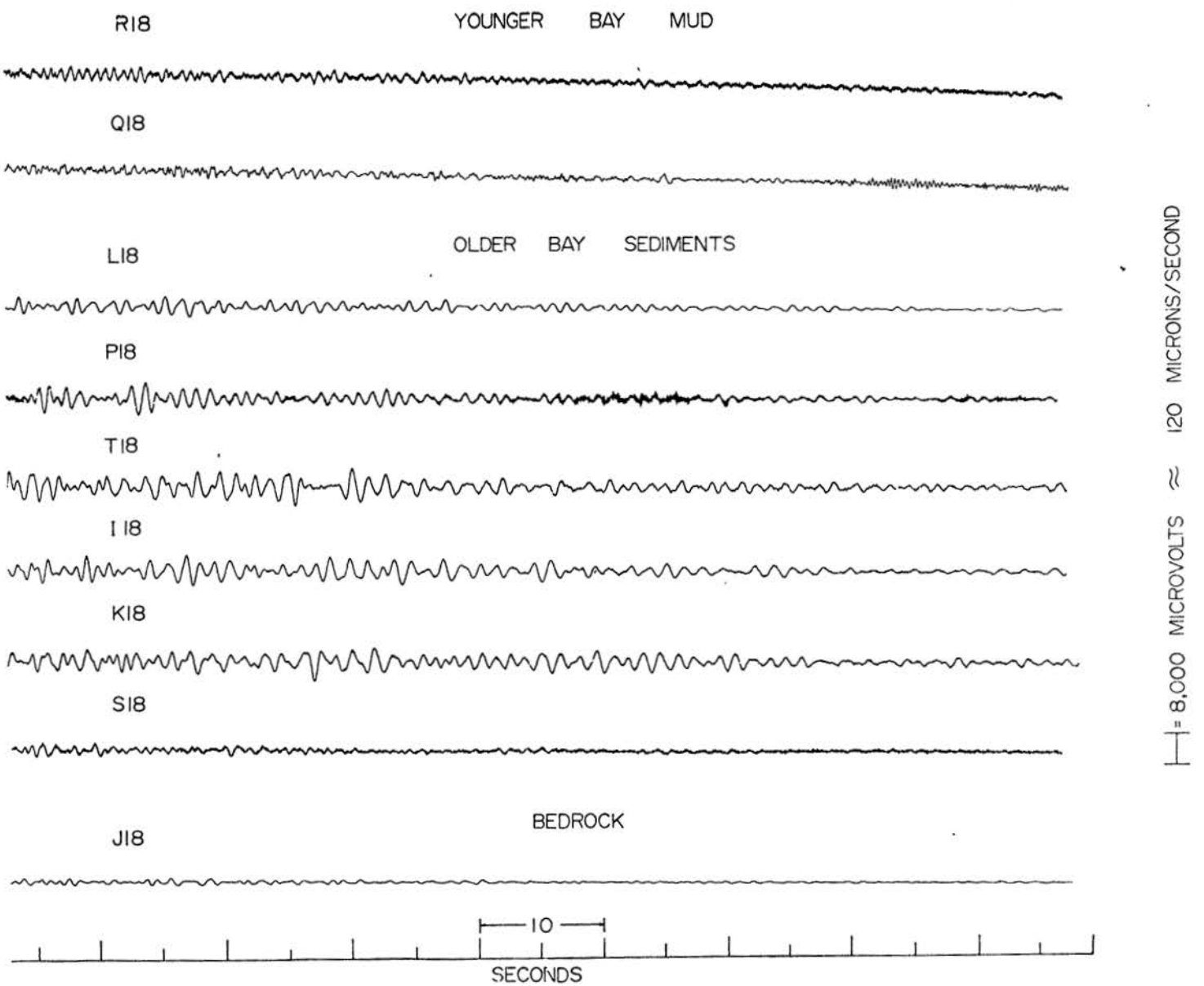
R18
YOUNGER BAY MUD
Q18
L18
OLDER BAY SEDIMENTS
P18
T18
I 18
K18
S18
J18
BEDROCK
10
SECONDS
= 8,000 MICROVOLTS ≈ 120 MICRONS/SECOND

Figure 8b

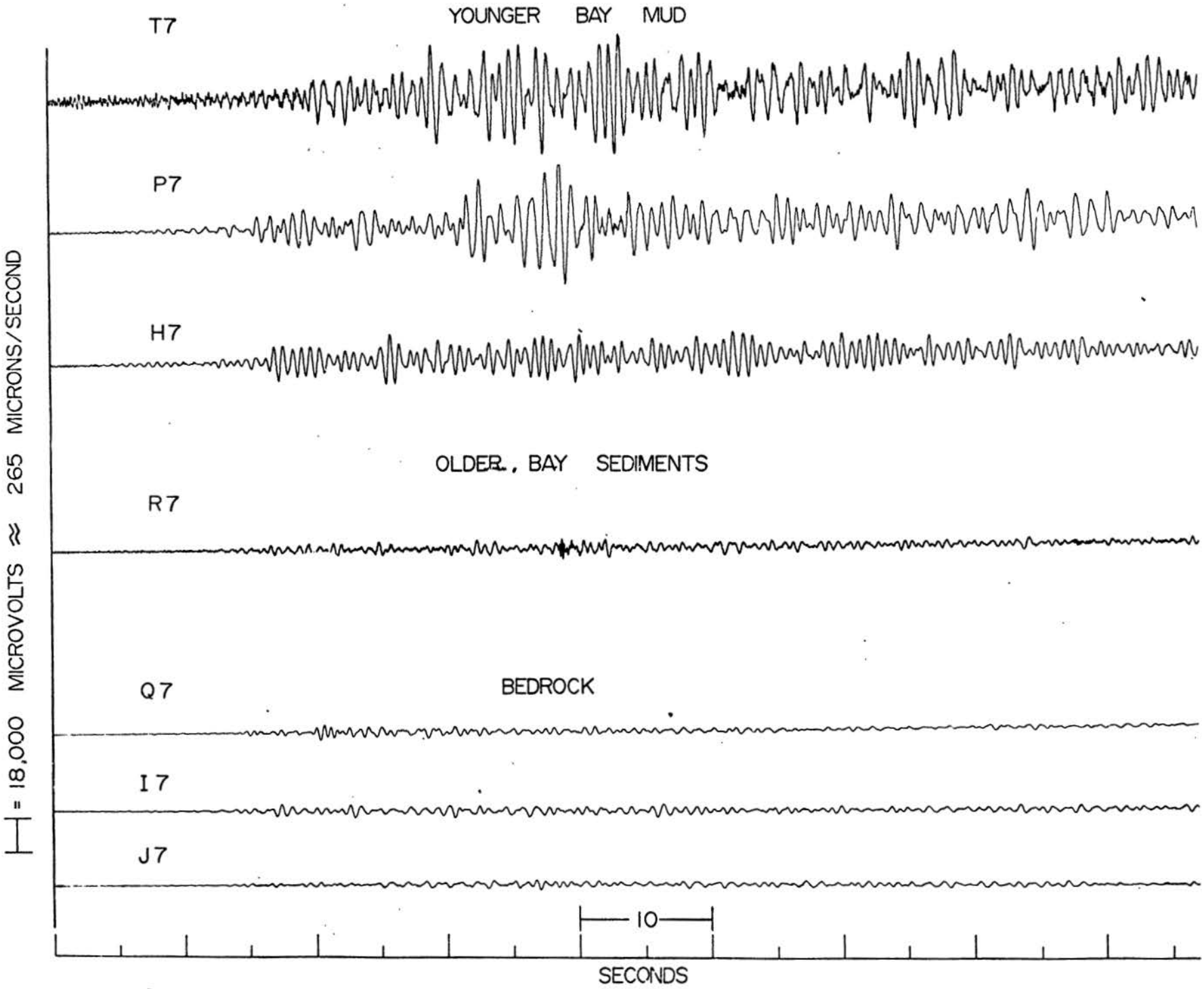
T7
YOUNGER BAY MUD
P7
H7
OLDER BAY SEDIMENTS
R7
Q7
BEDROCK
I7
J7
10
SECONDS
= 18,000 MICROVOLTS ≈ 265 MICRONS/SECOND

Figure 9a

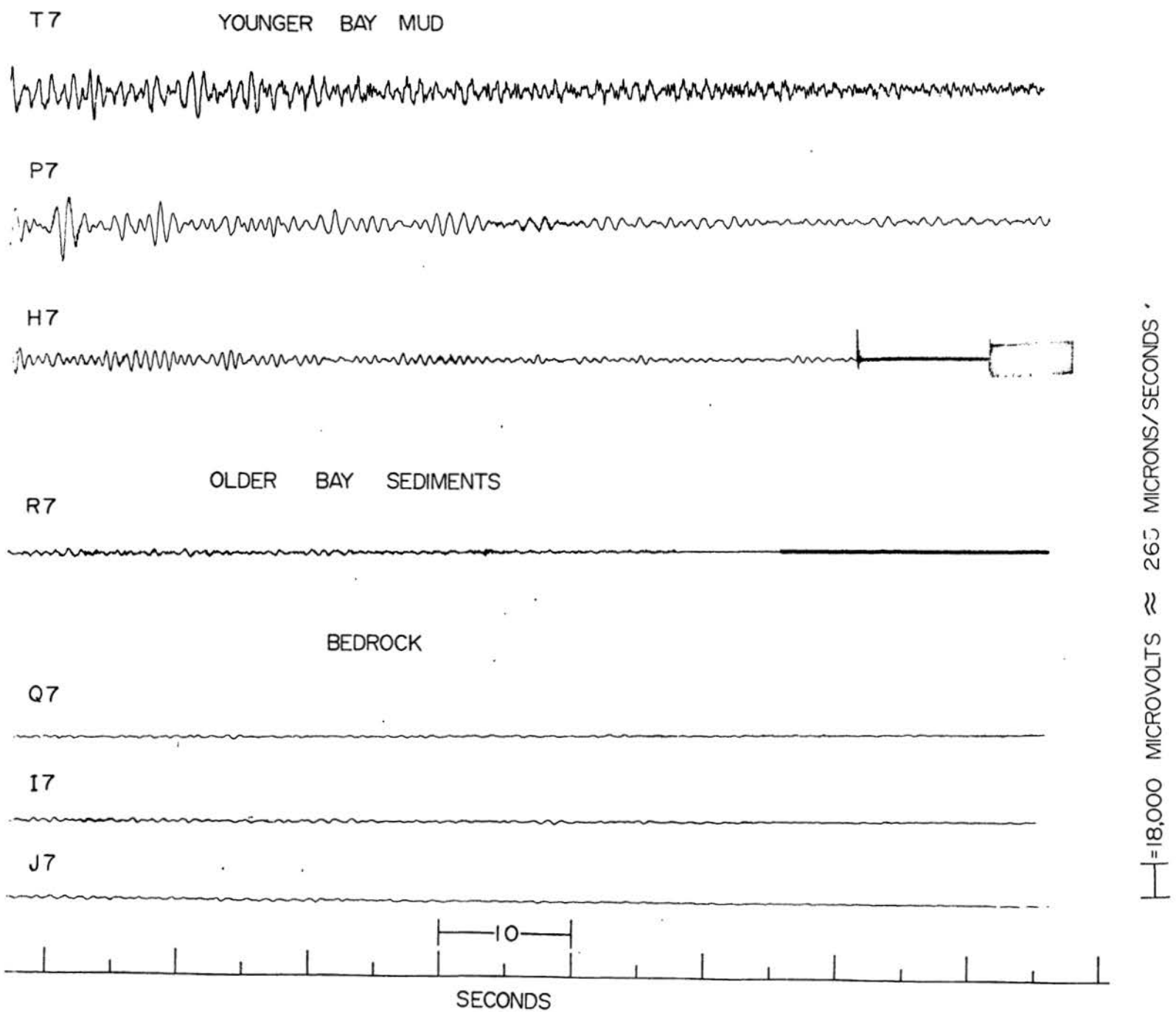
T7
YOUNGER BAY MUD
P7
H7
OLDER BAY SEDIMENTS
R7
BEDROCK
Q7
I7
J7
10
SECONDS
=18,000 MICROVOLTS ≈ 265 MICRONS/SECONDS

Figure 9b

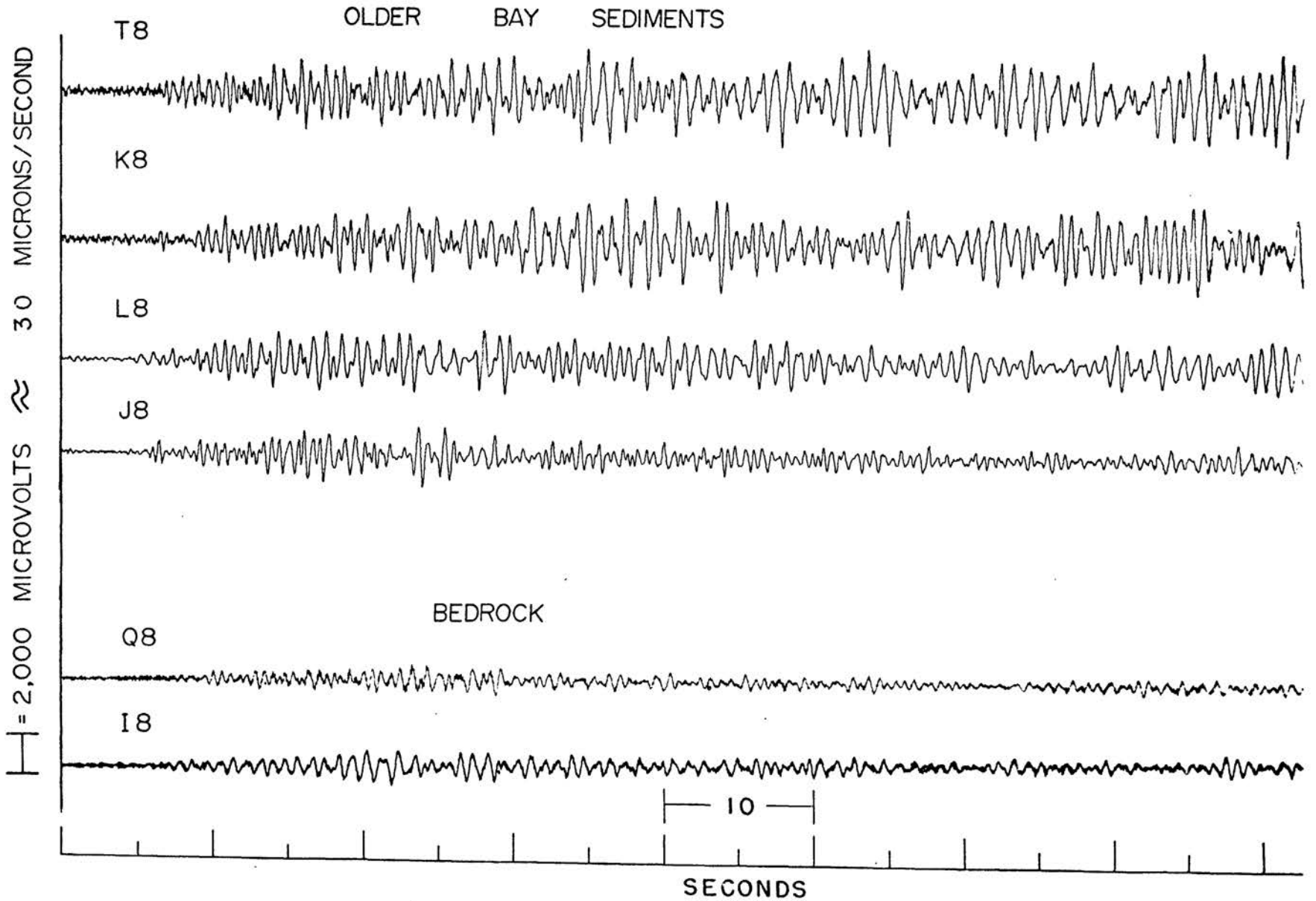
OLDER BAY SEDIMENTS
T8
K8
L8
J8
BEDROCK
Q8
I8
= 2,000 MICROVOLTS ≈ 30 MICRONS/SECOND
10
SECONDS

Figure 10a

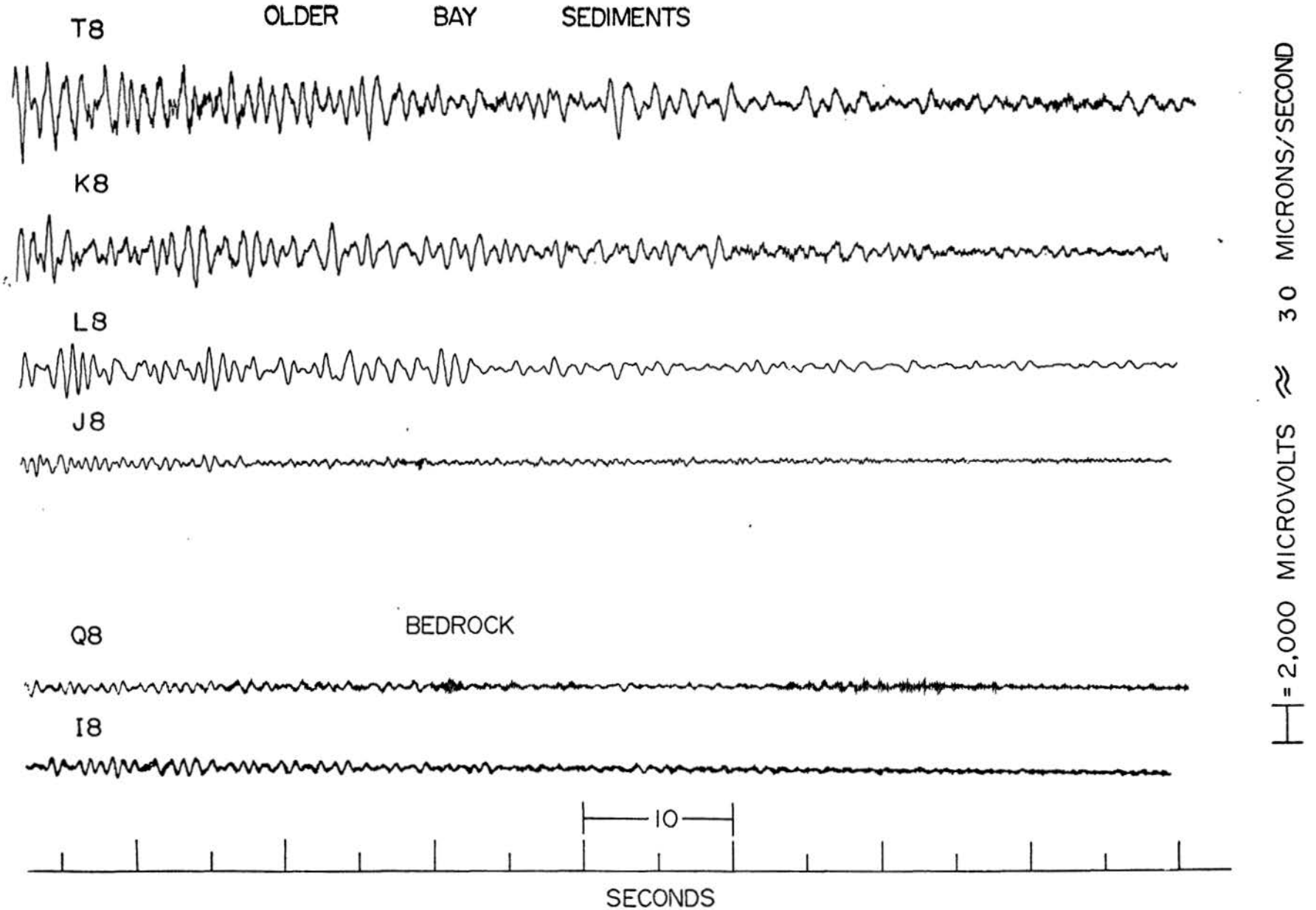
T8
OLDER BAY SEDIMENTS
K8
L8
J8
Q8
BEDROCK
I8
10
SECONDS
= 2,000 MICROVOLTS ≈ 30 MICRONS/SECOND

Figure 10b

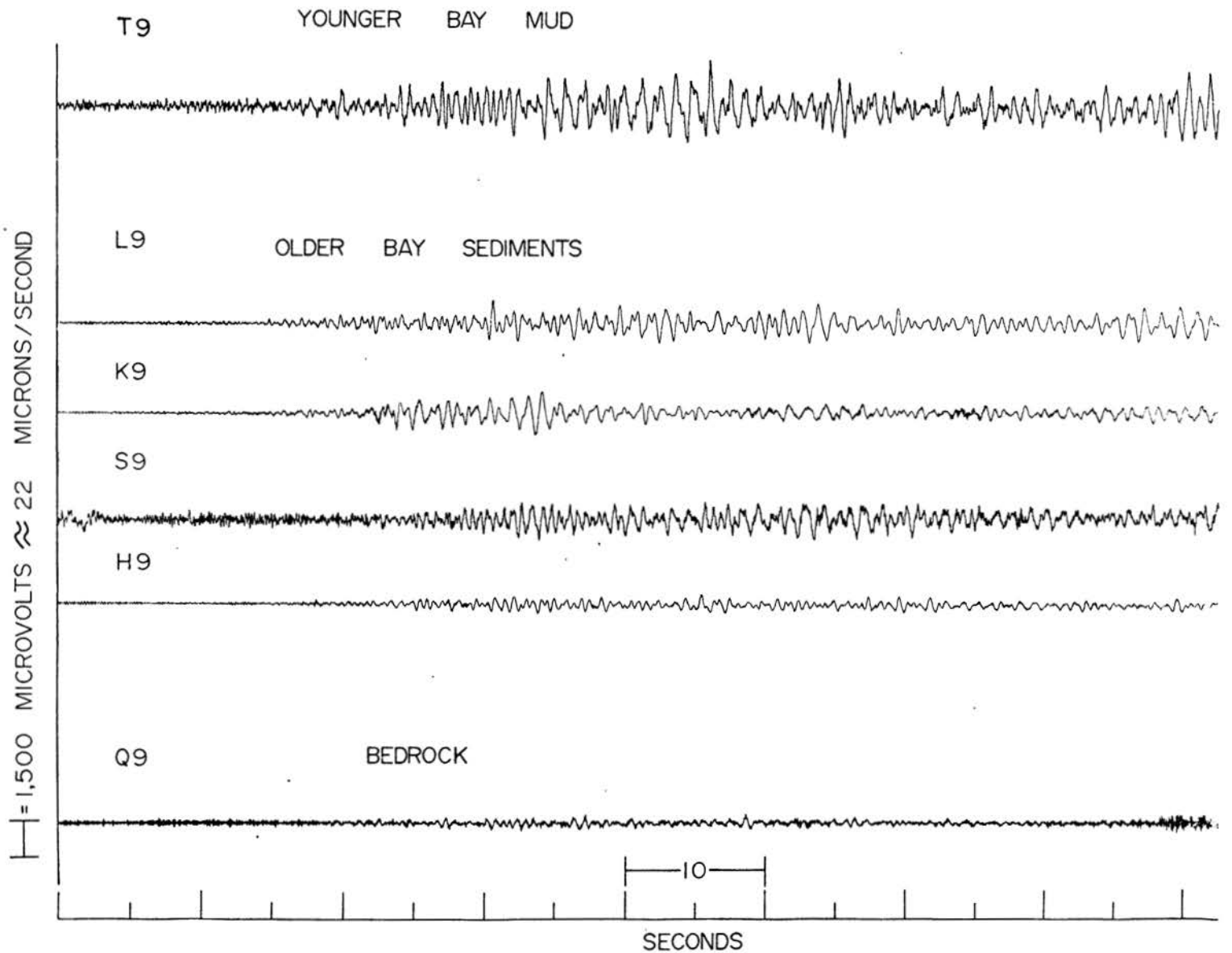
T9
YOUNGER BAY MUD
L9
OLDER BAY SEDIMENTS
K9
S9
H9
Q9
BEDROCK
= 1,500 MICROVOLTS ≈ 22 MICRONS/SECOND
10
SECONDS

Figure 11a

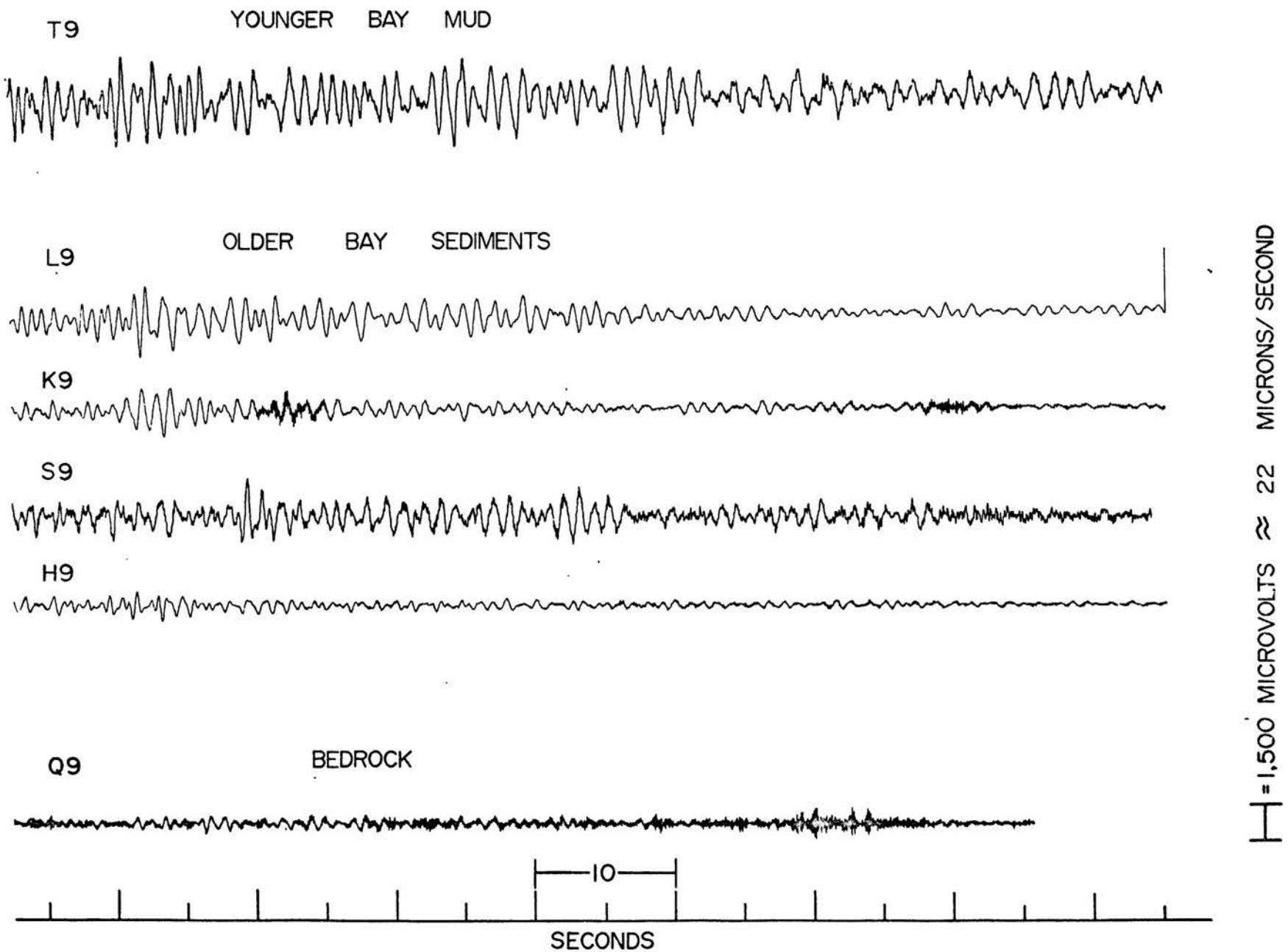
T9
YOUNGER BAY MUD
L9
OLDER BAY SEDIMENTS
K9
S9
H9
Q9
BEDROCK
10
SECONDS
1,500 MICROVOLTS ≈ 22 MICRONS/ SECOND

Figure 11b

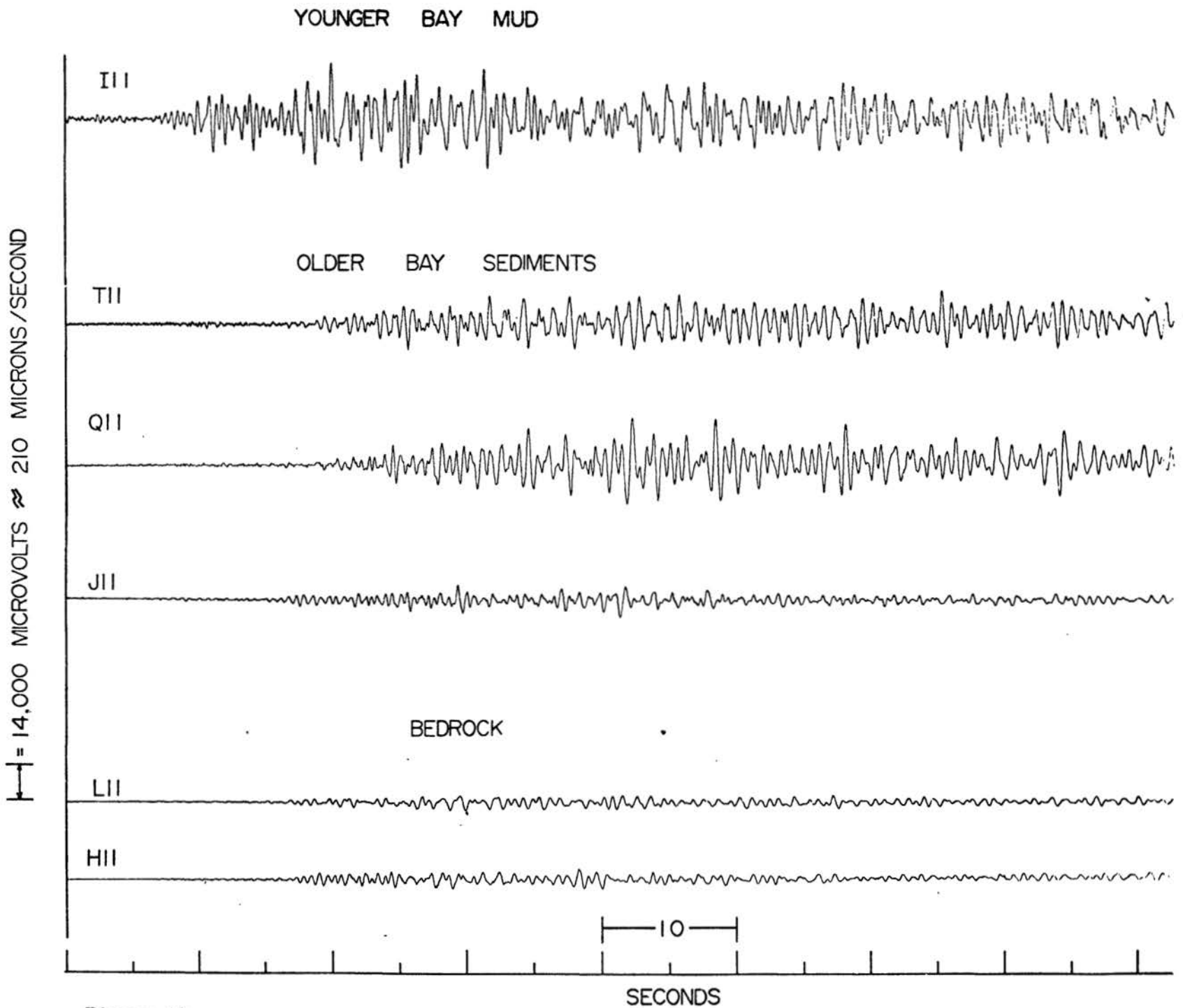
YOUNGER BAY MUD
I11
OLDER BAY SEDIMENTS
T11
Q11
J11
BEDROCK
L11
H11
= 14,000 MICROVOLTS ≈ 210 MICRONS/SECOND
10
SECONDS

Figure 12a

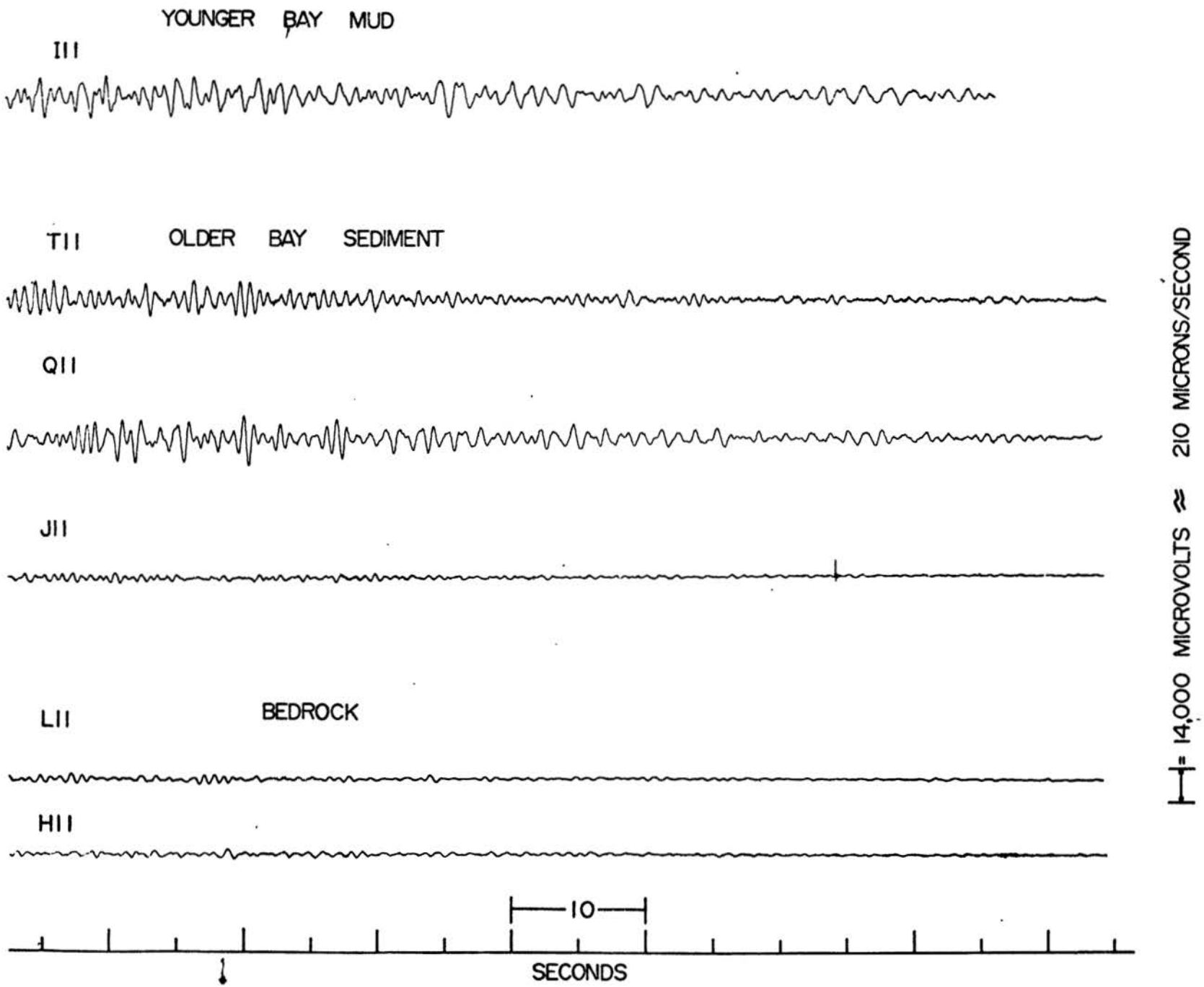
YOUNGER BAY MUD
III
TII
OLDER BAY SEDIMENT
QII
JII
LII
BEDROCK
HII
10
SECONDS
= 14,000 MICROVOLTS ≈ 210 MICRONS/SECOND

Figure 12b

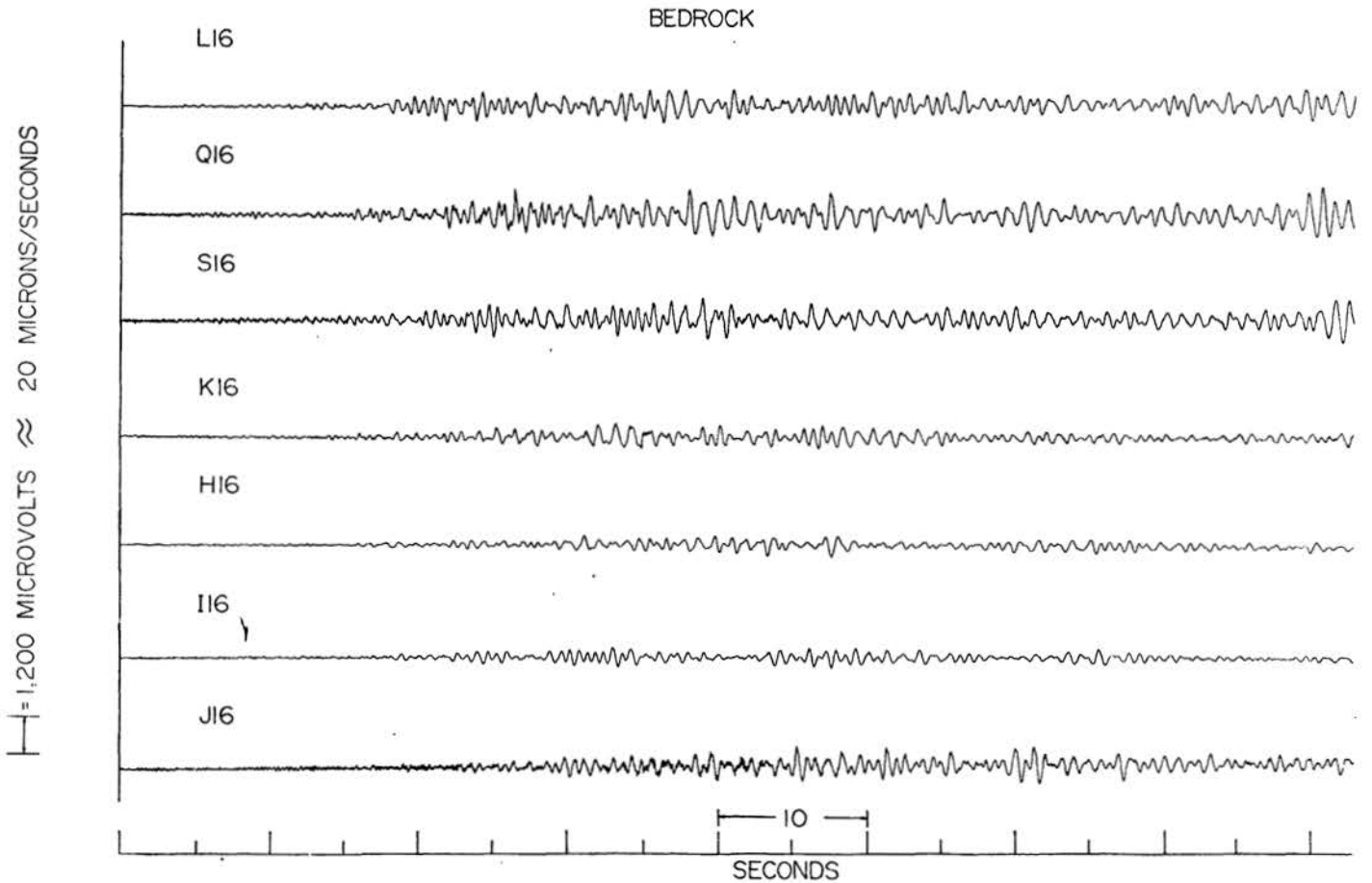
BEDROCK
L16
Q16
S16
K16
H16
I16
J16
= 1,200 MICROVOLTS ≈ 20 MICRONS/SECONDS
10
SECONDS

Figure 13a

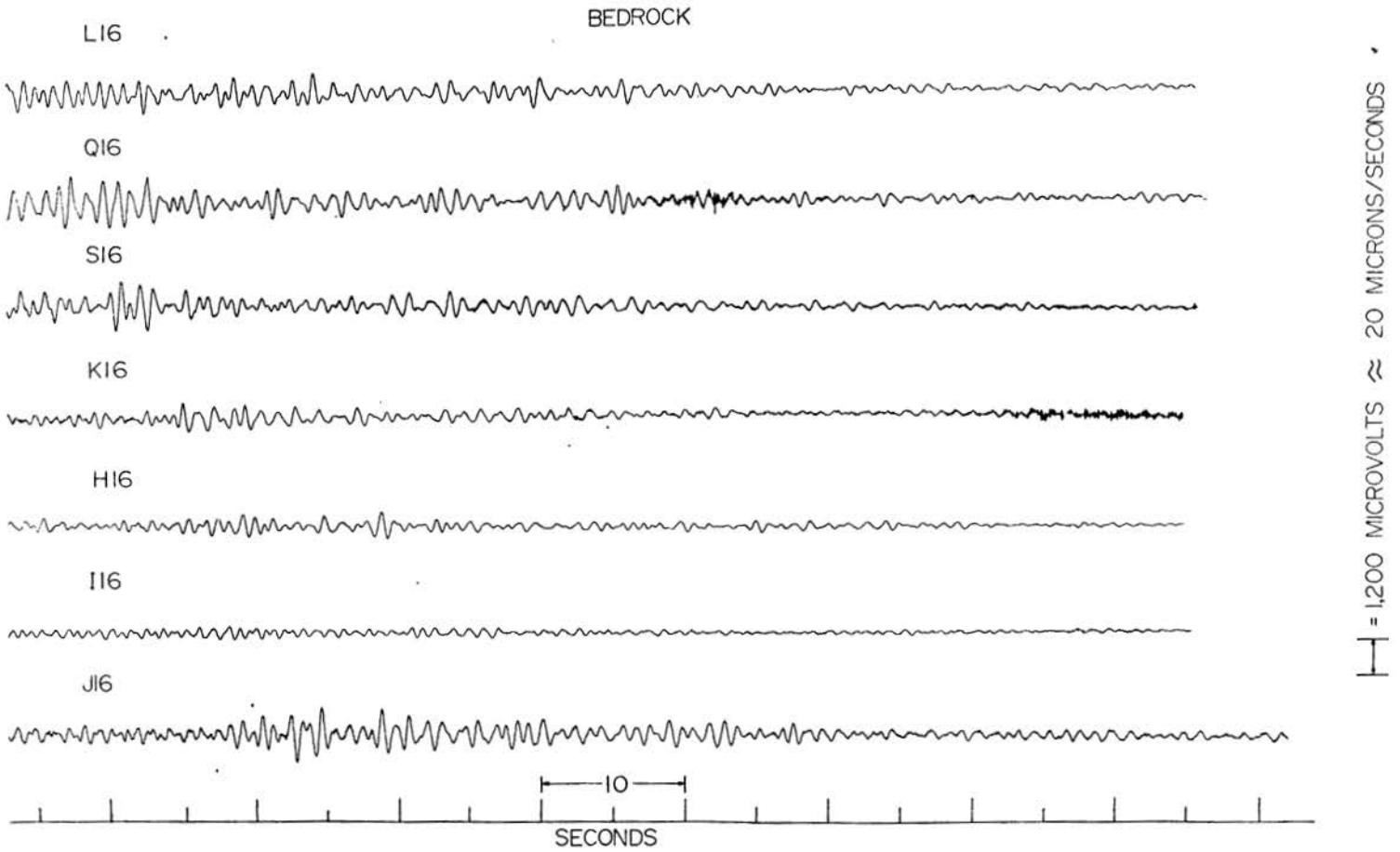
BEDROCK
L16
Q16
S16
K16
H16
I16
J16
10
SECONDS
= 1,200 MICROVOLTS ≈ 20 MICRONS/SECONDS

Figure 13b

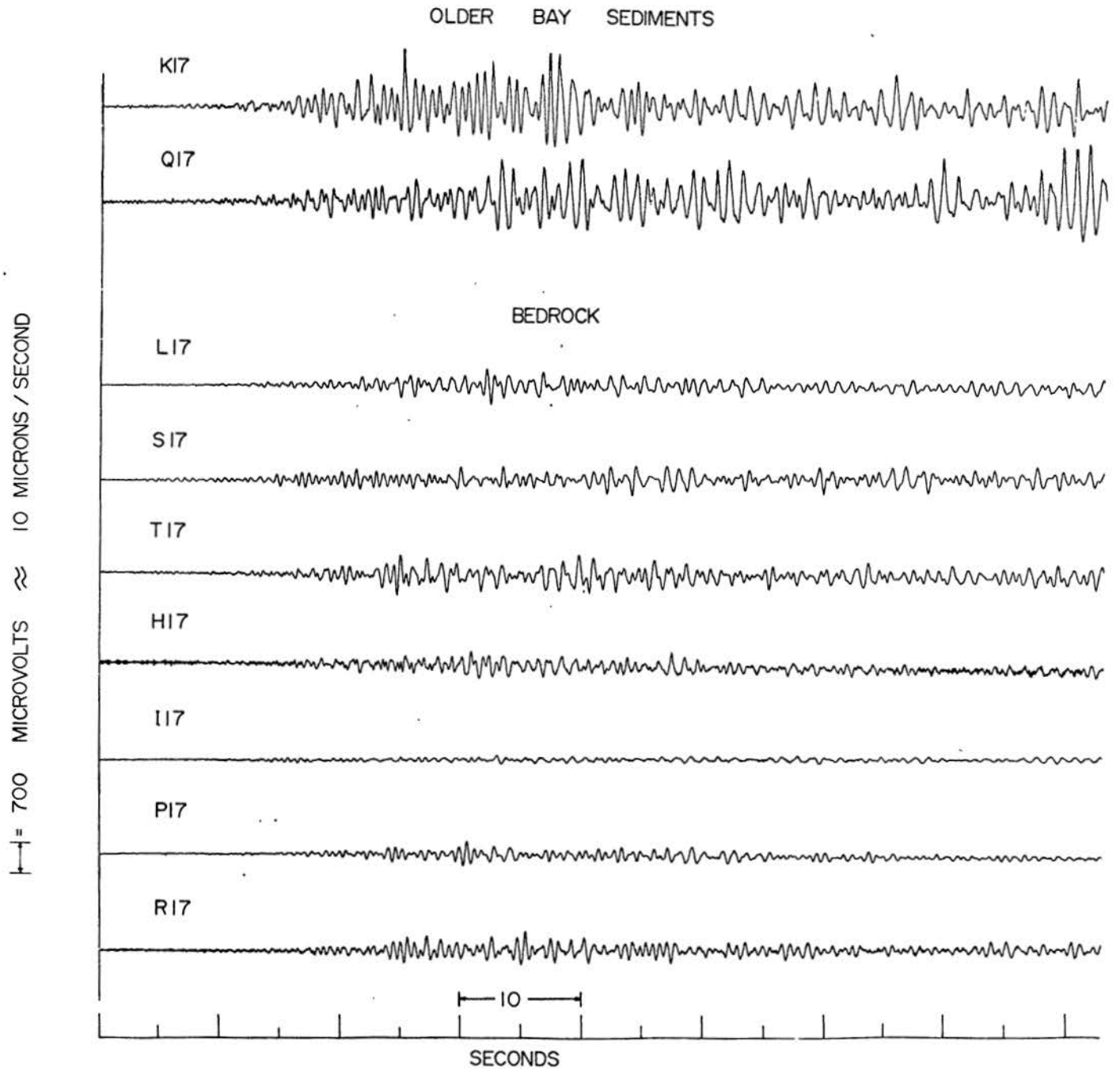
OLDER BAY SEDIMENTS
K17
Q17
BEDROCK
L17
S17
T17
H17
I17
P17
R17
10
SECONDS
= 700 MICROVOLTS ≈ 10 MICRONS / SECOND

Figure 14a

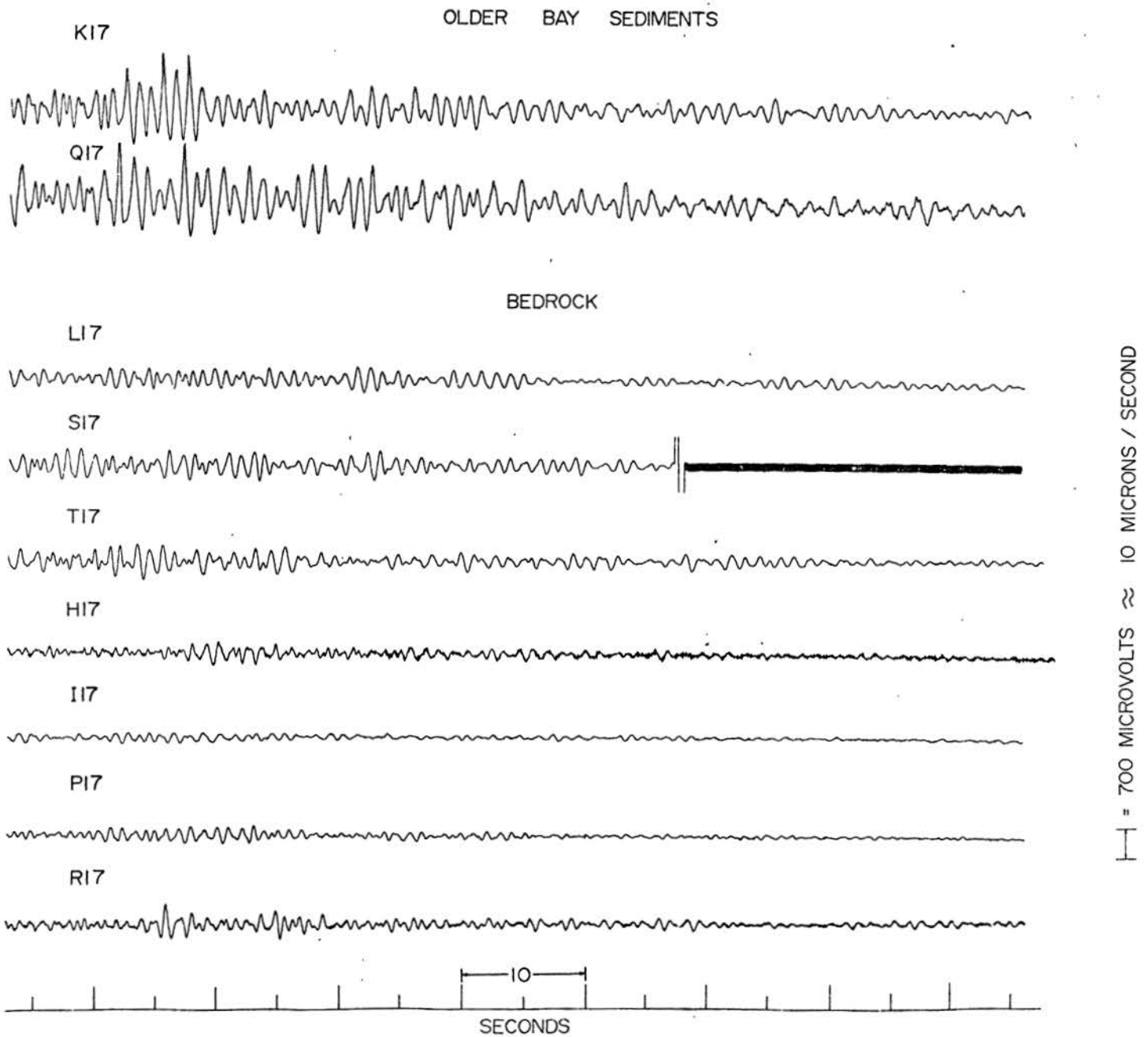
OLDER BAY SEDIMENTS
K17
Q17
BEDROCK
L17
S17
T17
H17
I17
P17
R17
10
SECONDS
= 700 MICROVOLTS ≈ 10 MICRONS / SECOND

Figure 14b

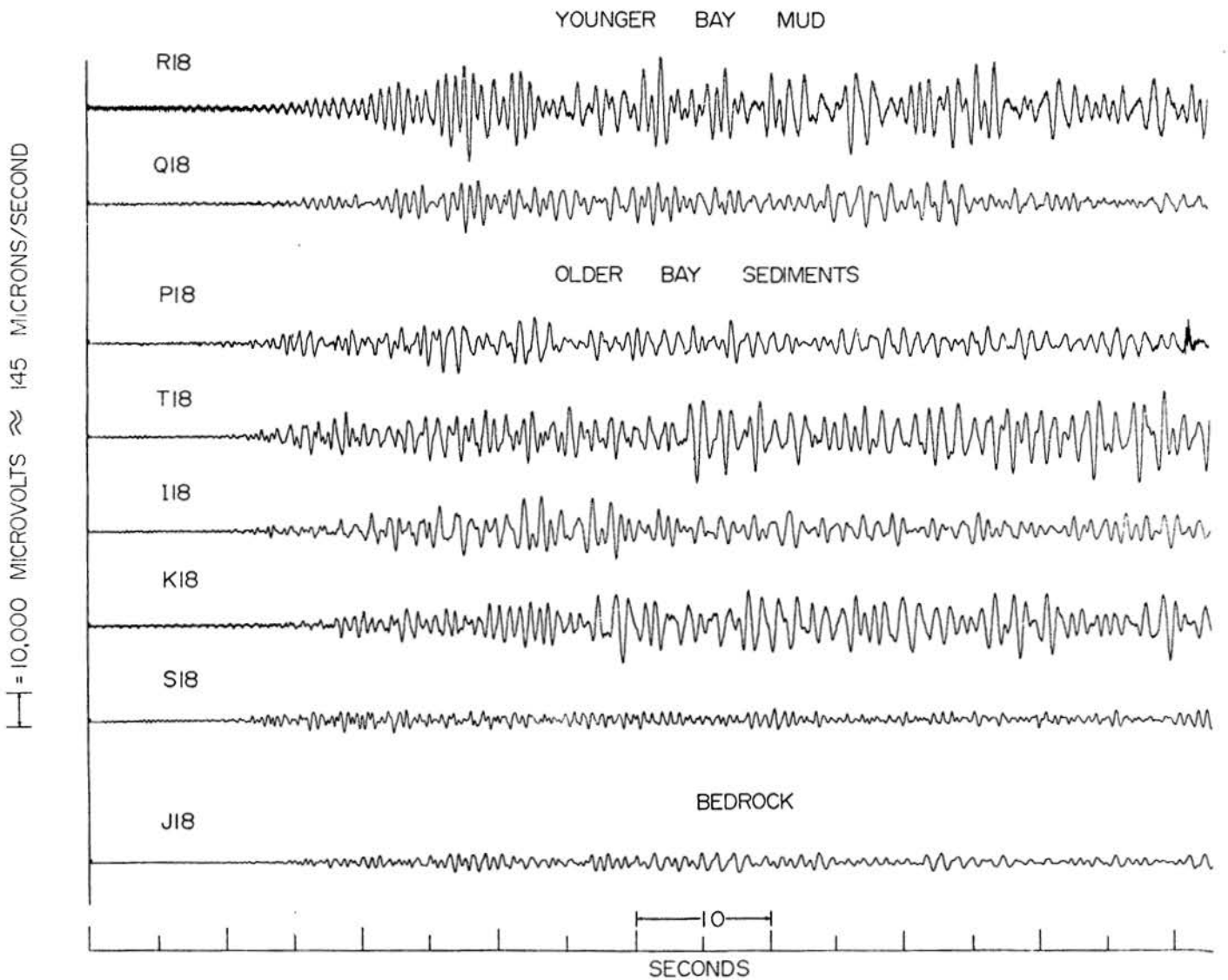
YOUNGER BAY MUD
R18
Q18
OLDER BAY SEDIMENTS
P18
T18
I18
K18
S18
BEDROCK
J18
= 10,000 MICROVOLTS ≈ 145 MICRONS/SECOND
10
SECONDS

Figure 15a

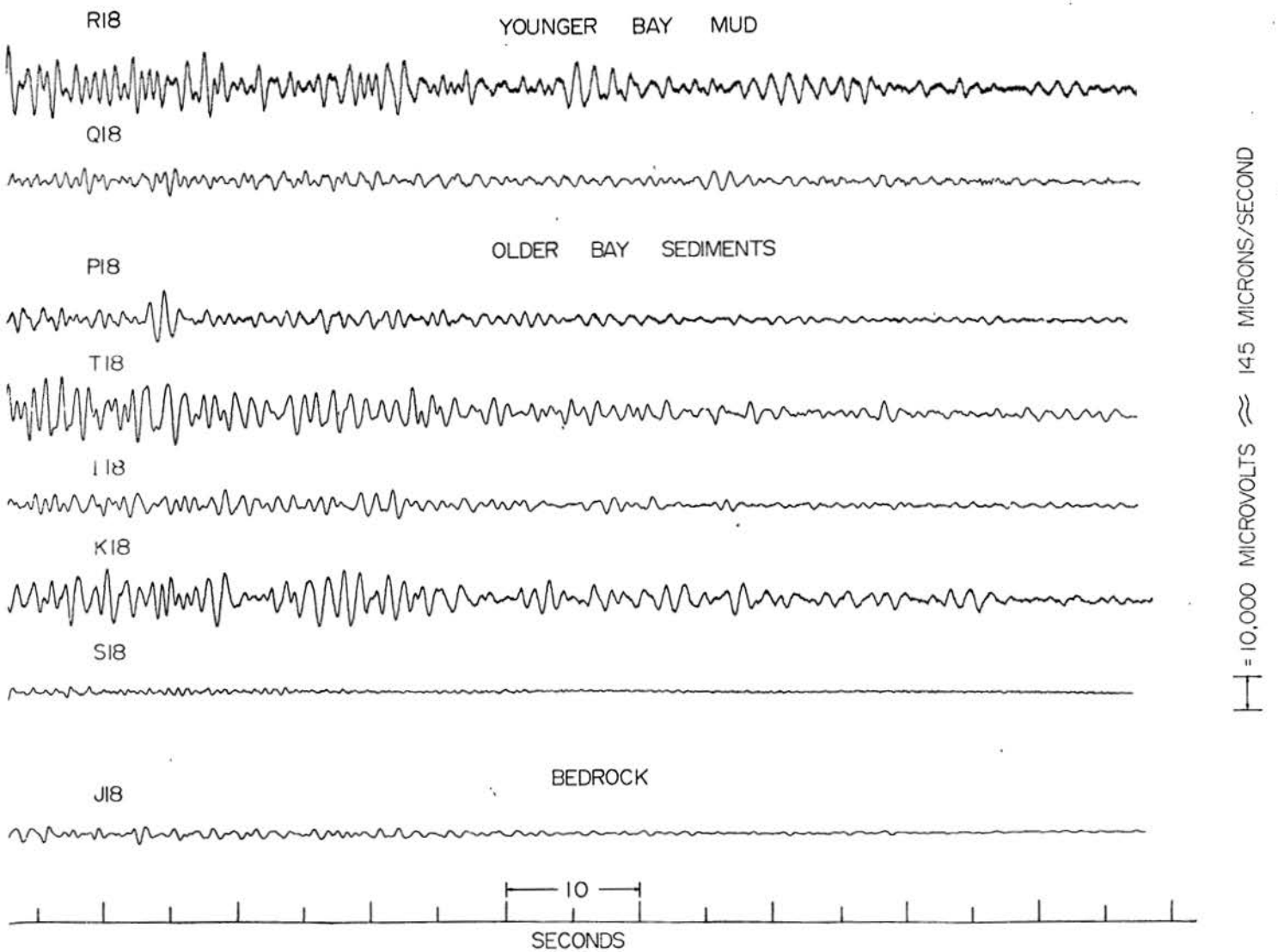
R18
YOUNGER BAY MUD
Q18
OLDER BAY SEDIMENTS
P18
T18
I18
K18
S18
BEDROCK
J18
10
SECONDS
= 10,000 MICROVOLTS ≈ 145 MICRONS/SECOND

Figure 15b

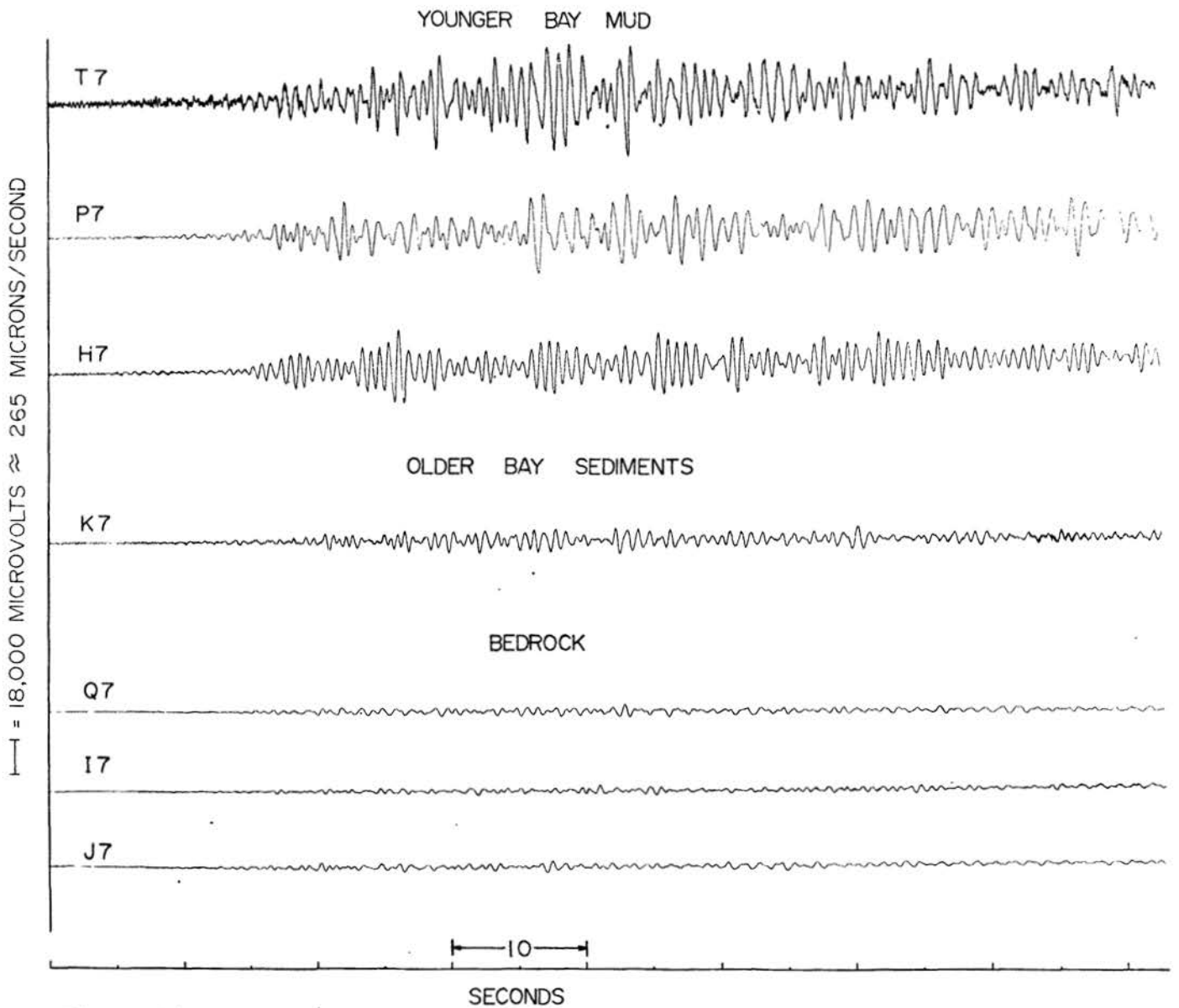
YOUNGER BAY MUD
T7
P7
H7
OLDER BAY SEDIMENTS
K7
BEDROCK
Q7
I7
J7
I = 18,000 MICROVOLTS ≈ 265 MICRONS/SECOND
10
SECONDS

Figure 16a

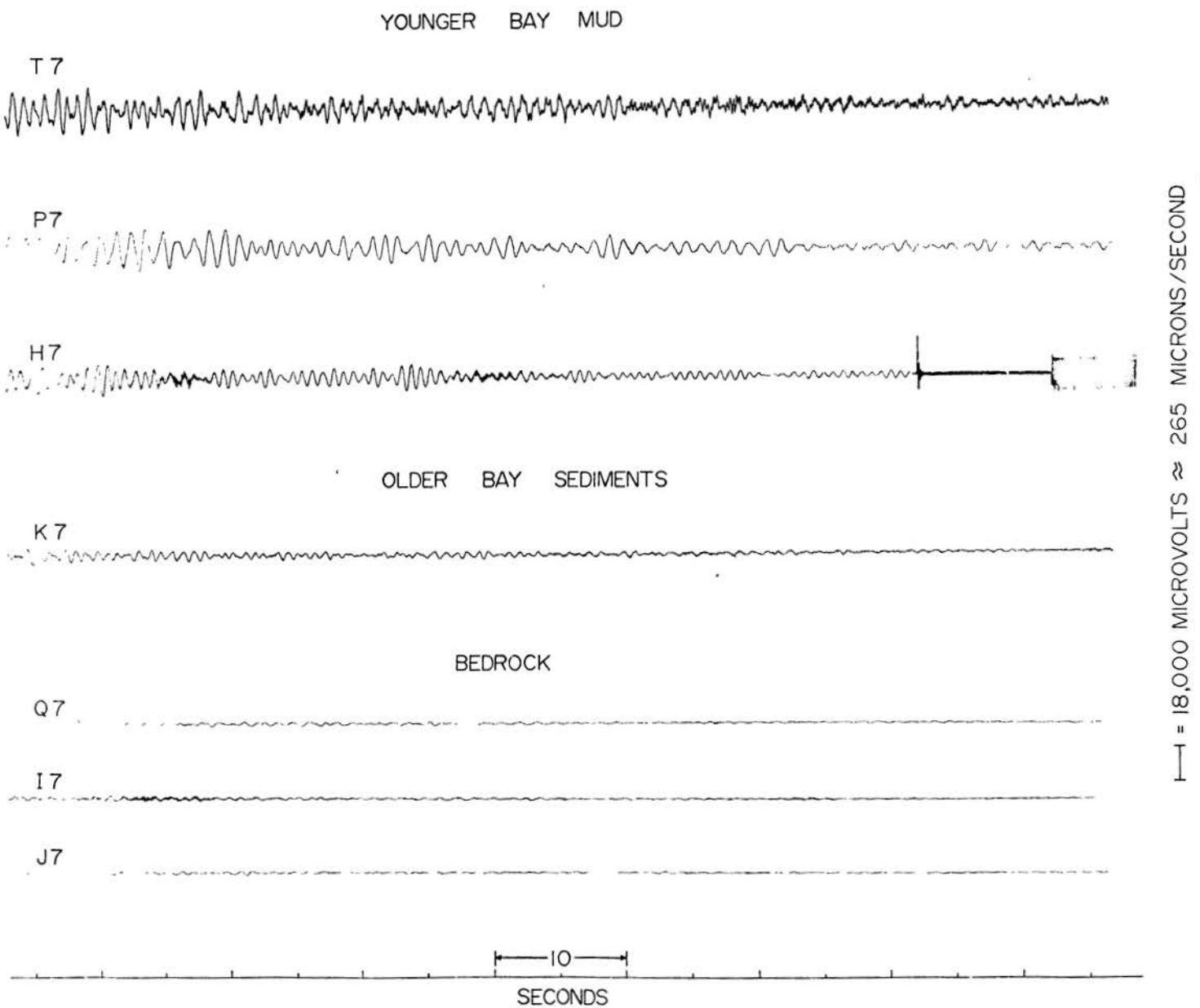
YOUNGER BAY MUD
T7
P7
H7
OLDER BAY SEDIMENTS
K7
BEDROCK
Q7
I7
J7
10
SECONDS
= 18,000 MICROVOLTS ≈ 265 MICRONS/SECOND

Figure 16b

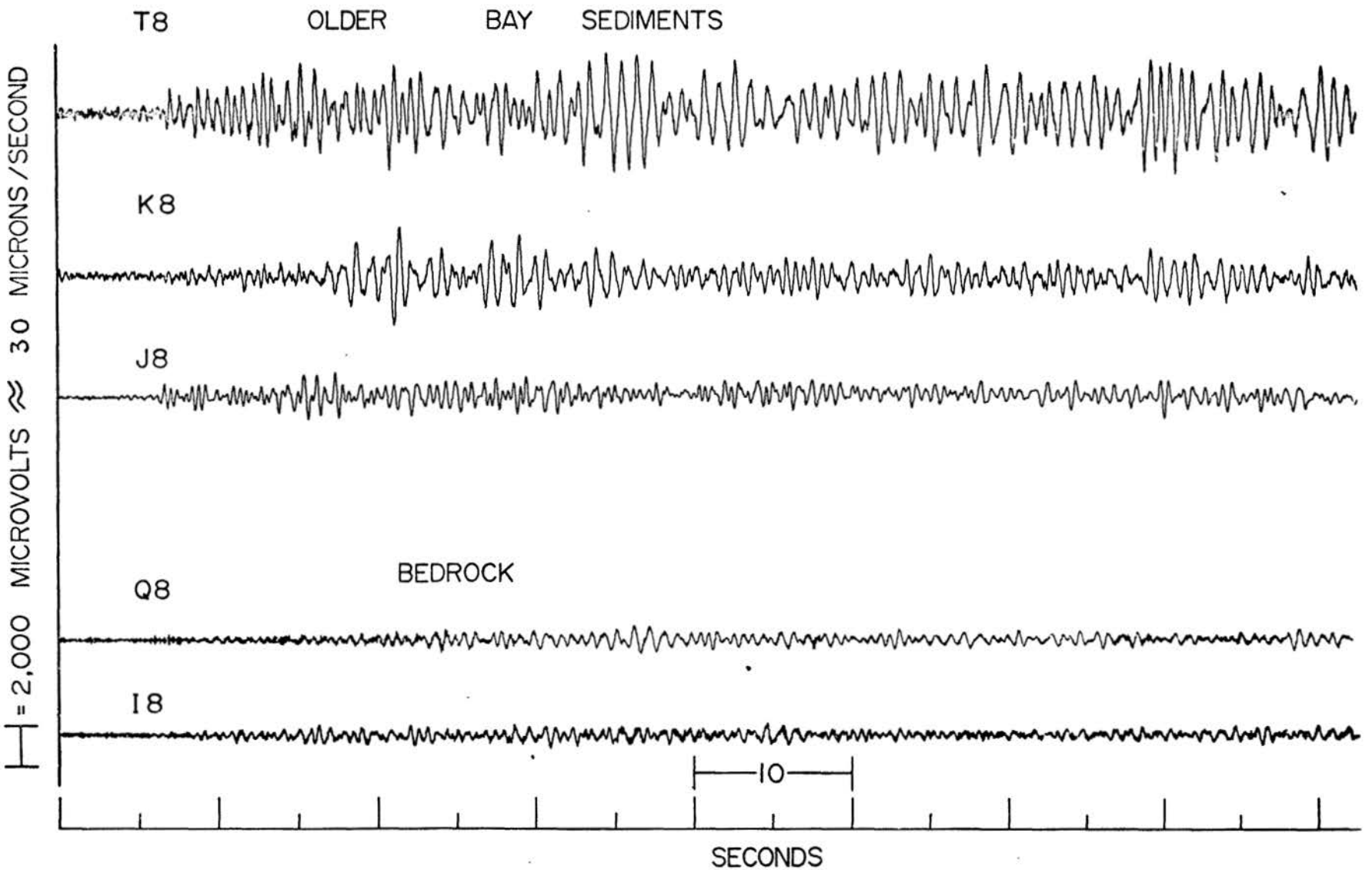
T8
OLDER
BAY
SEDIMENTS
K8
J8
Q8
BEDROCK
I8
= 2,000 MICROVOLTS ≈ 30 MICRONS/SECOND
10
SECONDS

Figure 17a

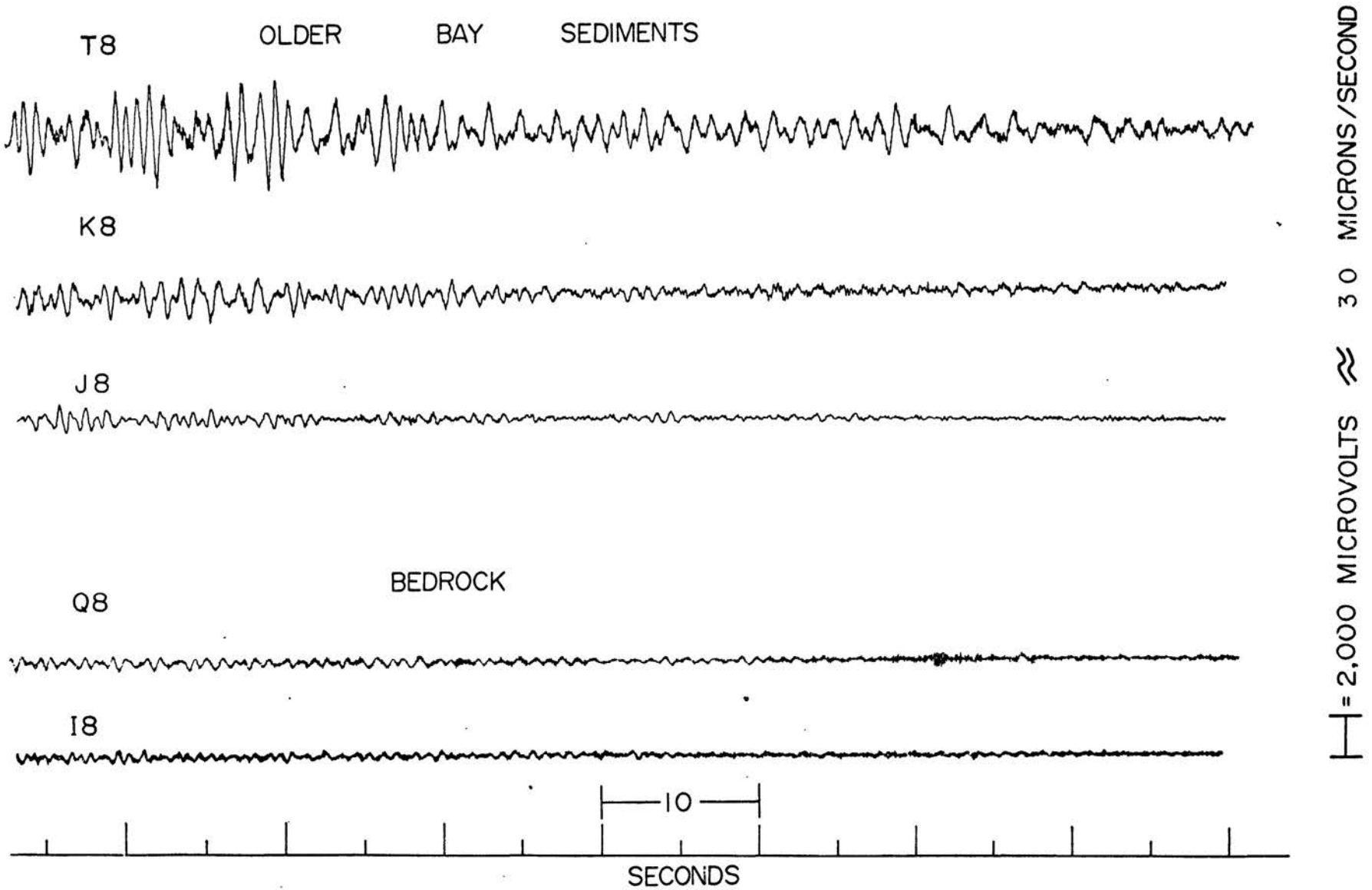
T8
OLDER BAY SEDIMENTS
K8
J8
BEDROCK
Q8
I8
10
SECONDS
= 2,000 MICROVOLTS ≈ 30 MICRONS/SECOND

Figure 17b

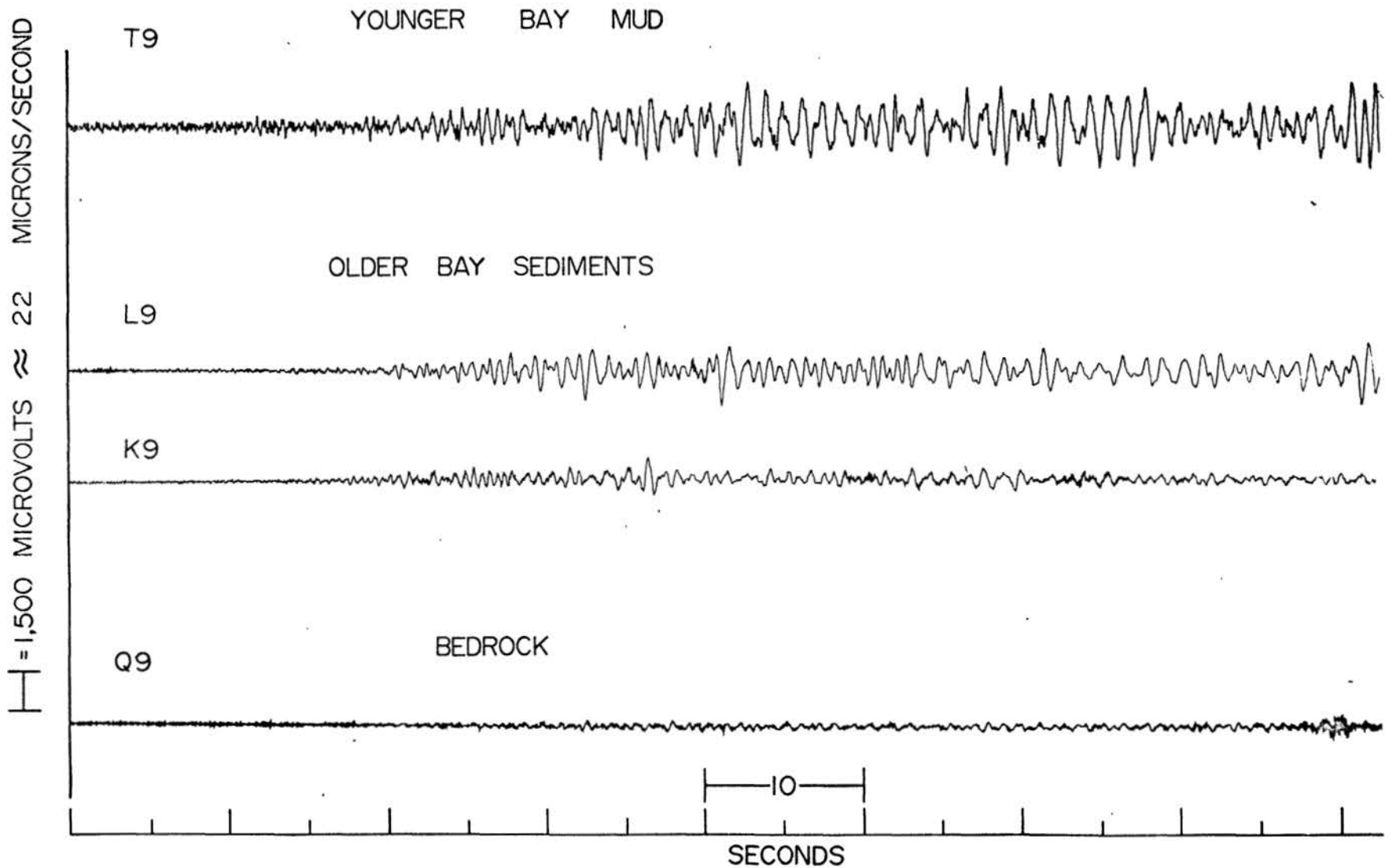
T9
YOUNGER BAY MUD
OLDER BAY SEDIMENTS
L9
K9
Q9
BEDROCK
= 1,500 MICROVOLTS ≈ 22 MICRONS/SECOND
10
SECONDS

Figure 18a

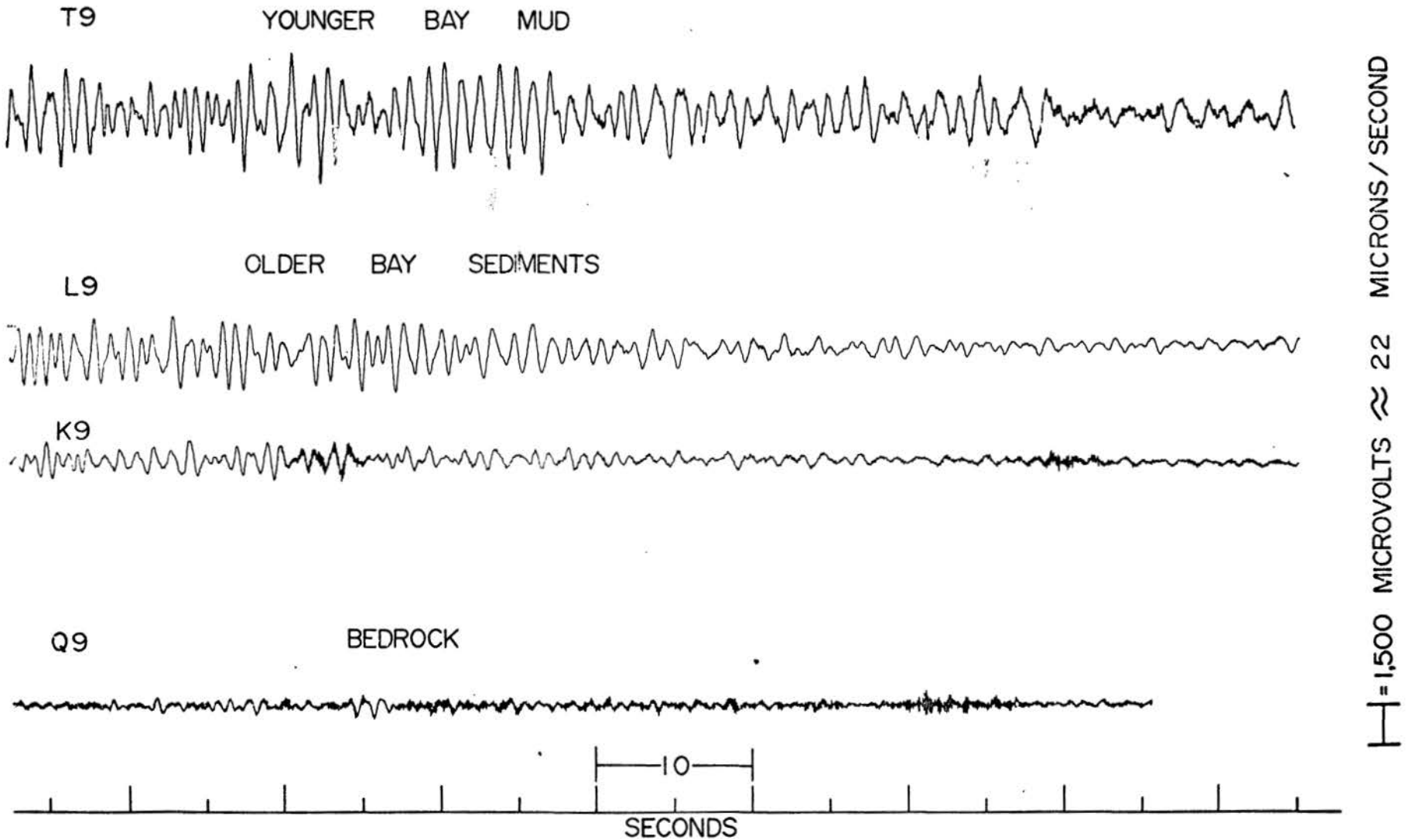
T9
YOUNGER BAY MUD
L9
OLDER BAY SEDIMENTS
K9
Q9
BEDROCK
10
SECONDS
1,500 MICROVOLTS ≈ 22 MICRONS / SECOND

Figure 18b

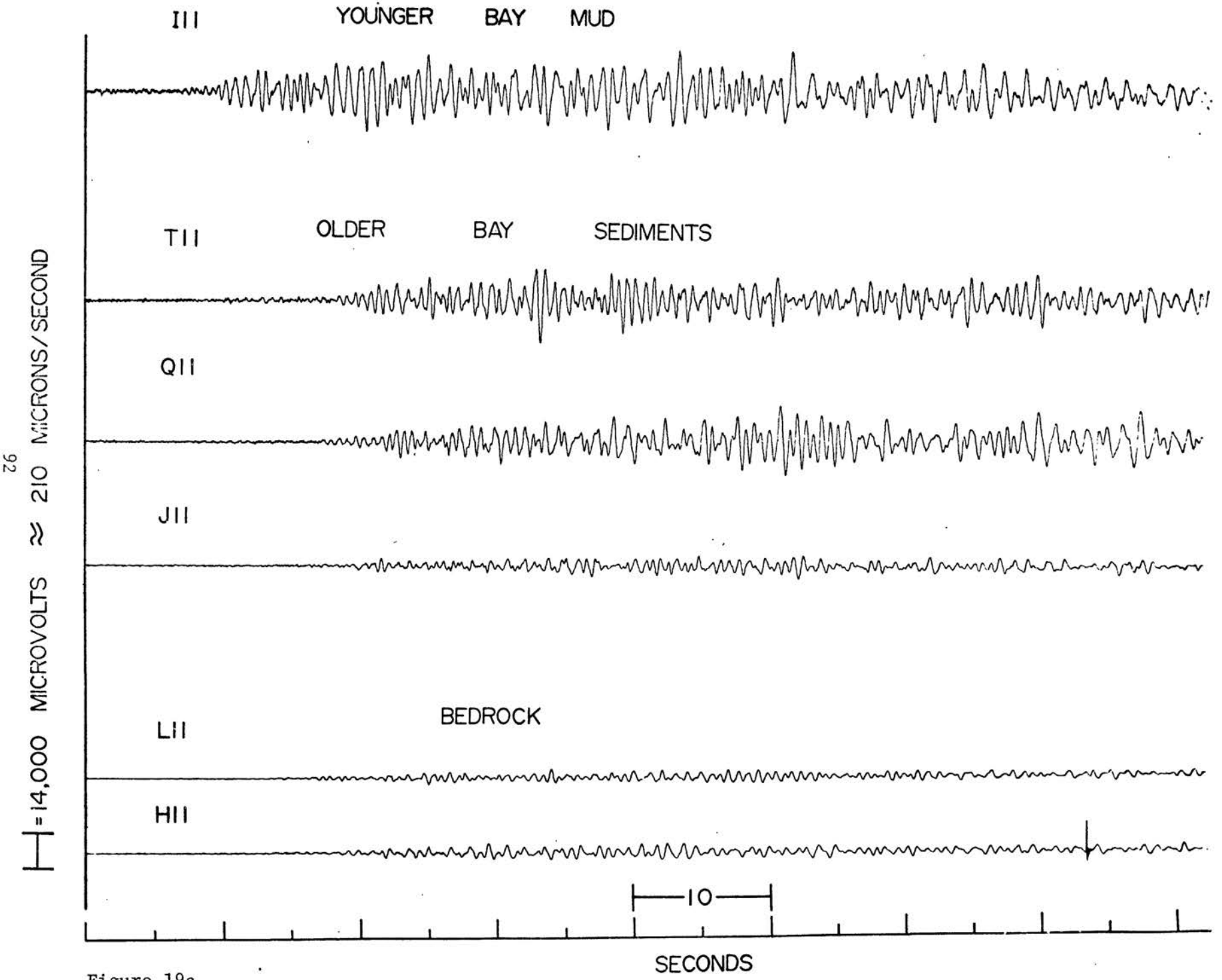
I11
YOUNGER BAY MUD
T11
OLDER BAY SEDIMENTS
Q11
J11
L11
BEDROCK
H11
=14,000 MICROVOLTS ≈ 210 MICRONS/SECOND
10
SECONDS

Figure 19a

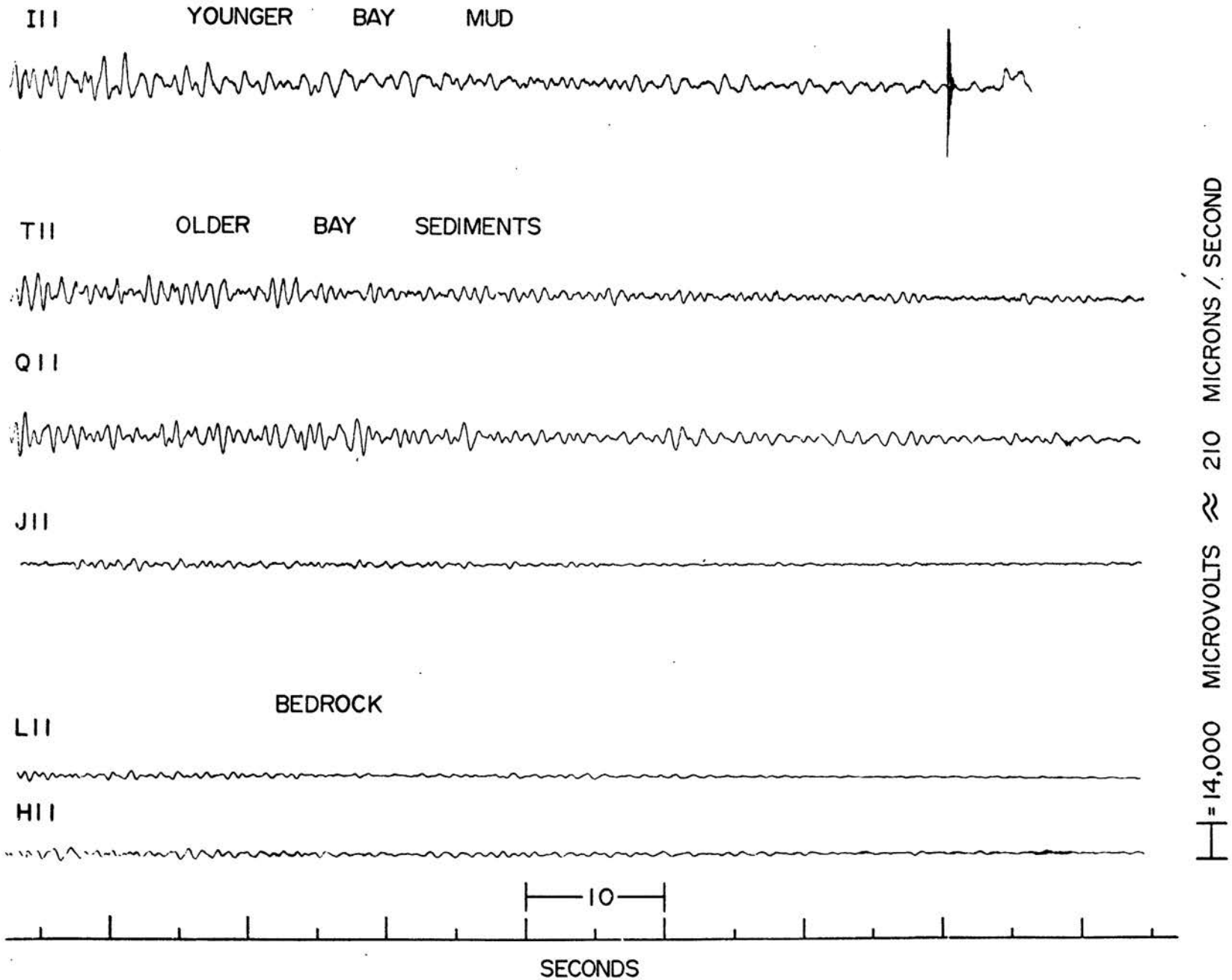
I11
YOUNGER BAY MUD
T11
OLDER BAY SEDIMENTS
Q11
J11
BEDROCK
L11
H11
10
SECONDS
= 14,000 MICROVOLTS ≈ 210 MICRONS / SECOND

Figure 19b

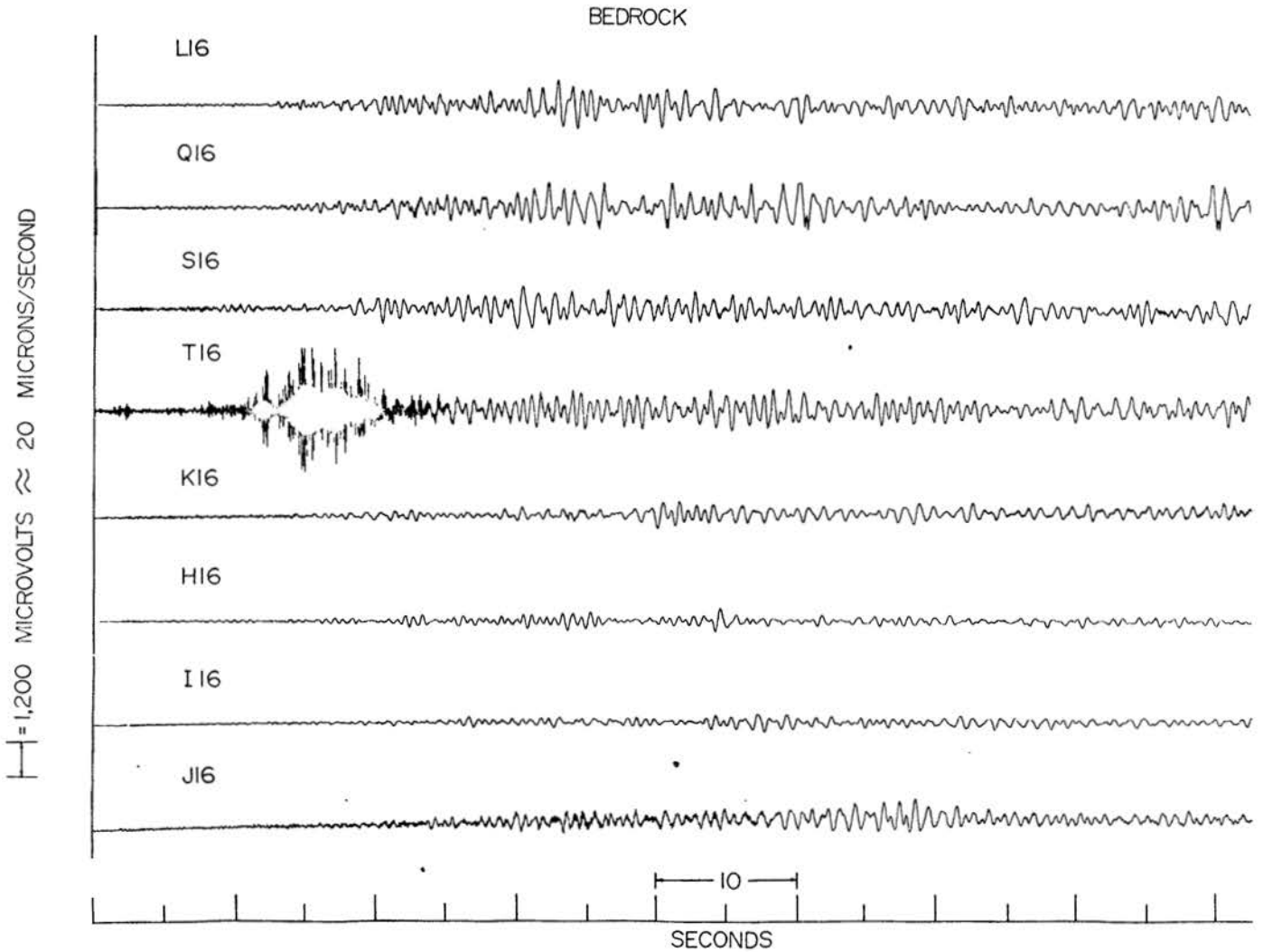
BEDROCK
L16
Q16
S16
T16
K16
H16
I16
J16
= 1,200 MICROVOLTS ≈ 20 MICRONS/SECOND
10
SECONDS

Figure 20a

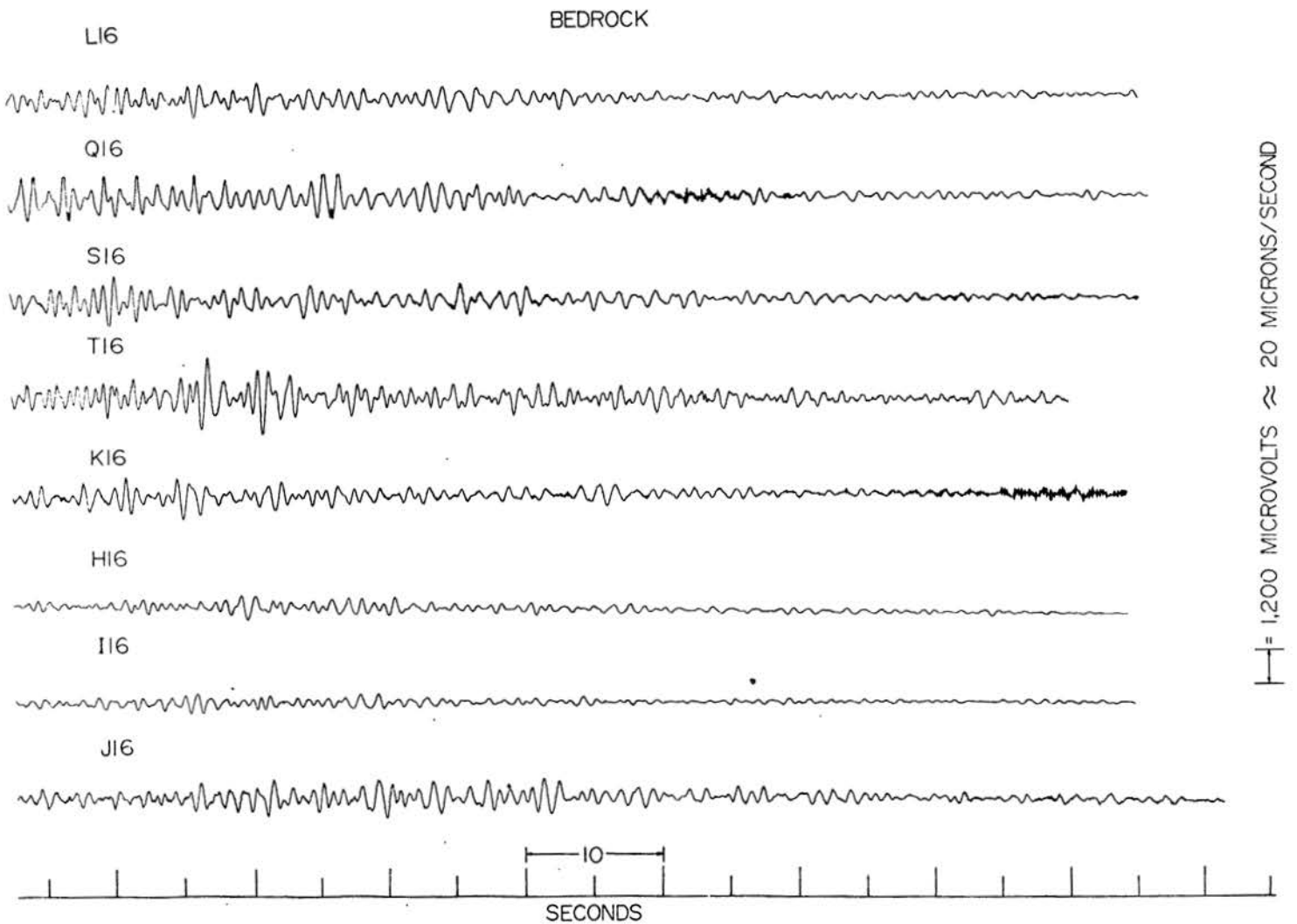
BEDROCK
L16
Q16
S16
T16
K16
H16
I16
J16
10
SECONDS
= 1,200 MICROVOLTS ≈ 20 MICRONS/SECOND

Figure 20b

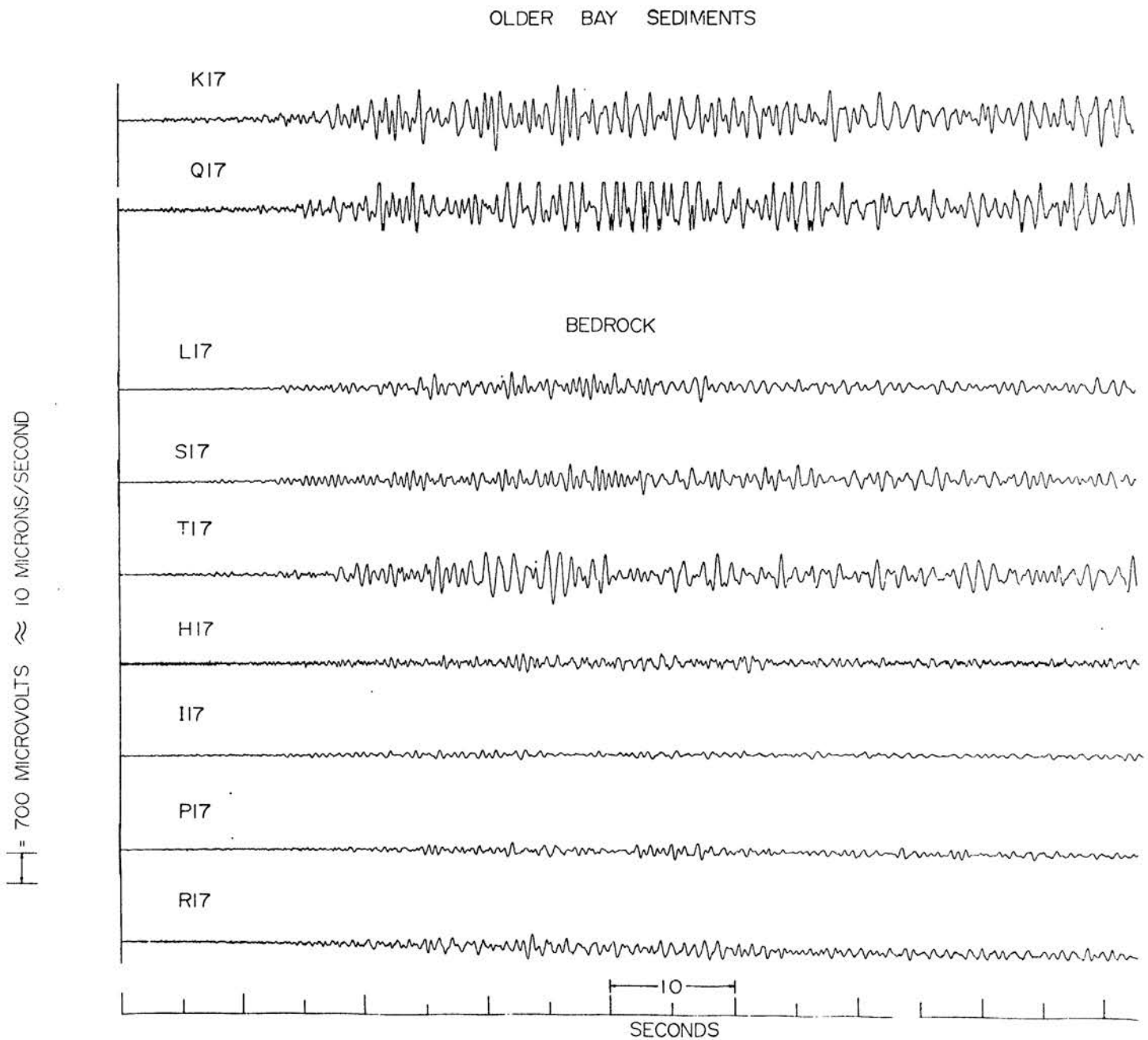
OLDER BAY SEDIMENTS
K17
Q17
BEDROCK
L17
S17
T17
H17
I17
P17
R17
10
SECONDS
= 700 MICROVOLTS ≈ 10 MICRONS/SECOND

Figure 21a

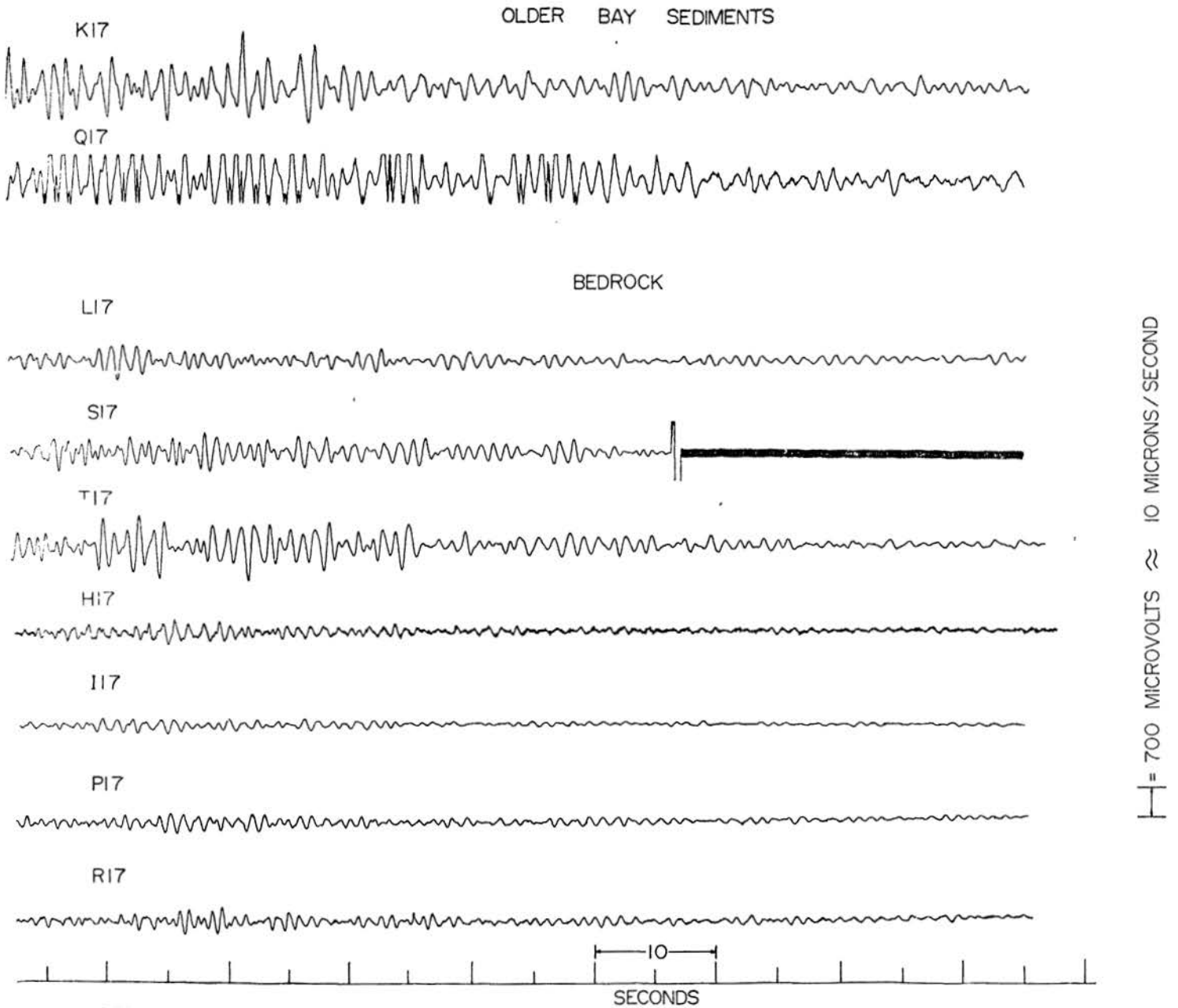
OLDER BAY SEDIMENTS
K17
Q17
BEDROCK
L17
S17
T17
H17
I17
P17
R17
10
SECONDS
= 700 MICROVOLTS ≈ 10 MICRONS/SECOND

Figure 21b

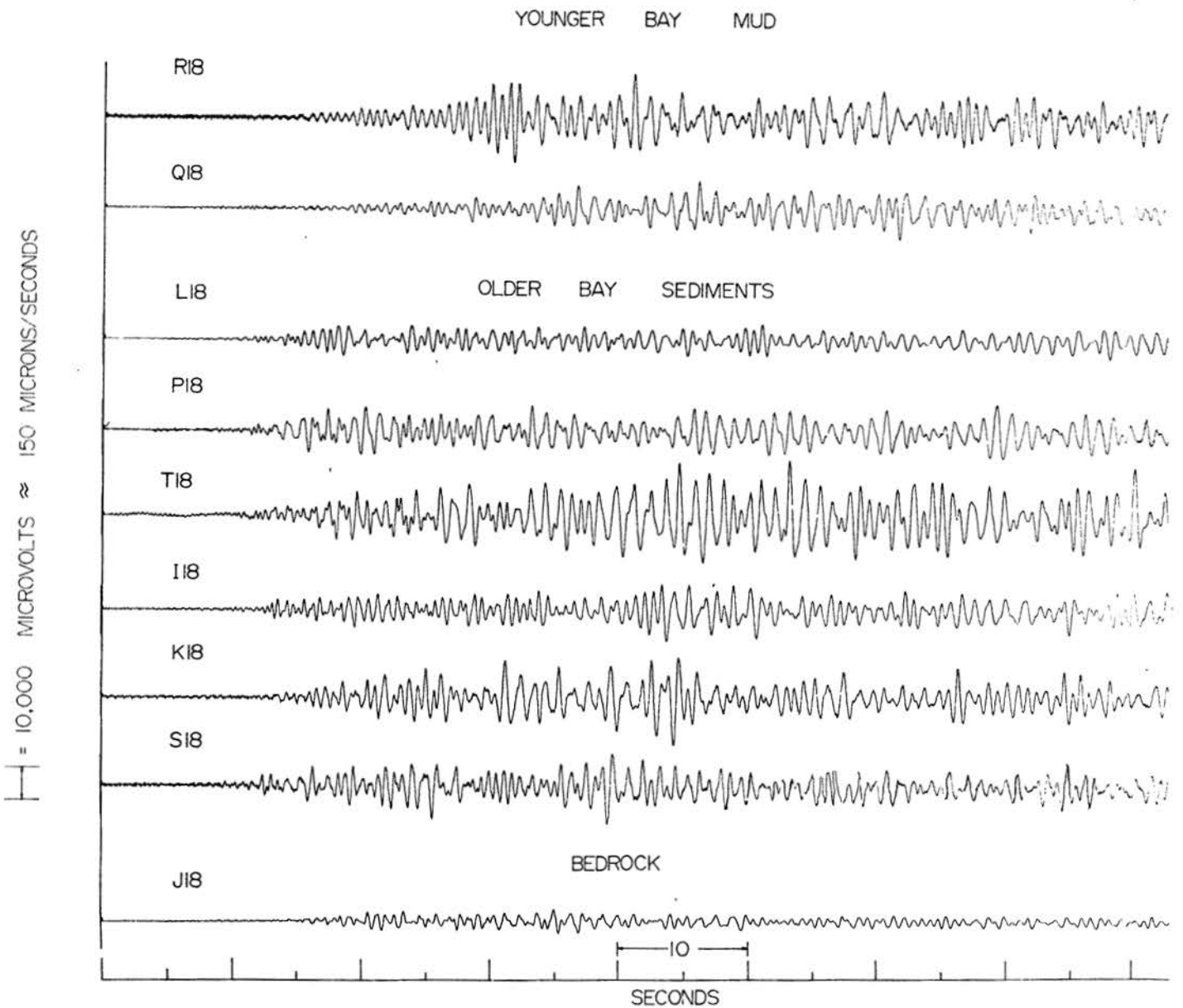
YOUNGER BAY MUD
R18
Q18
L18
OLDER BAY SEDIMENTS
P18
T18
I18
K18
S18
BEDROCK
J18
10
SECONDS
= 10,000 MICROVOLTS ≈ 150 MICRONS/SECONDS

Figure 22a

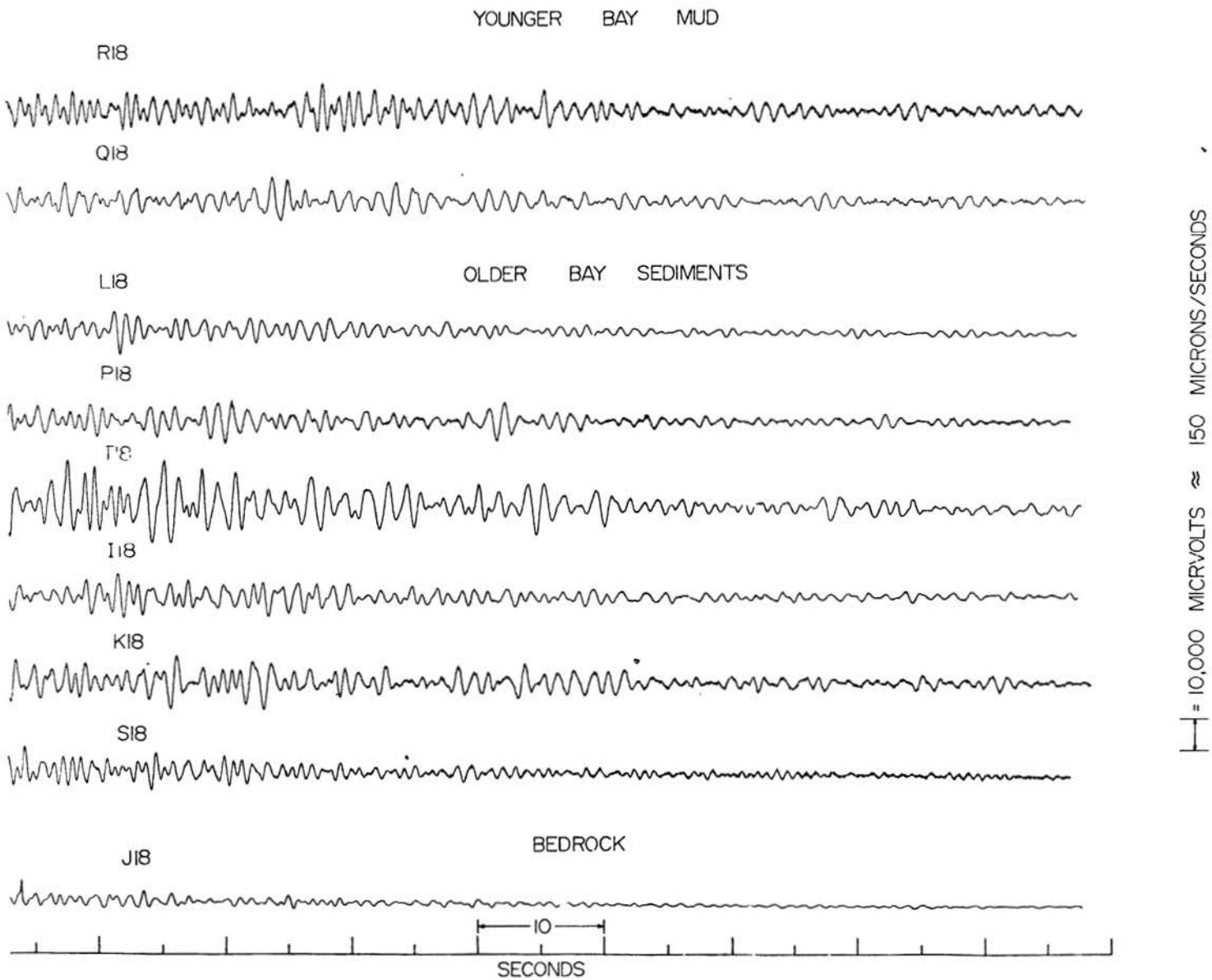
YOUNGER BAY MUD
R18
Q18
OLDER BAY SEDIMENTS
L18
P18
T18
I18
K18
S18
BEDROCK
J18
10
SECONDS
= 10,000 MICROVOLTS ≈ 150 MICRONS/SECONDS

Figure 22b

Figure 23

Horizontal Analog Amplifications on Geologic Map

(in map pouch)

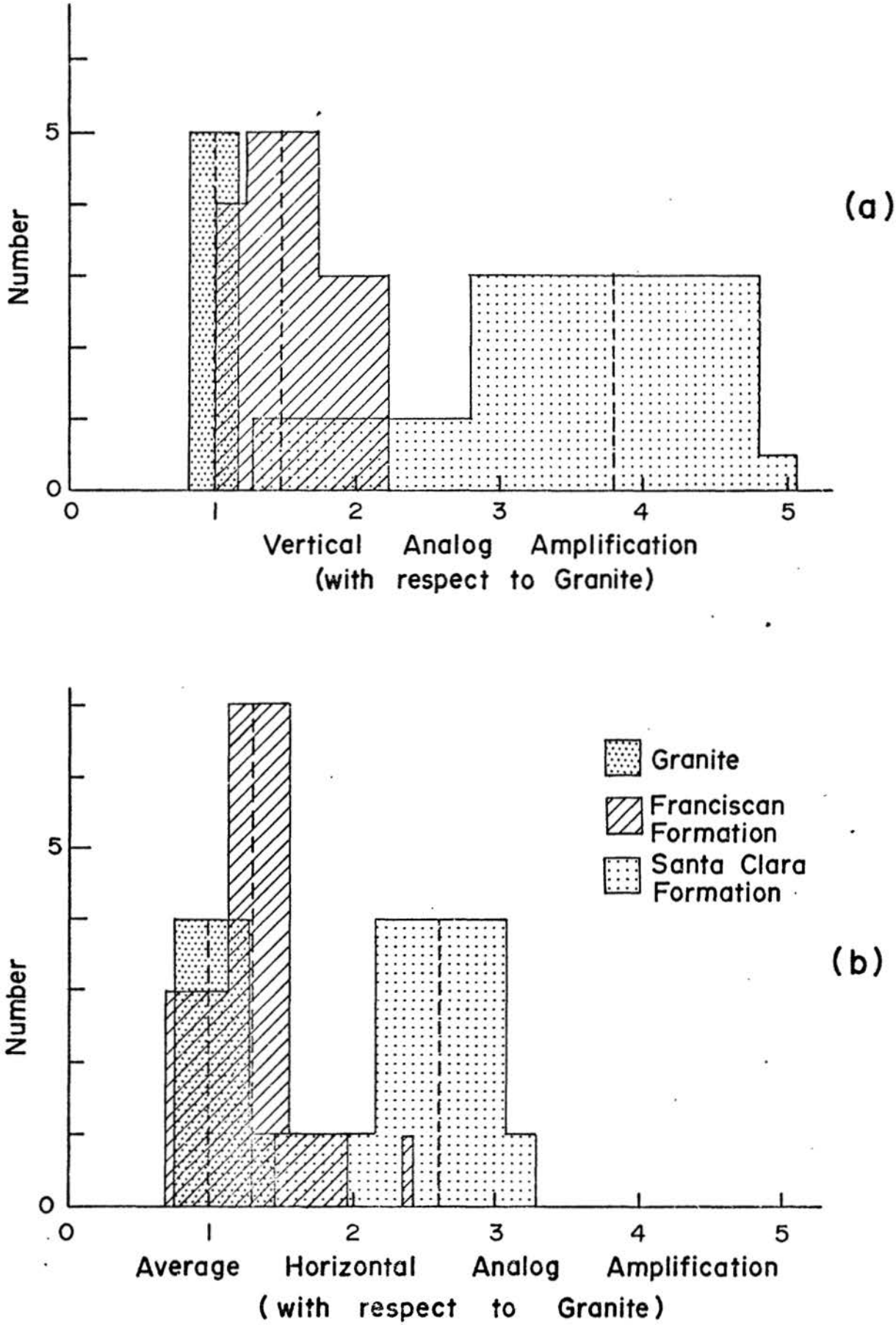
Number
5
0
0
1
2
3
4
5
Vertical Analog Amplification
(with respect to Granite)
(a)
Granite
Franciscan Formation
Santa Clara Formation
Number
5
0
0
1
2
3
4
5
Average Horizontal Analog Amplification
(with respect to Granite)
(b)

Figure 24

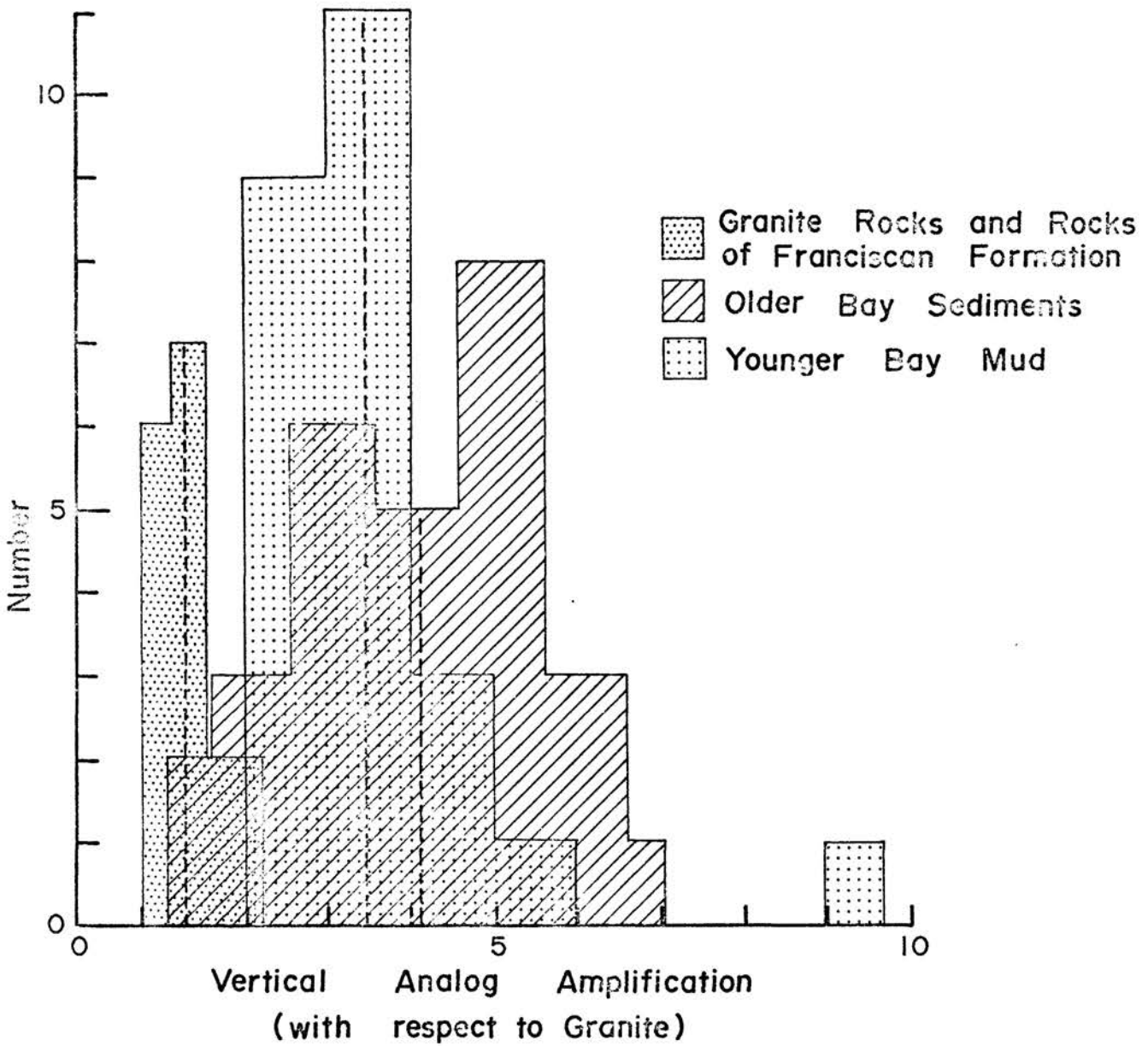
Granite Rocks and Rocks of Franciscan Formation
Older Bay Sediments
Younger Bay Mud
Number
0
5
10
0
5
10
Vertical Analog Amplification
(with respect to Granite)

Figure 25

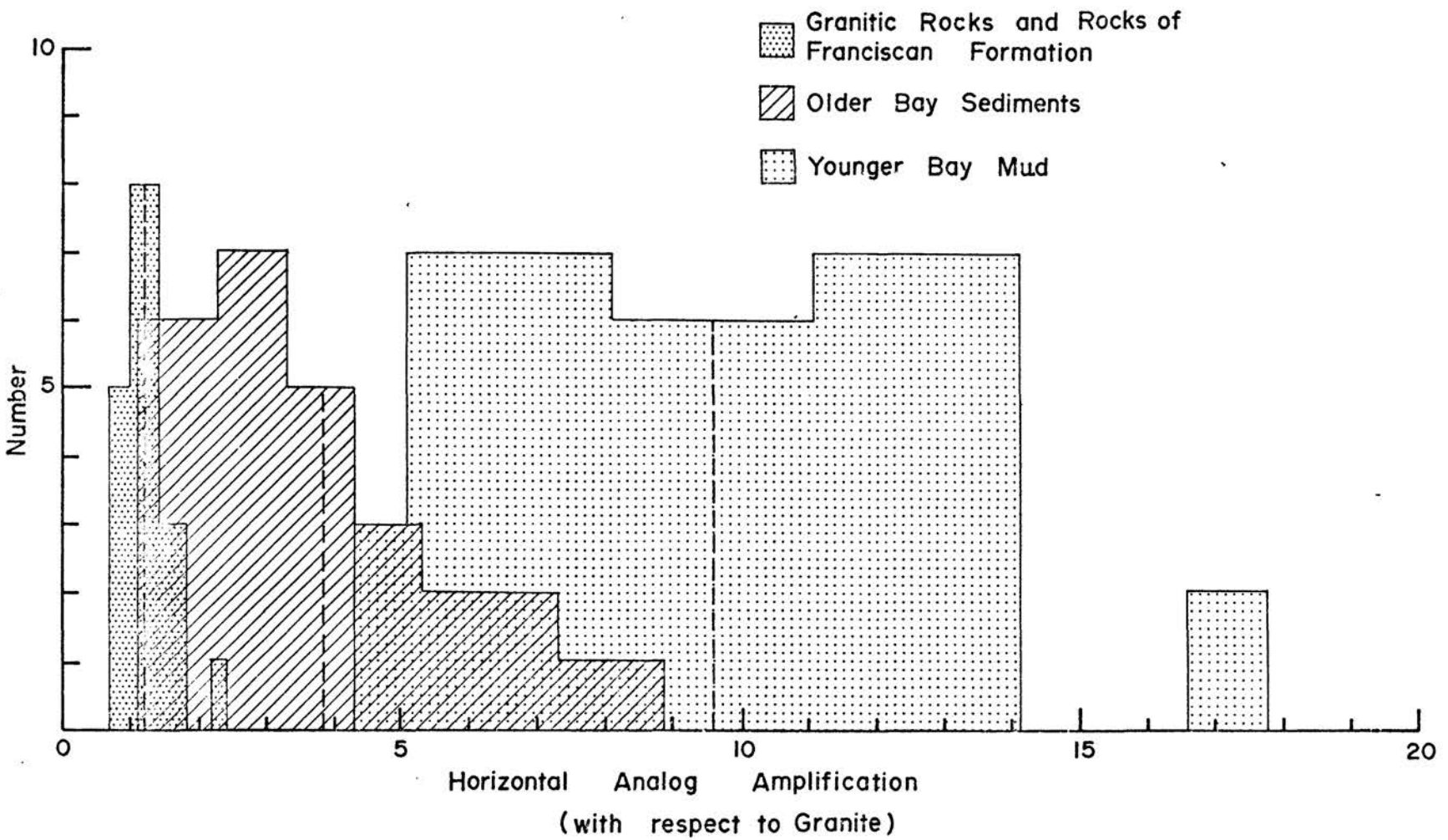
Granitic Rocks and Rocks of Franciscan Formation
Older Bay Sediments
Younger Bay Mud
Number
10
5
0
5
10
15
20
Horizontal Analog Amplification
(with respect to Granite)

Figure 26

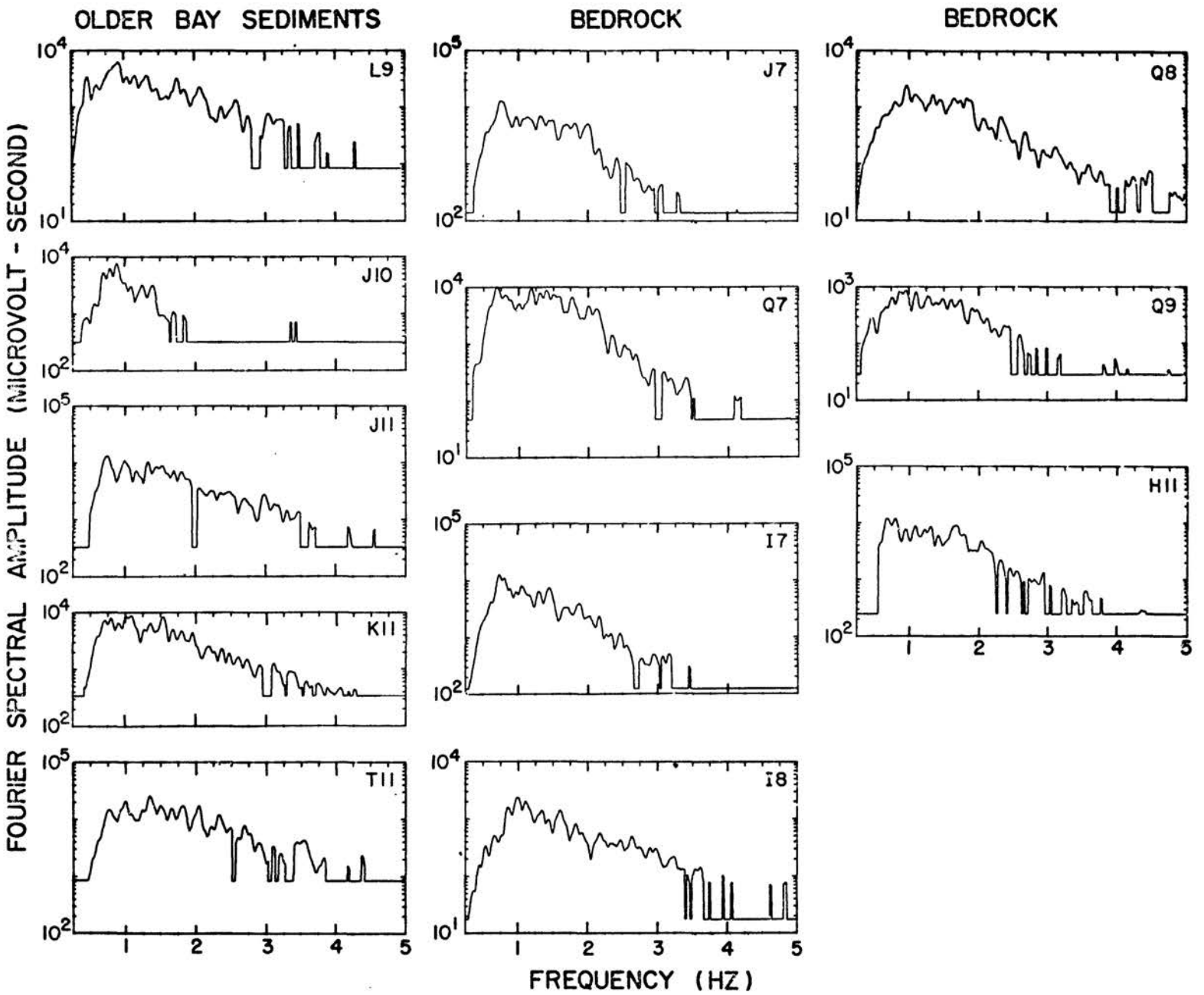
OLDER BAY SEDIMENTS
BEDROCK
BEDROCK
FOURIER SPECTRAL AMPLITUDE (MICROVOLT - SECOND)
L9
J10
J11
K11
T11
J7
Q7
I7
I8
Q8
Q9
H11
FREQUENCY (HZ)

Figure 27

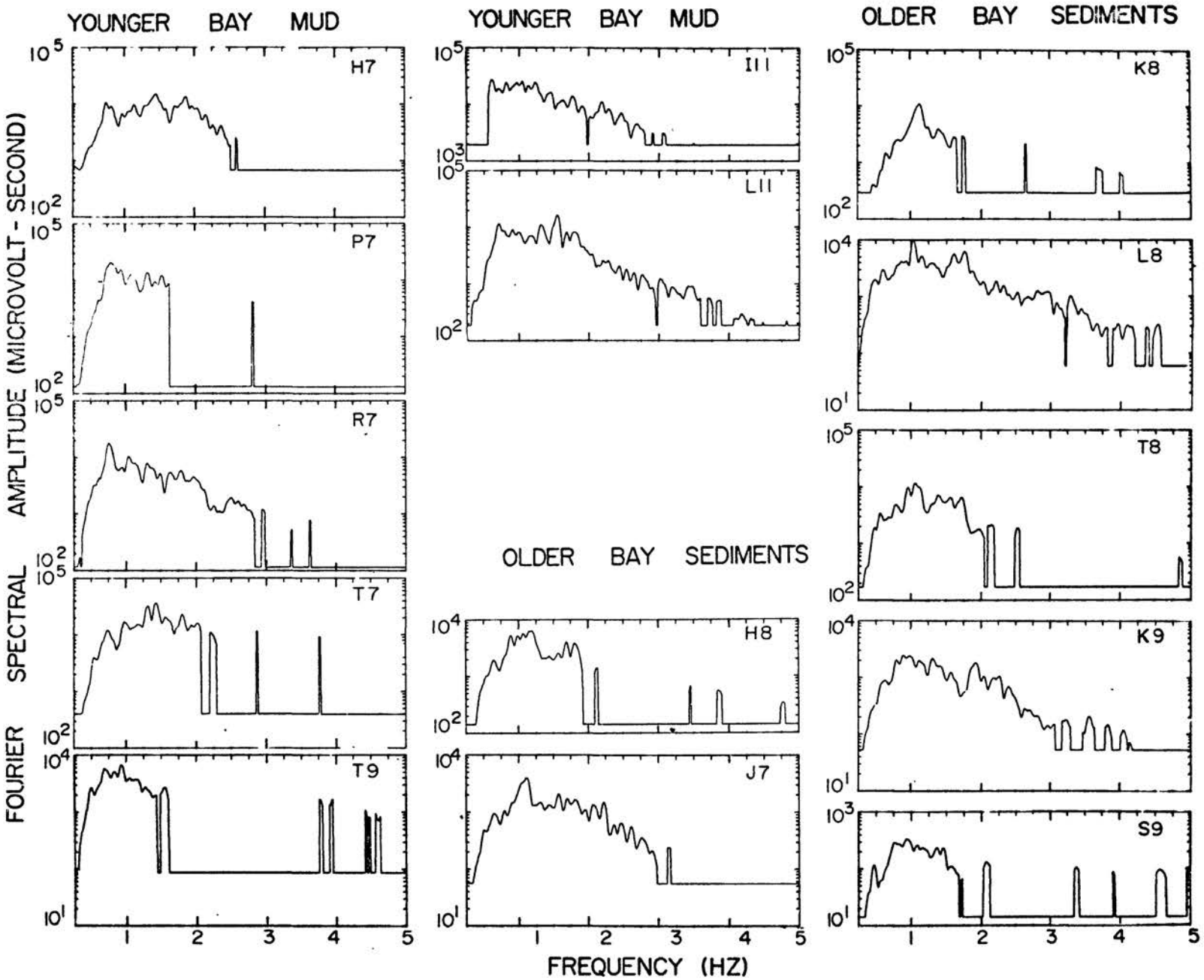
YOUNGER BAY MUD
YOUNGER BAY MUD
OLDER BAY SEDIMENTS
OLDER BAY SEDIMENTS
FOURIER SPECTRAL AMPLITUDE (MICROVOLT - SECOND)
FREQUENCY (HZ)
H7
P7
R7
T7
T9
I11
L11
H8
J7
K8
L8
T8
K9
S9

Figure 28

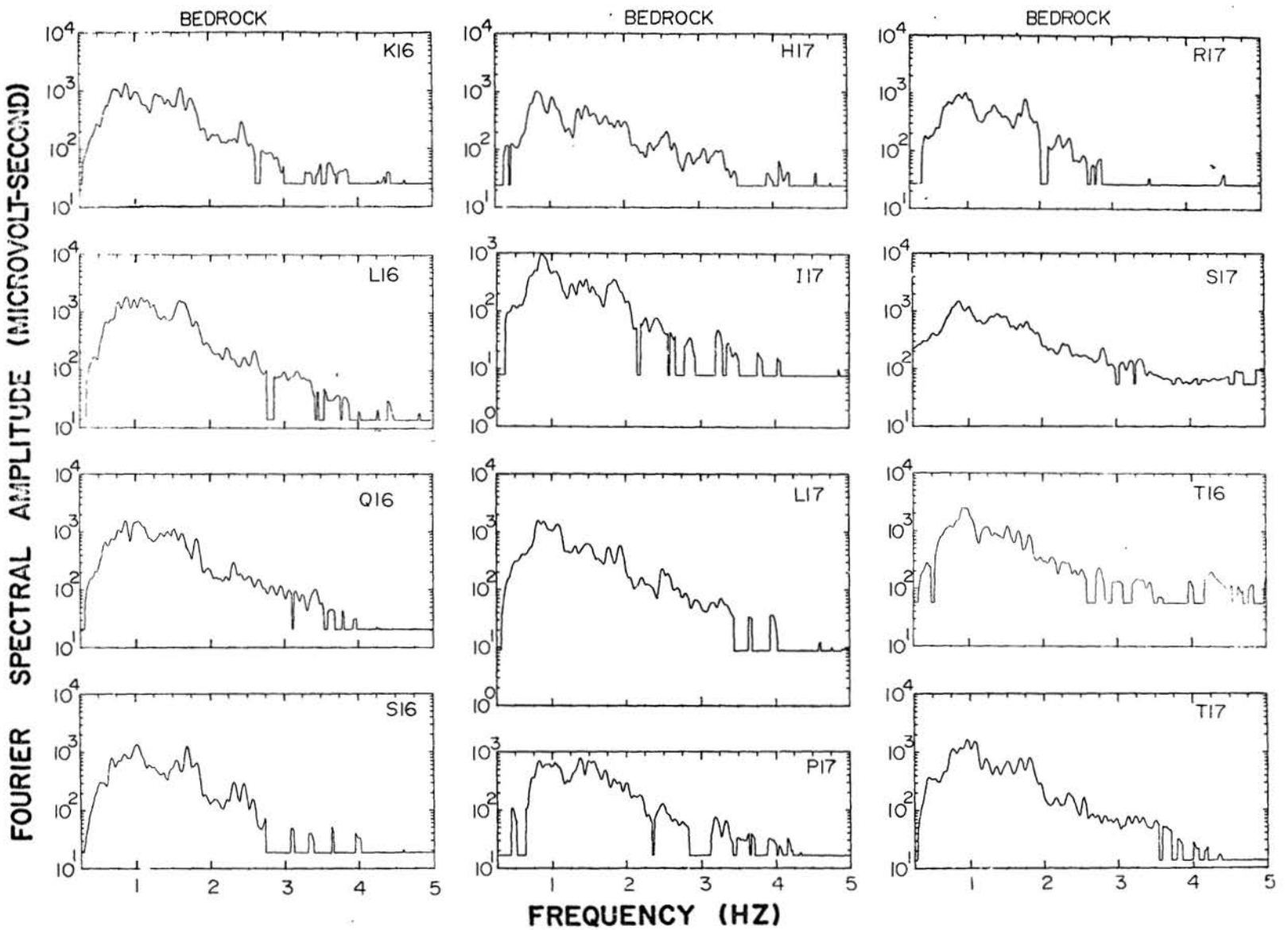
BEDROCK
K16
H17
R17
L16
I17
S17
Q16
L17
T16
S16
P17
T17
FOURIER SPECTRAL AMPLITUDE (MICROVOLT-SECOND)
FREQUENCY (HZ)

Figure 29

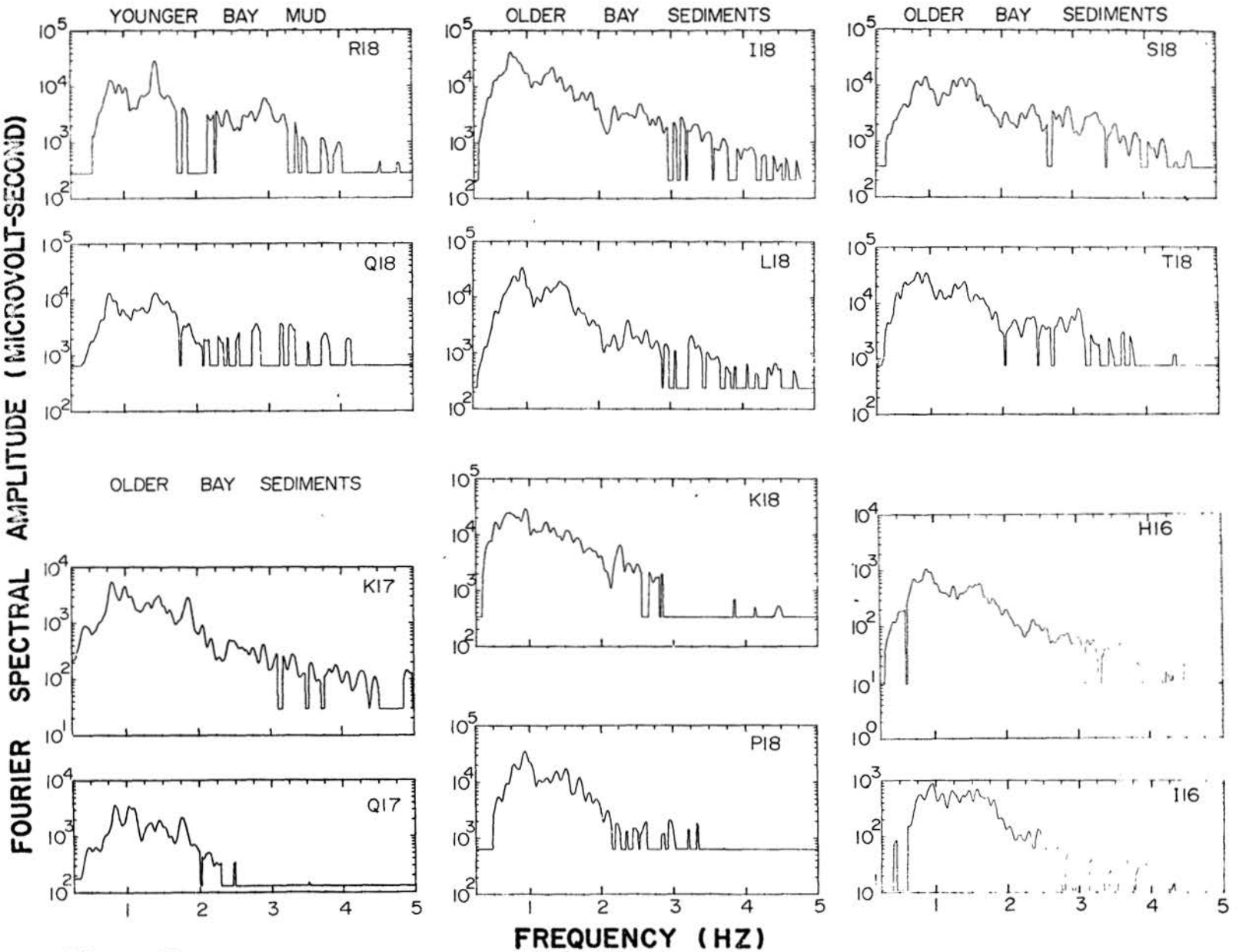
YOUNGER BAY MUD
OLDER BAY SEDIMENTS
OLDER BAY SEDIMENTS
OLDER BAY SEDIMENTS
R18
I18
S18
Q18
L18
T18
K18
K17
H16
P18
Q17
I16
FOURIER SPECTRAL AMPLITUDE (MICROVOLT-SECOND)
FREQUENCY (HZ)

Figure 30

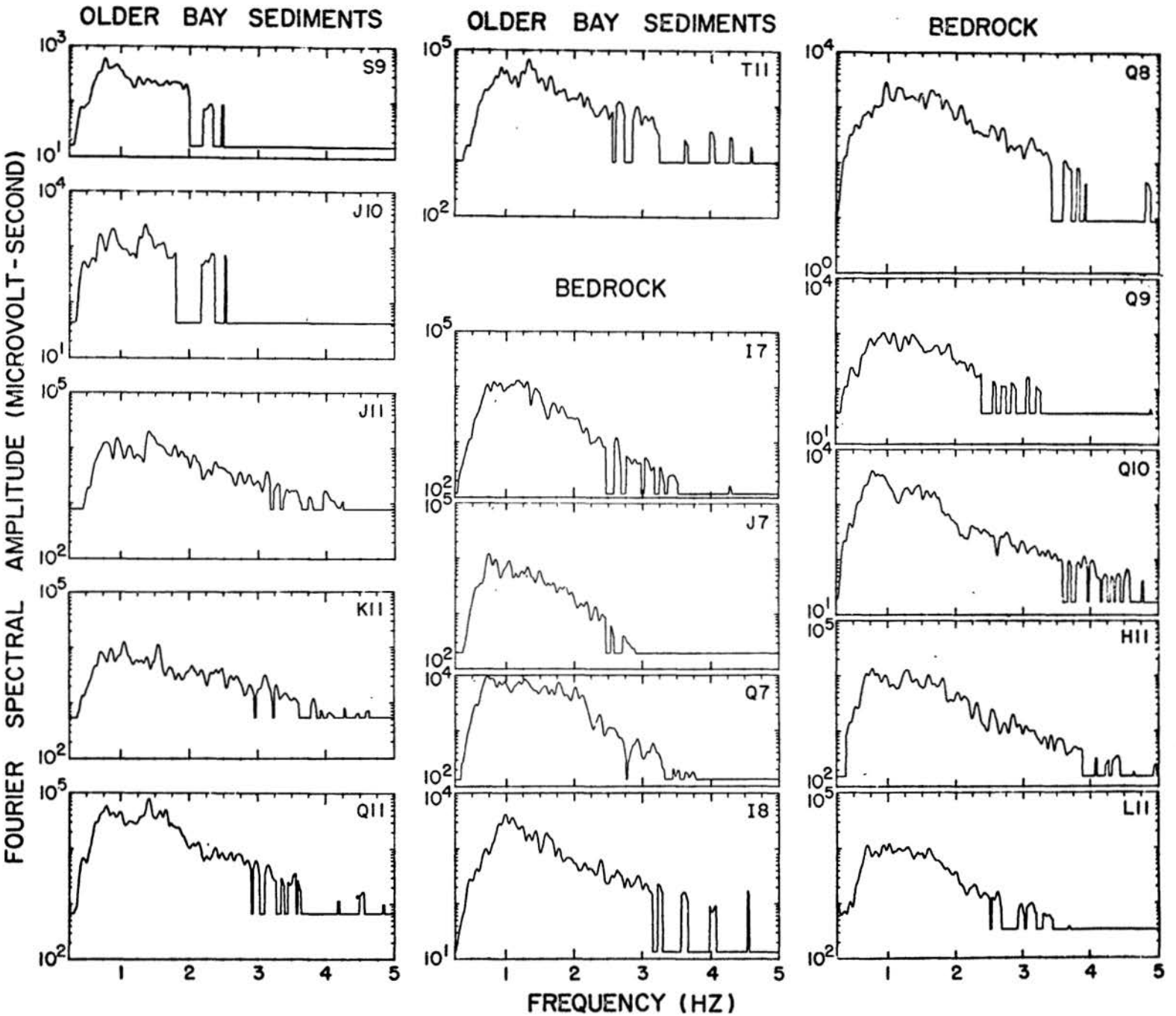
OLDER BAY SEDIMENTS
OLDER BAY SEDIMENTS
BEDROCK
BEDROCK
S9
J10
J11
K11
Q11
T11
I7
J7
Q7
I8
Q8
Q9
Q10
H11
L11
FOURIER SPECTRAL AMPLITUDE (MICROVOLT-SECOND)
FREQUENCY (HZ)

Figure 31

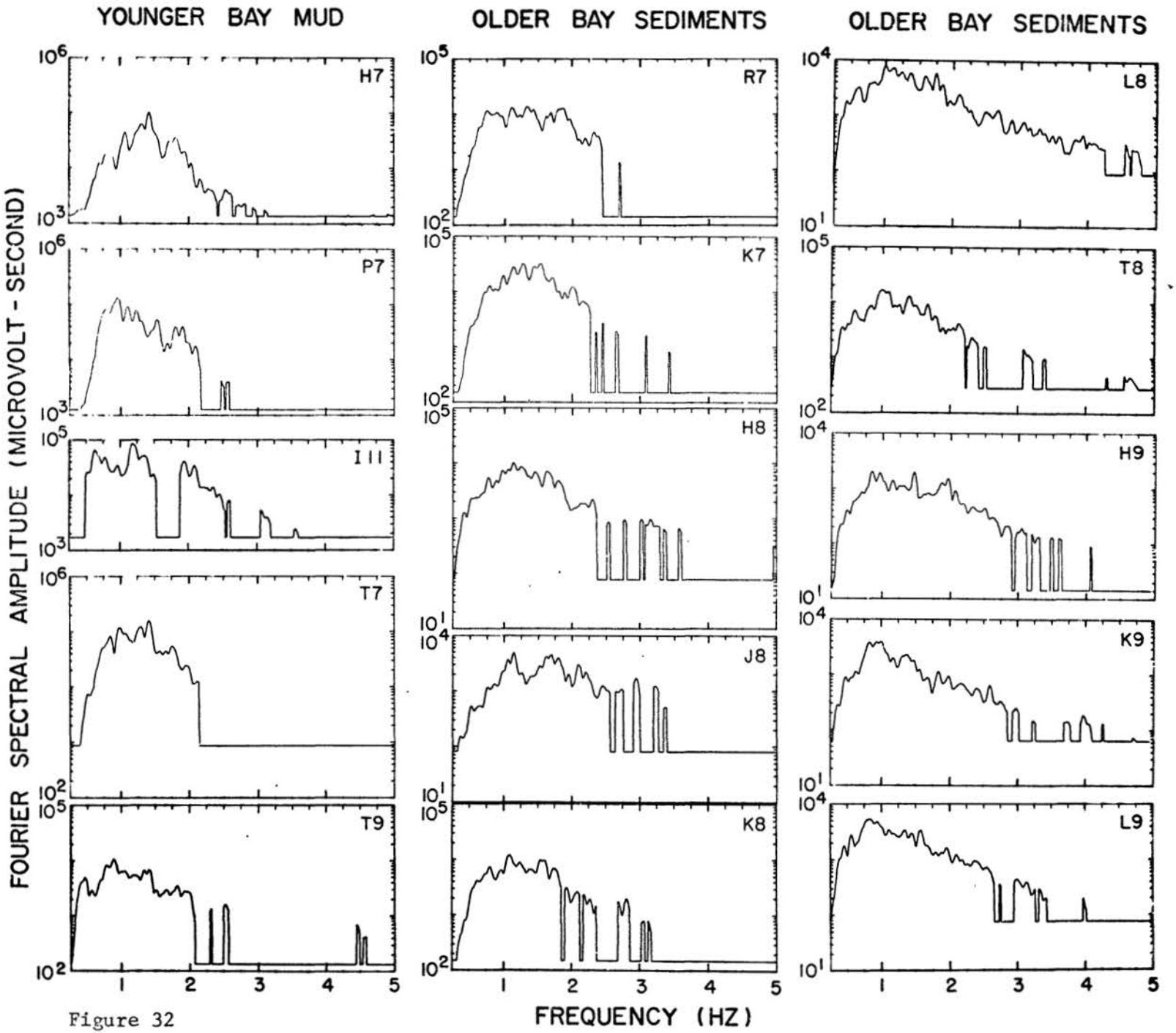
YOUNGER BAY MUD
OLDER BAY SEDIMENTS
OLDER BAY SEDIMENTS
FOURIER SPECTRAL AMPLITUDE (MICROVOLT - SECOND)
FREQUENCY (HZ)
H7
P7
I 11
T7
T9
R7
K7
H8
J8
K8
L8
T8
H9
K9
L9

Figure 32

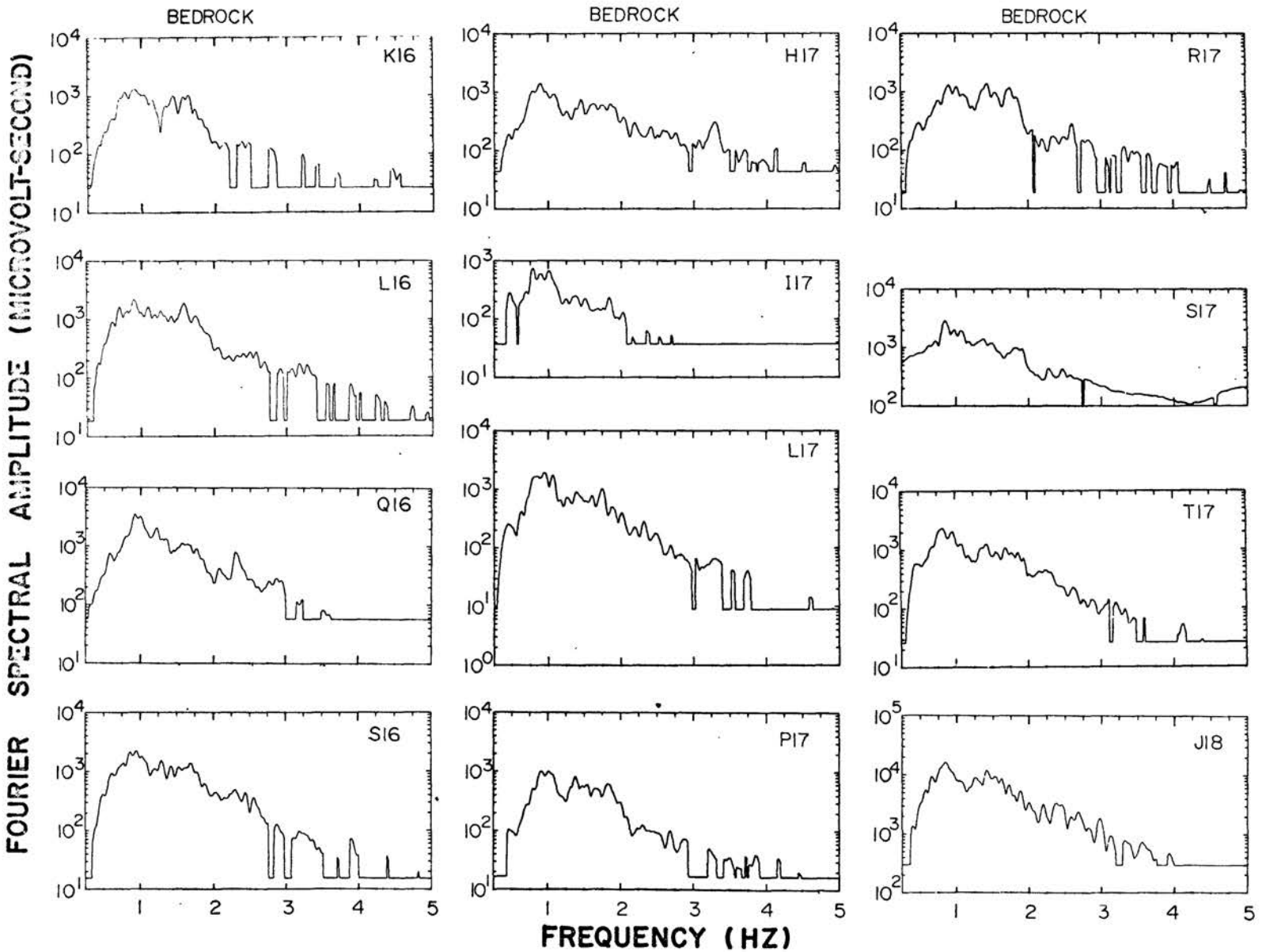
BEDROCK
K16
H17
R17
L16
I17
S17
L17
Q16
T17
S16
P17
J18
FOURIER SPECTRAL AMPLITUDE (MICROVOLT-SECOND)
FREQUENCY (HZ)

Figure 33

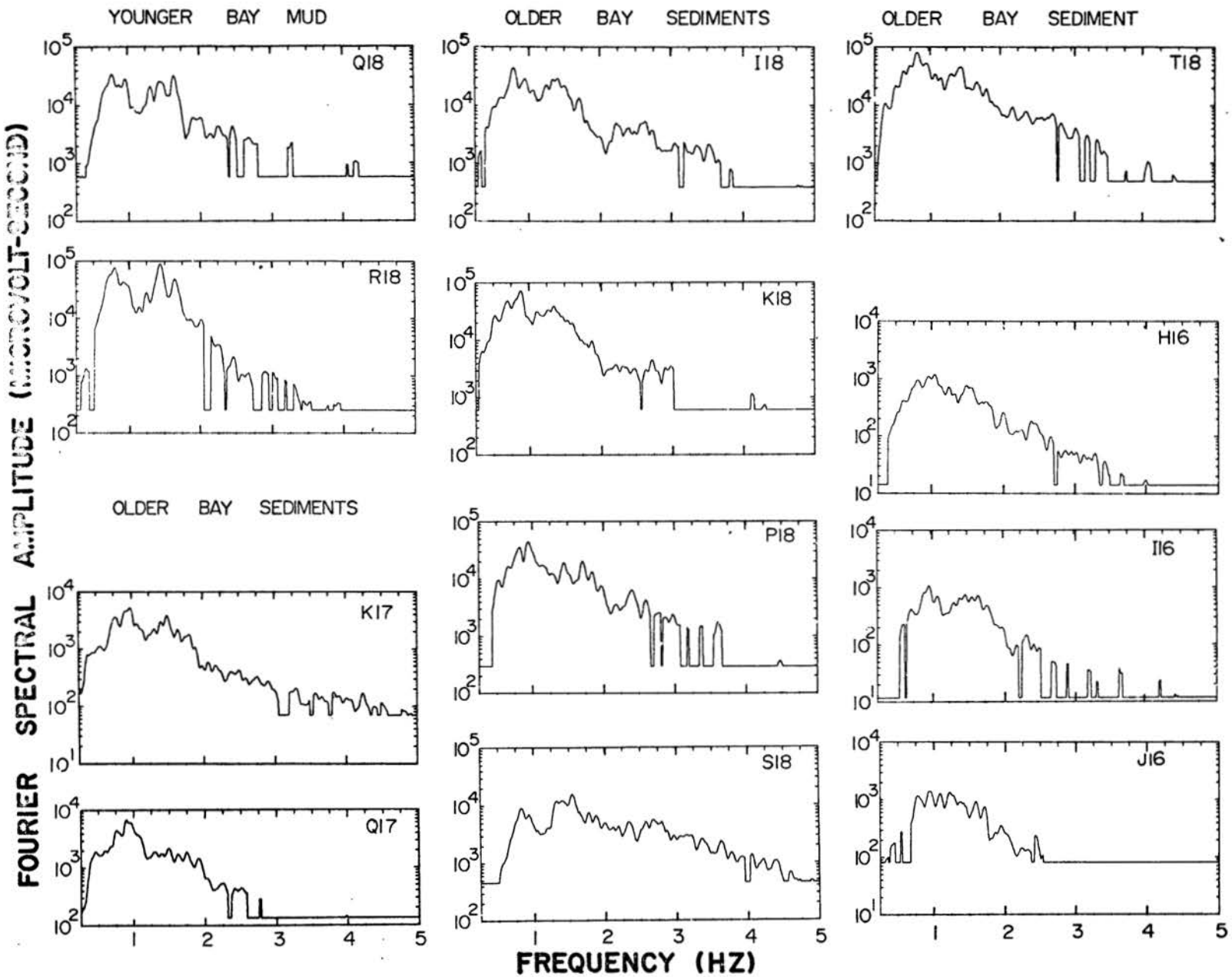
YOUNGER BAY MUD
OLDER BAY SEDIMENTS
OLDER BAY SEDIMENT
OLDER BAY SEDIMENTS
Q18
R18
K17
Q17
I18
K18
P18
S18
T18
H16
I16
J16
FOURIER SPECTRAL AMPLITUDE (MICROVOLT-SECOND)
FREQUENCY (HZ)

Figure 34

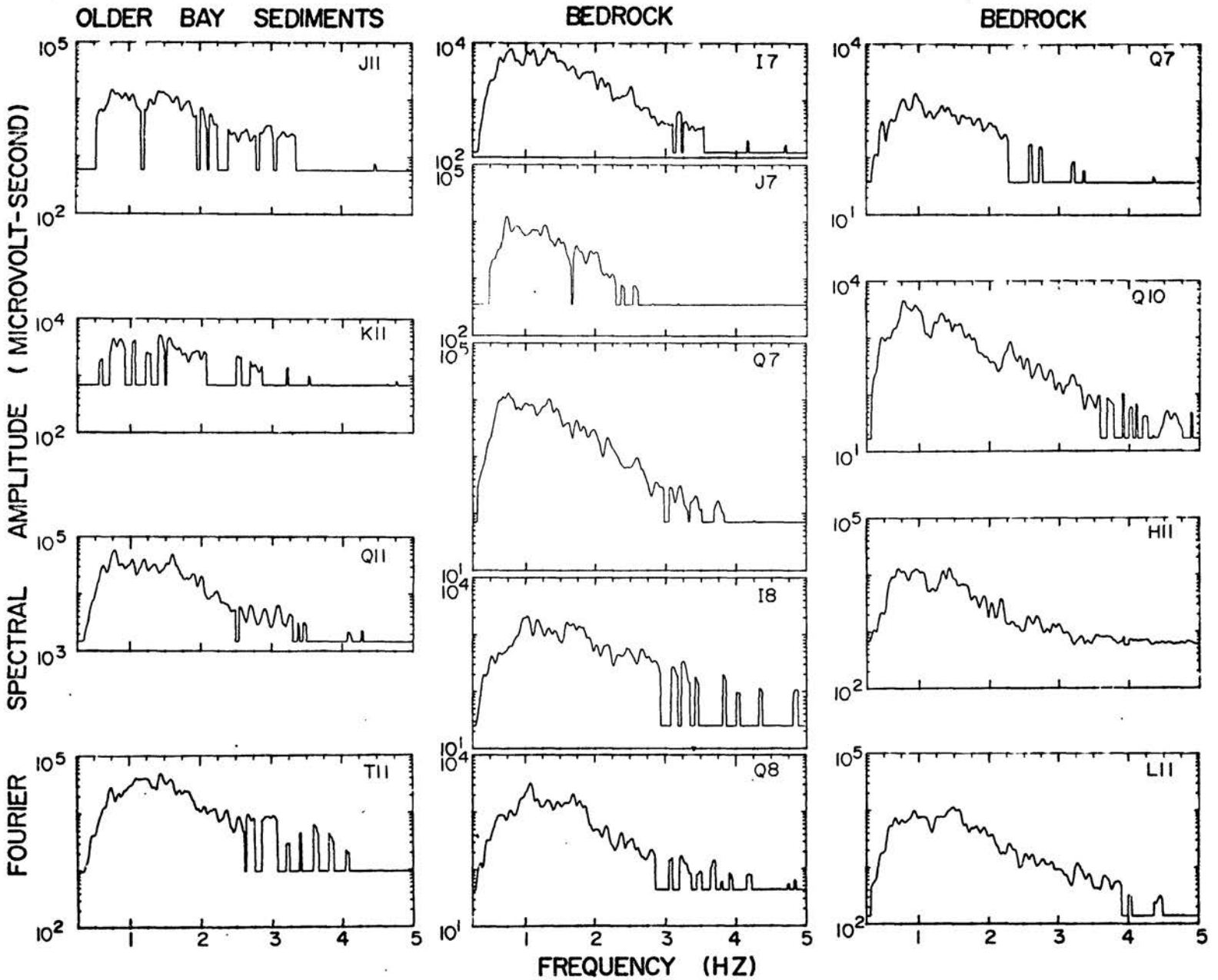
OLDER BAY SEDIMENTS
BEDROCK
BEDROCK
FOURIER SPECTRAL AMPLITUDE (MICROVOLT-SECOND)
FREQUENCY (HZ)
J11
K11
Q11
T11
I7
J7
Q7
I8
Q8
Q7
Q10
H11
L11

Figure 35

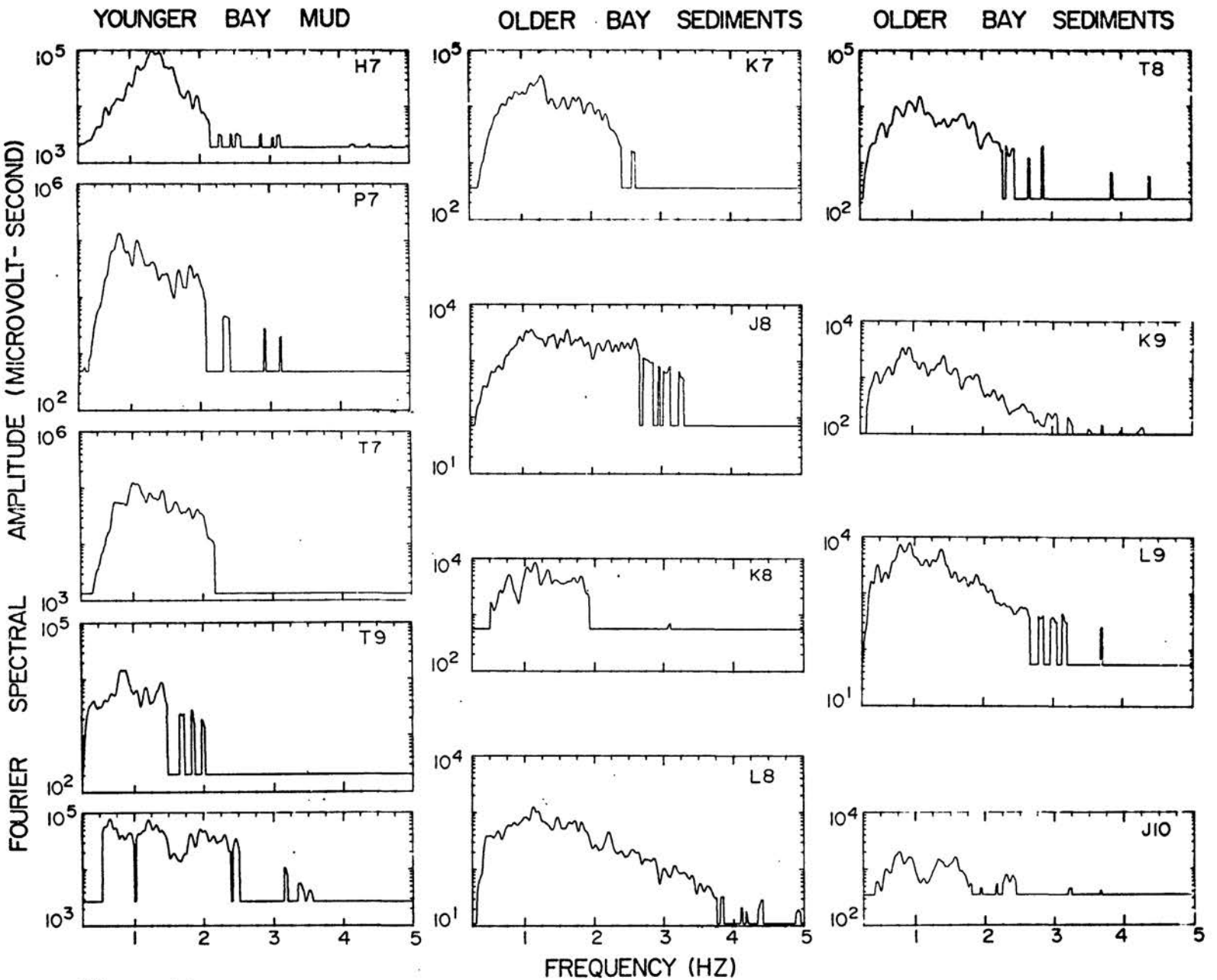
YOUNGER BAY MUD
OLDER BAY SEDIMENTS
OLDER BAY SEDIMENTS
FOURIER SPECTRAL AMPLITUDE (MICROVOLT- SECOND)
H7
P7
T7
T9
K7
J8
K8
L8
T8
K9
L9
J10
FREQUENCY (HZ)

Figure 36

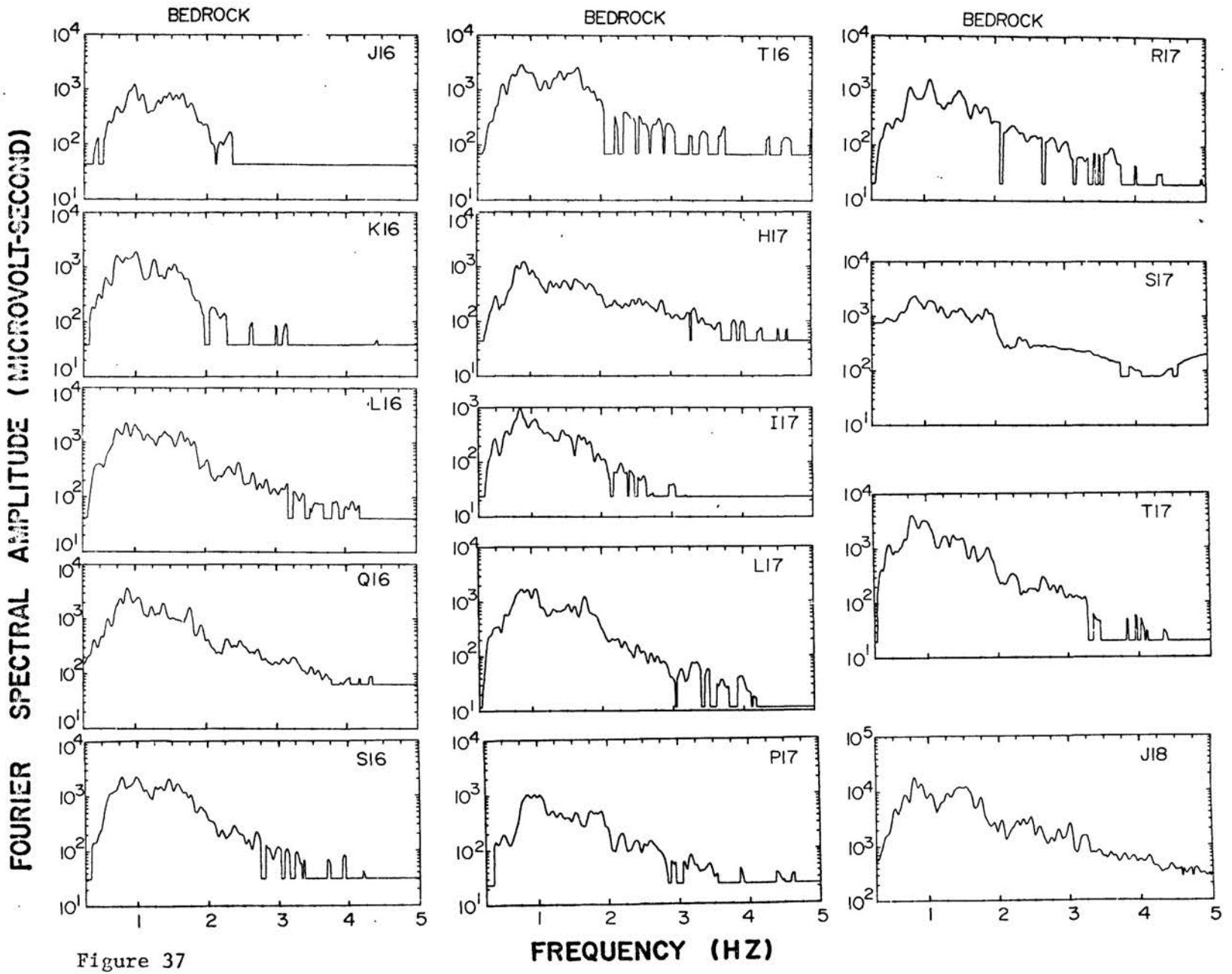
BEDROCK
BEDROCK
BEDROCK
J16
K16
L16
Q16
S16
T16
H17
I17
L17
P17
R17
S17
T17
J18
FOURIER SPECTRAL AMPLITUDE (MICROVOLT-SECOND)
FREQUENCY (HZ)

Figure 37

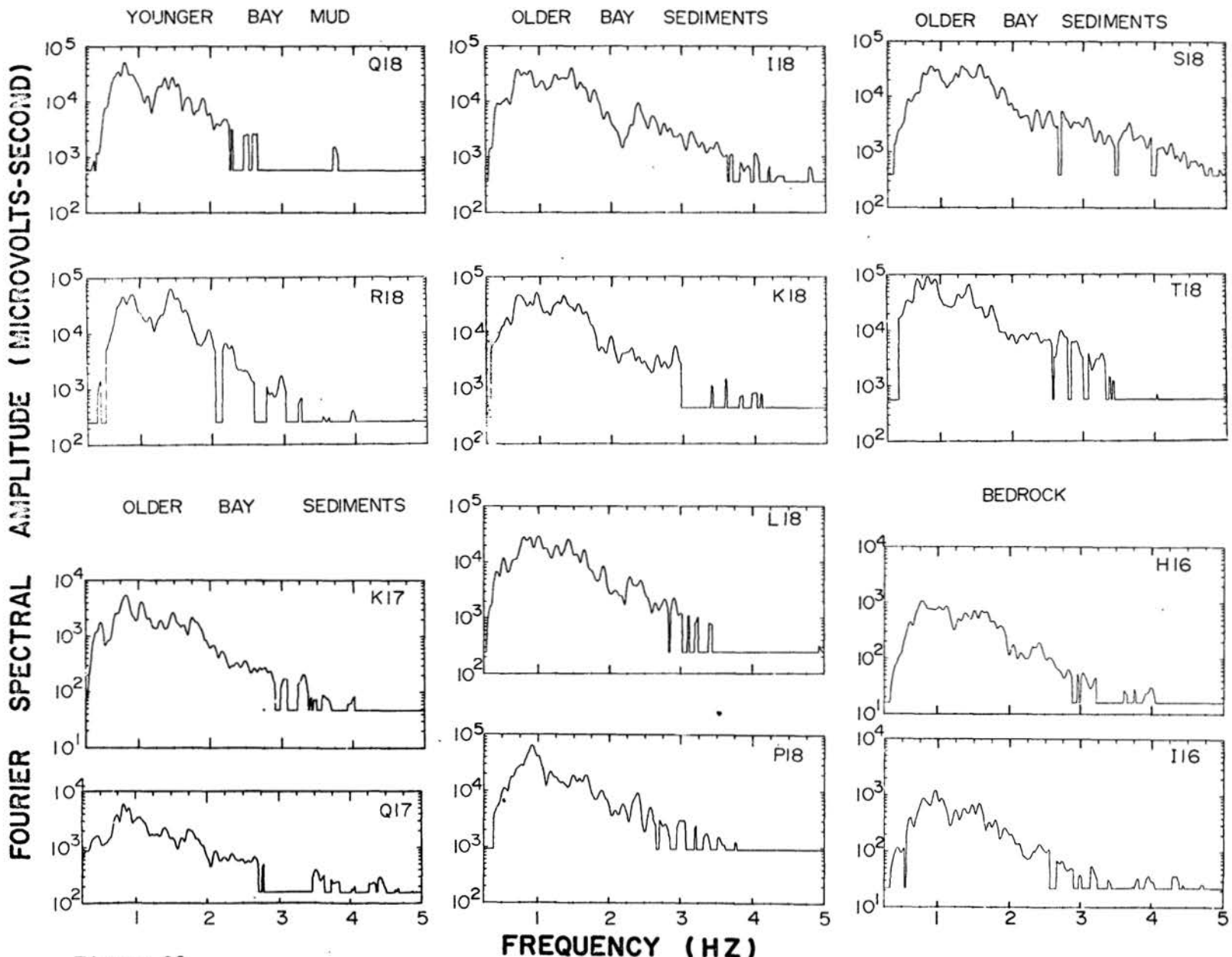
YOUNGER BAY MUD
OLDER BAY SEDIMENTS
OLDER BAY SEDIMENTS
OLDER BAY SEDIMENTS
BEDROCK
Q18
I18
S18
R18
K18
T18
K17
L18
H16
Q17
P18
I16
FOURIER SPECTRAL AMPLITUDE (MICROVOLTS-SECOND)
FREQUENCY (HZ)

Figure 38

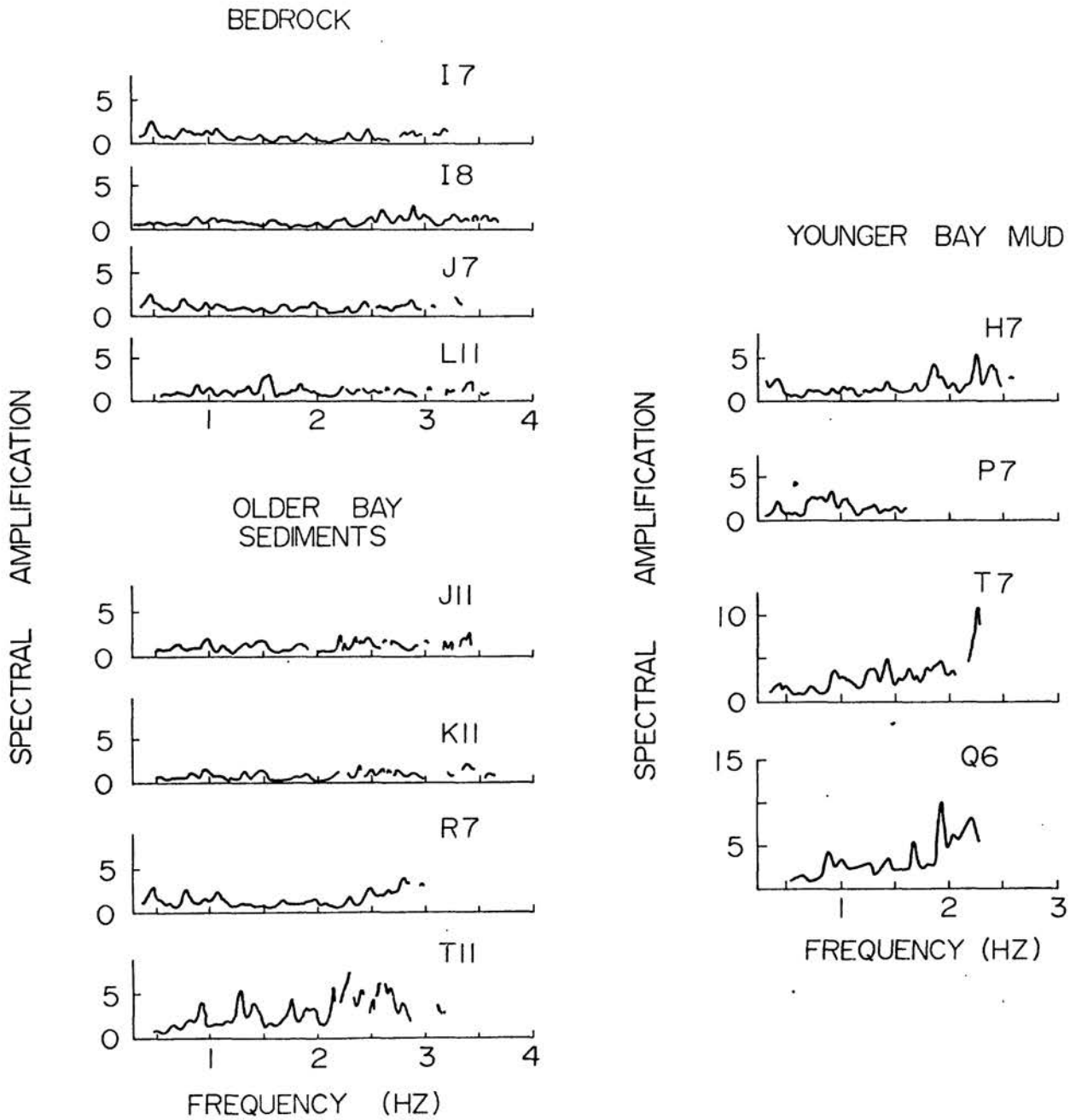
BEDROCK
I7
I8
J7
L11
OLDER BAY SEDIMENTS
J11
K11
R7
T11
YOUNGER BAY MUD
H7
P7
T7
Q6
SPECTRAL AMPLIFICATION
FREQUENCY (HZ)

Figure 39

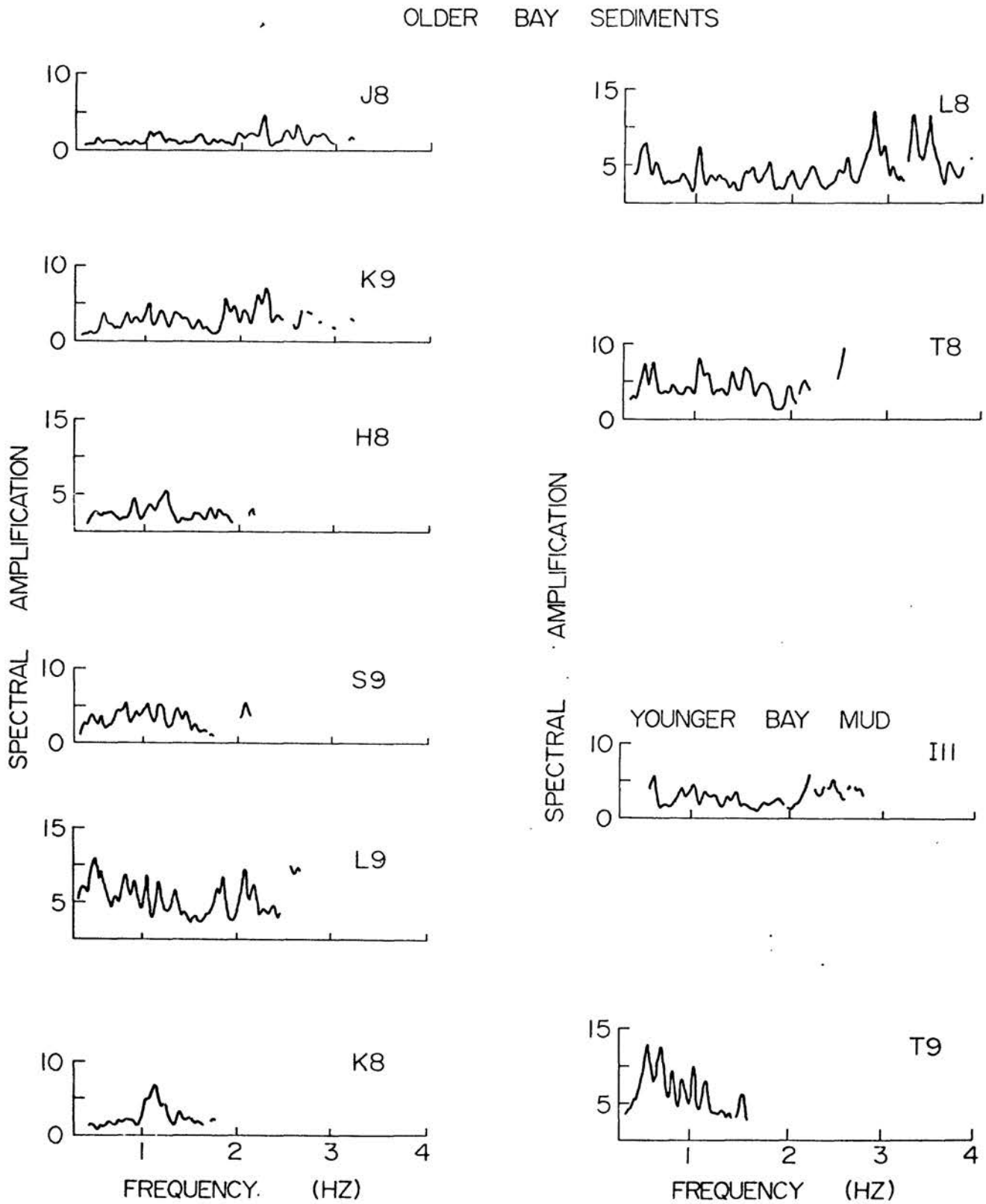
OLDER BAY SEDIMENTS
J8
K9
H8
S9
L9
K8
L8
T8
YOUNGER BAY MUD
I11
T9
SPECTRAL AMPLIFICATION
FREQUENCY (HZ)

Figure 40

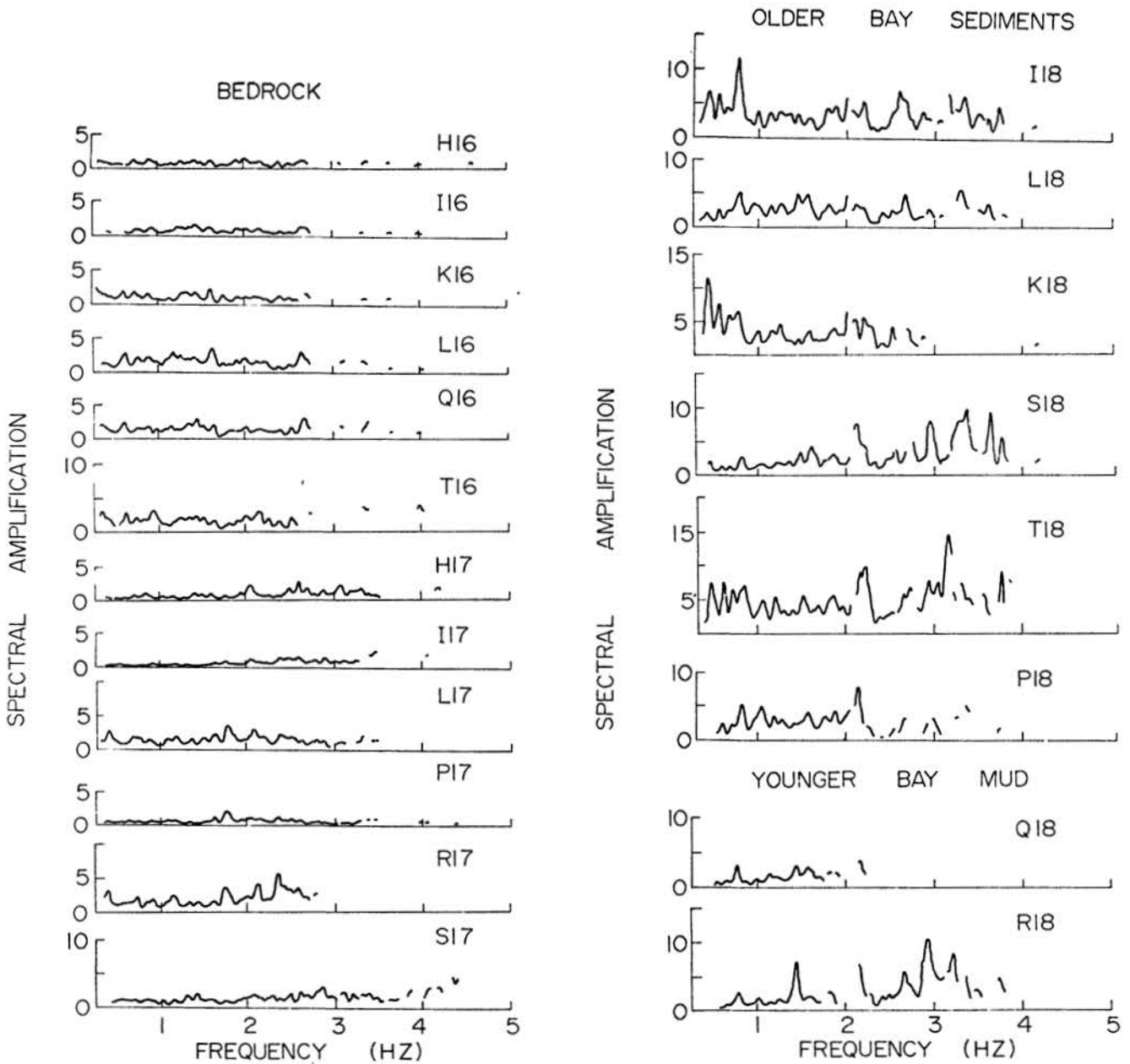
BEDROCK
OLDER BAY SEDIMENTS
YOUNGER BAY MUD
SPECTRAL AMPLIFICATION
H16
I16
K16
L16
Q16
T16
H17
I17
L17
P17
R17
S17
I18
L18
K18
S18
T18
P18
Q18
R18
FREQUENCY (HZ)

Figure 41

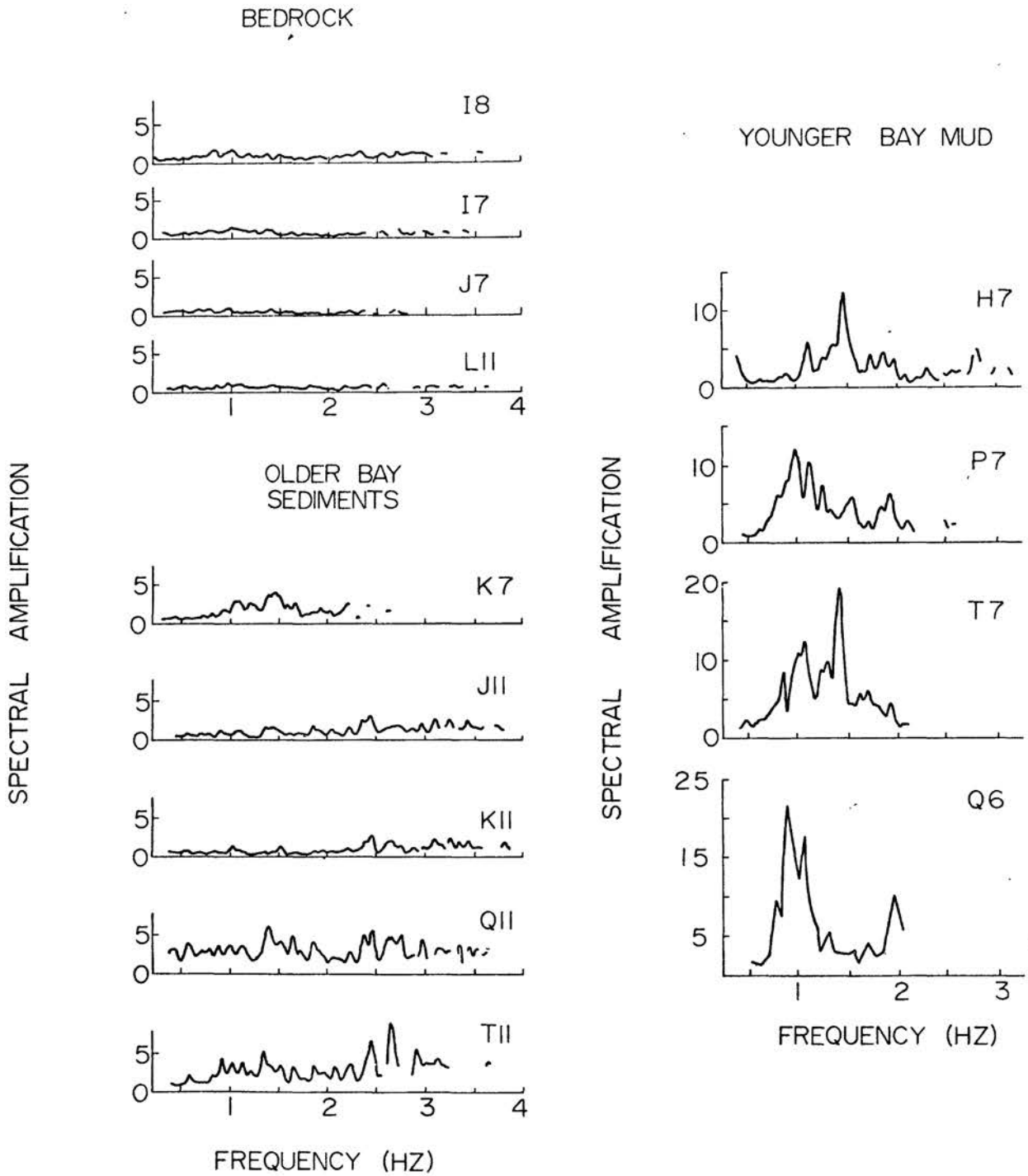
BEDROCK
I8
I7
J7
LII
OLDER BAY SEDIMENTS
K7
JII
KII
QII
TII
YOUNGER BAY MUD
H7
P7
T7
Q6
SPECTRAL AMPLIFICATION
FREQUENCY (HZ)

Figure 42

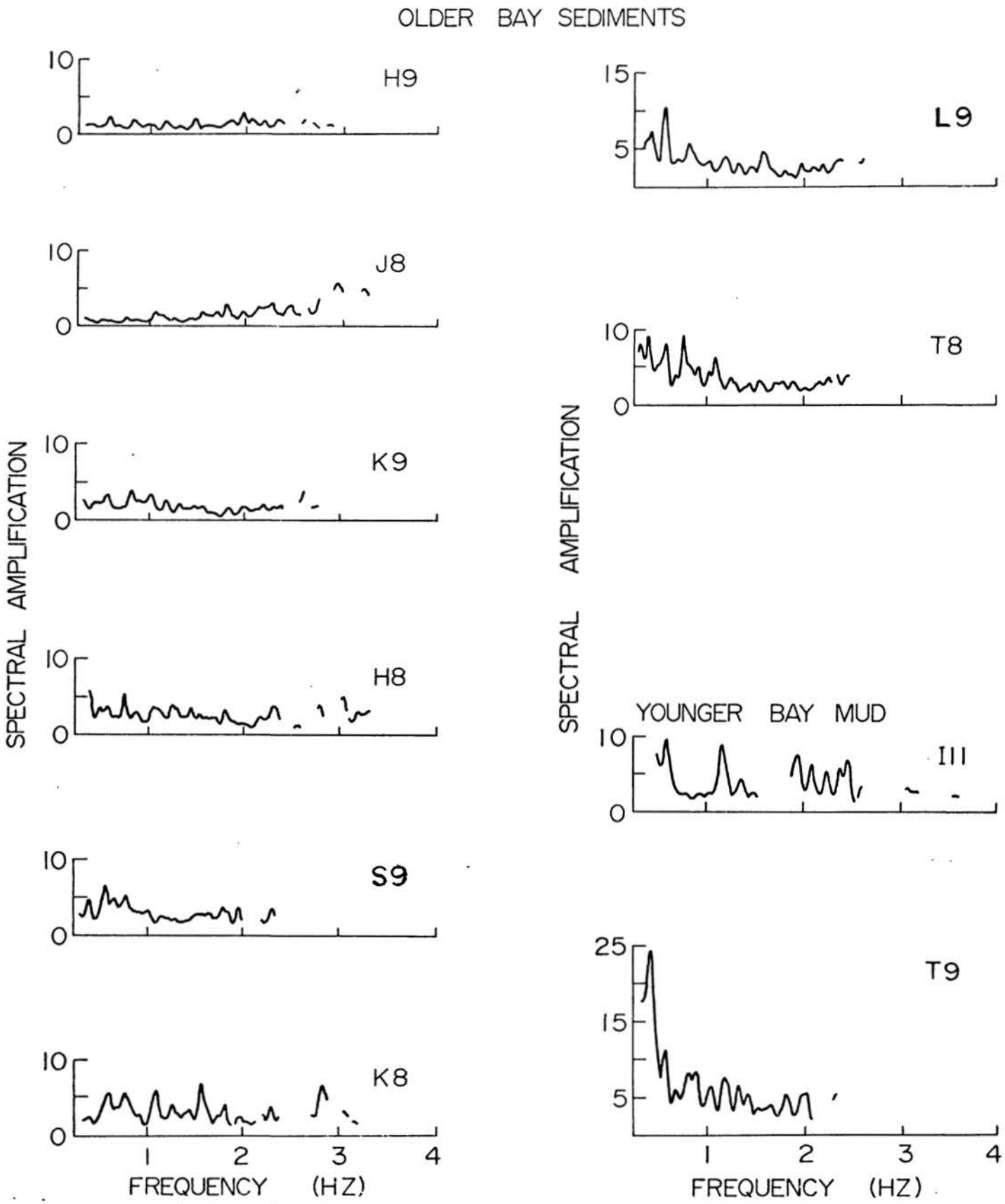
OLDER BAY SEDIMENTS
H9
J8
K9
H8
S9
K8
L9
T8
YOUNGER BAY MUD
III
T9
SPECTRAL AMPLIFICATION
SPECTRAL AMPLIFICATION
FREQUENCY (HZ)
FREQUENCY (HZ)

Figure 43

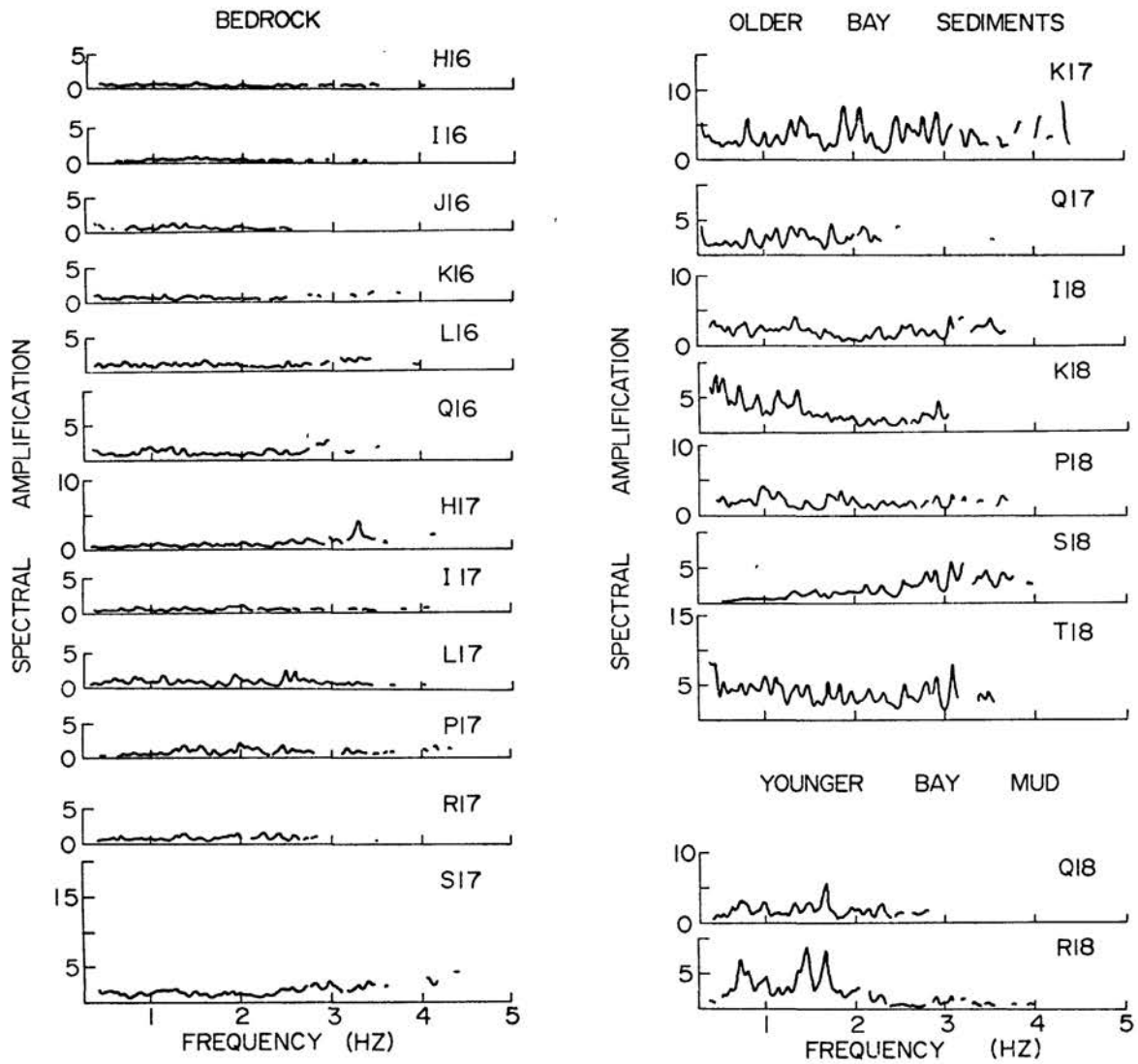
BEDROCK
OLDER BAY SEDIMENTS
YOUNGER BAY MUD
SPECTRAL AMPLIFICATION
H16
I16
J16
K16
L16
Q16
H17
I17
L17
P17
R17
S17
K17
Q17
I18
K18
P18
S18
T18
Q18
R18
FREQUENCY (HZ)

Figure 44

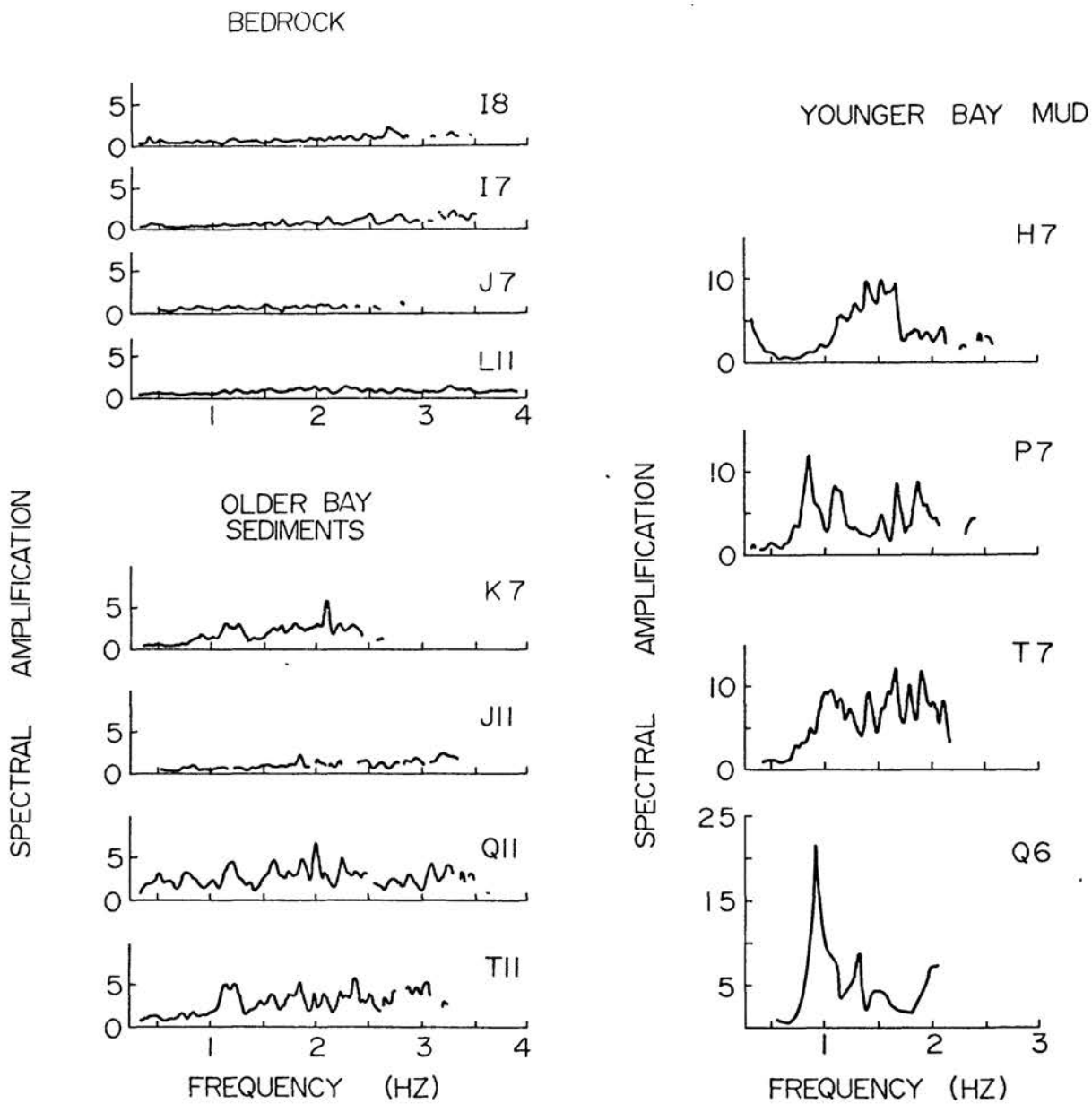
BEDROCK
I8
I7
J7
LII
OLDER BAY SEDIMENTS
K7
JII
QII
TII
YOUNGER BAY MUD
H7
P7
T7
Q6
SPECTRAL AMPLIFICATION
FREQUENCY (HZ)

Figure 45

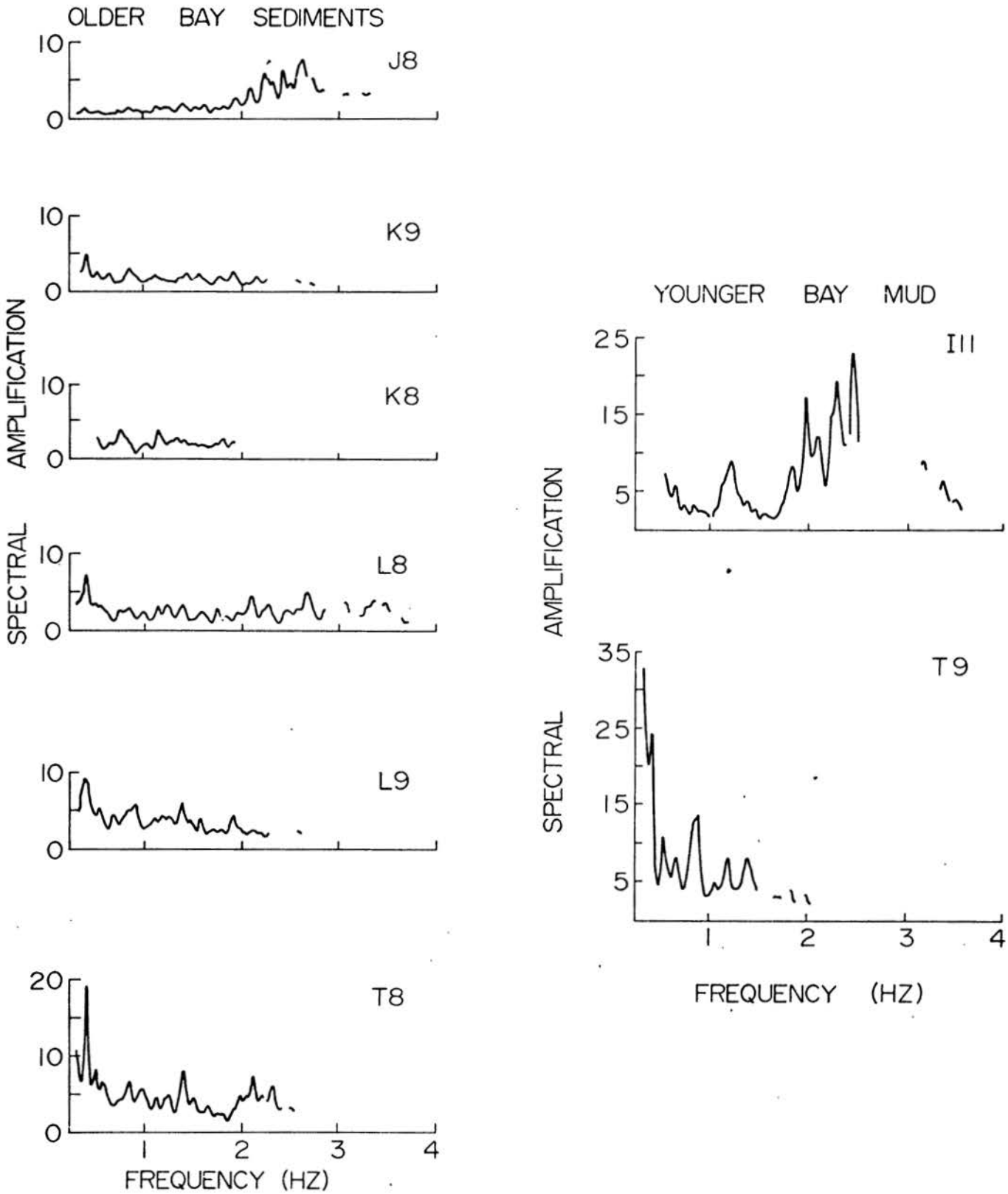
OLDER BAY SEDIMENTS
J8
K9
K8
L8
L9
T8
SPECTRAL AMPLIFICATION
FREQUENCY (HZ)
YOUNGER BAY MUD
I11
T9
SPECTRAL AMPLIFICATION
FREQUENCY (HZ)

Figure 46

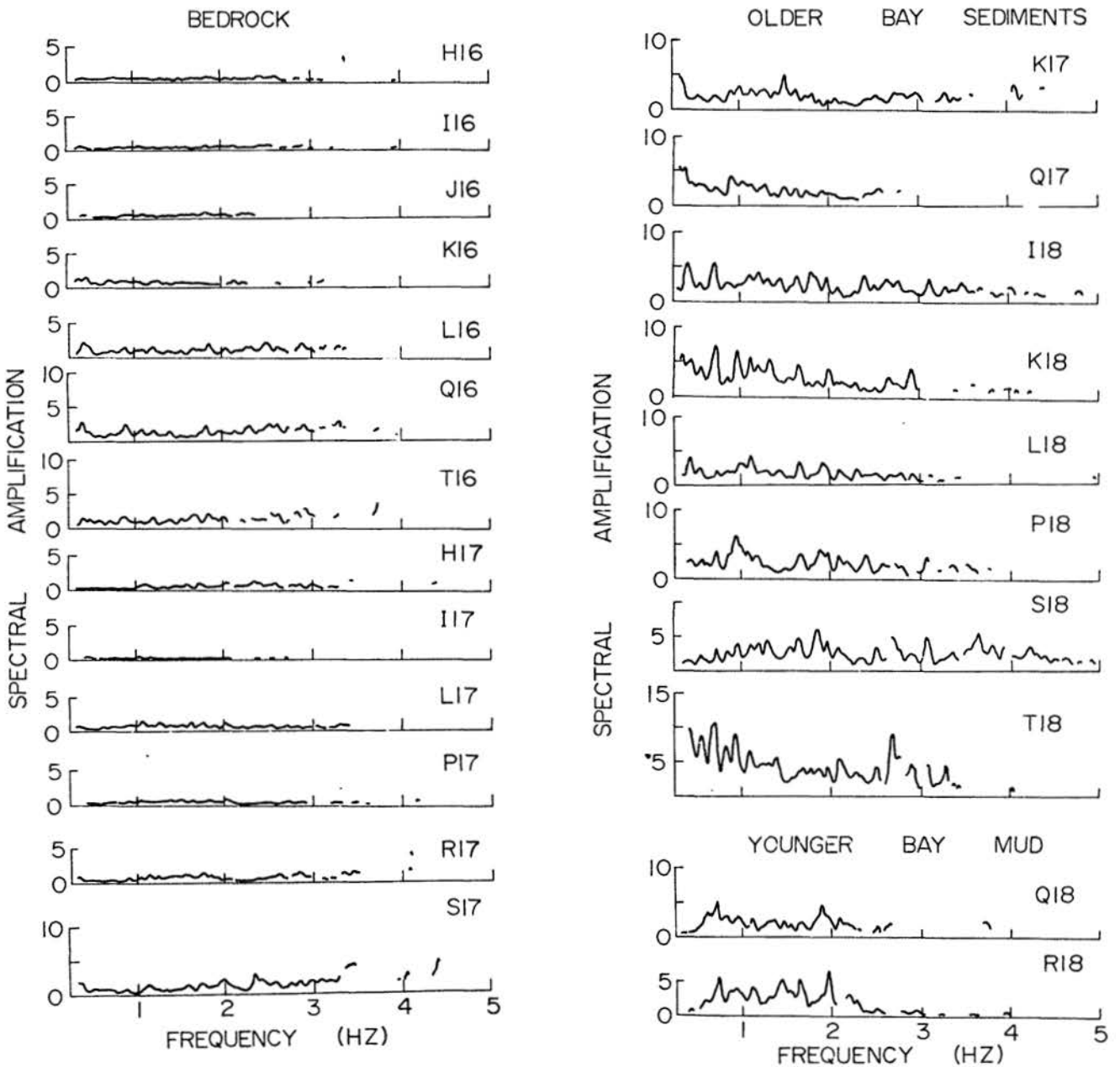
BEDROCK
H16
I16
J16
K16
L16
Q16
T16
H17
I17
L17
P17
R17
S17
SPECTRAL AMPLIFICATION
FREQUENCY (HZ)
OLDER BAY SEDIMENTS
K17
Q17
I18
K18
L18
P18
S18
T18
YOUNGER BAY MUD
Q18
R18
SPECTRAL AMPLIFICATION
FREQUENCY (HZ)

Figure 47

Figure 48

Average Horizontal Spectral Amplification on Geologic Map

(in map pouch)

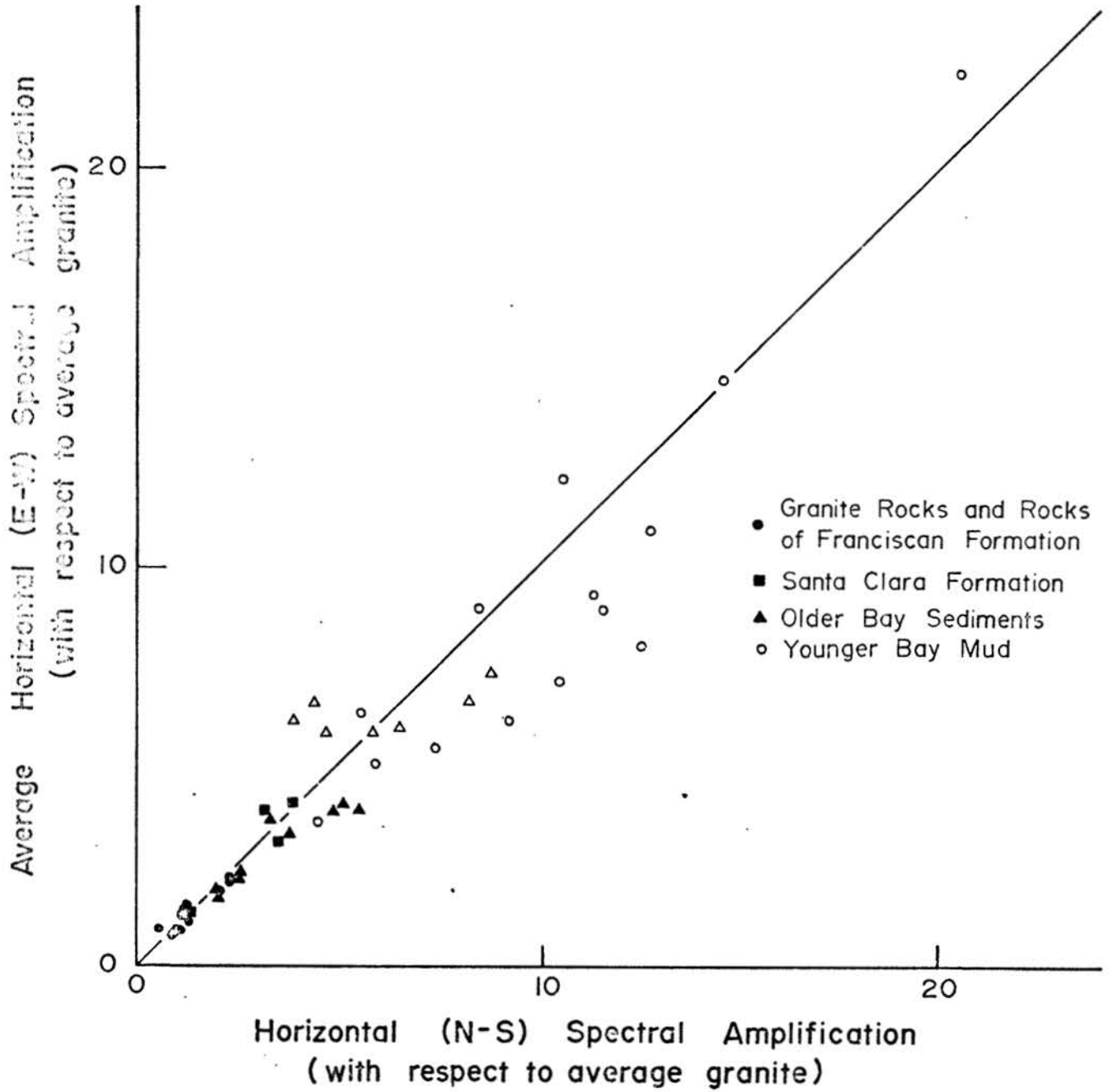
Average Horizontal (E-W) Spectral Amplification
(with respect to average granite)
20
10
0
0
10
20
Horizontal (N-S) Spectral Amplification
(with respect to average granite)
Granite Rocks and Rocks of Franciscan Formation
Santa Clara Formation
Older Bay Sediments
Younger Bay Mud

Figure 49

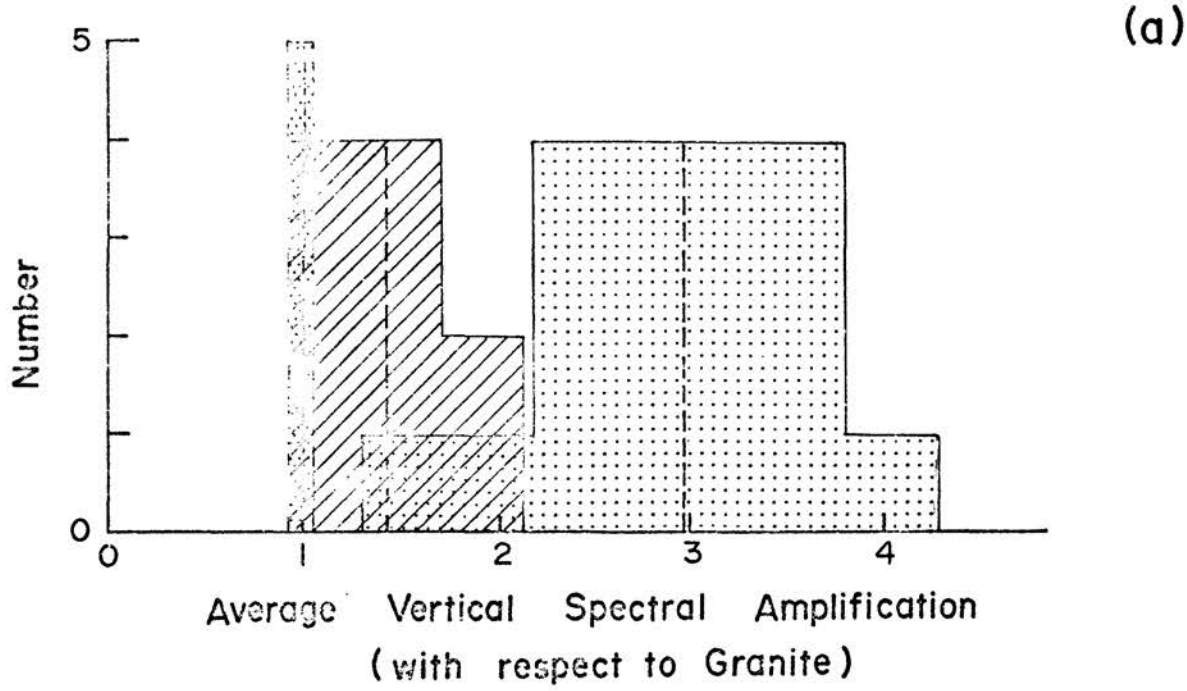
(a)
5
0
Number
0
1
2
3
4
Average Vertical Spectral Amplification
(with respect to Granite)

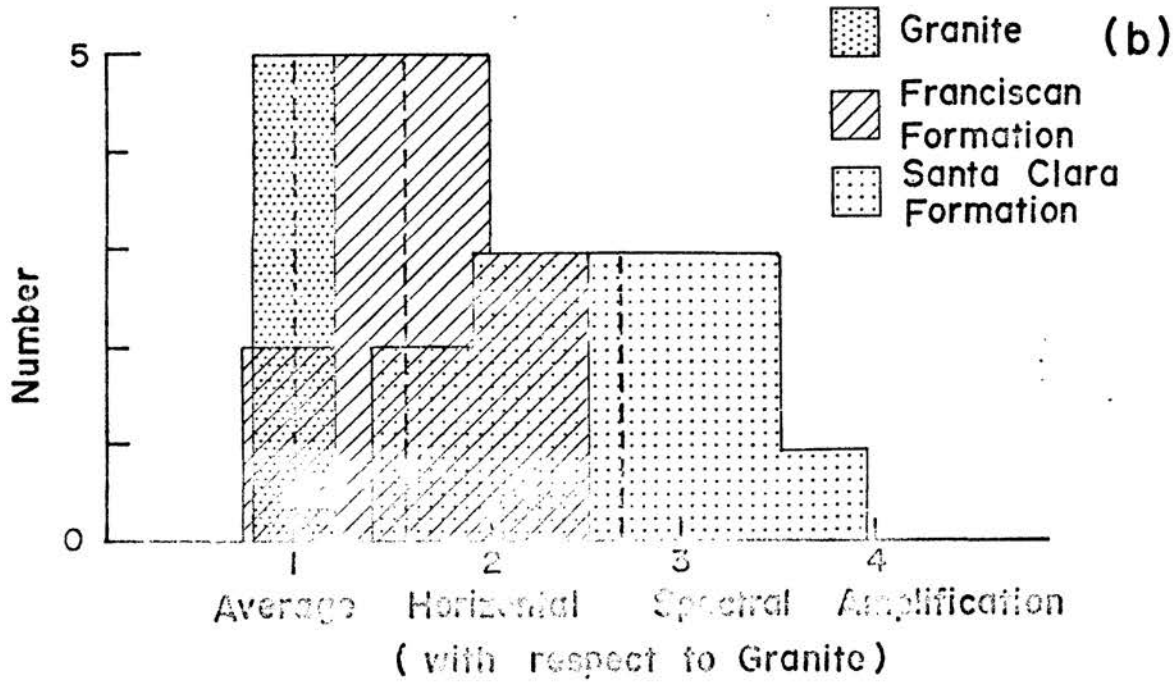
Granite
Franciscan Formation
Santa Clara Formation
(b)
5
0
Number
1
2
3
4
Average Horizontal Spectral Amplification
(with respect to Granite)

Figure 50

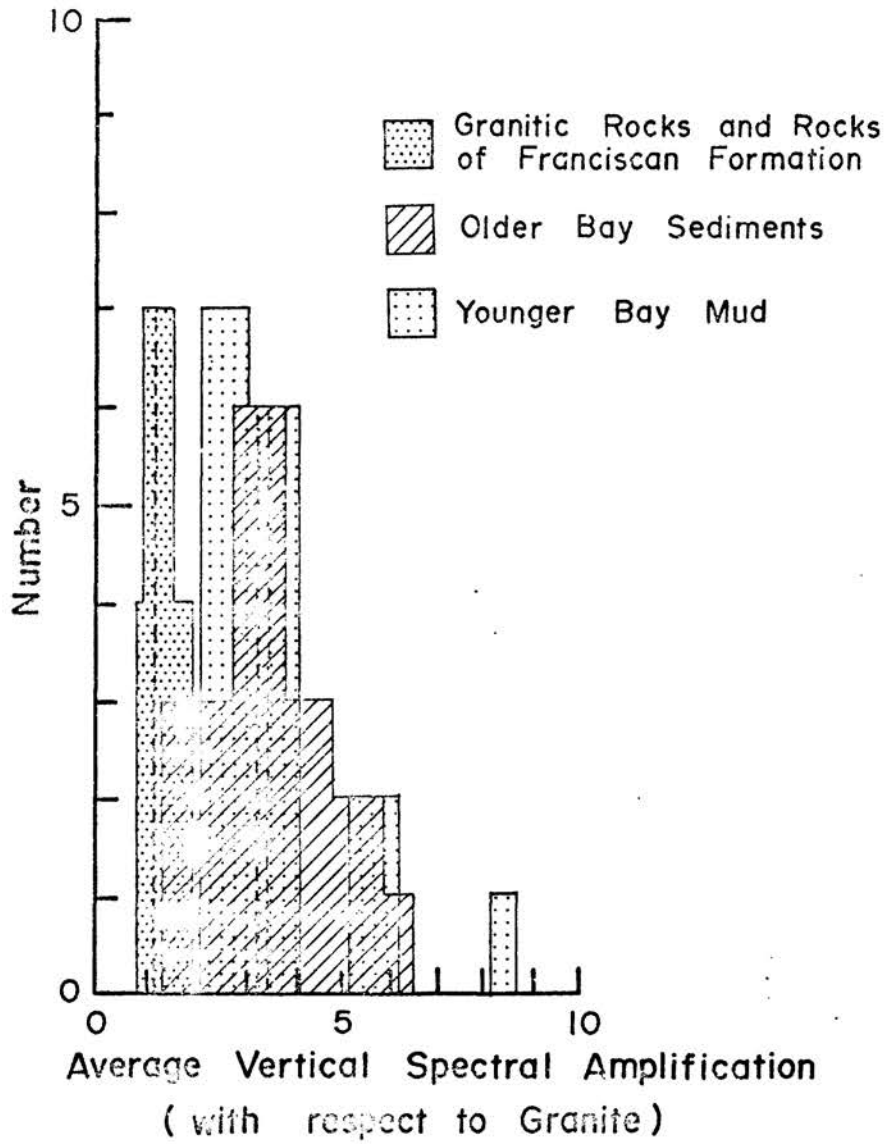
10
5
0
Number
Granitic Rocks and Rocks of Franciscan Formation
Older Bay Sediments
Younger Bay Mud
0
5
10
Average Vertical Spectral Amplification
(with respect to Granite)

Figure 51

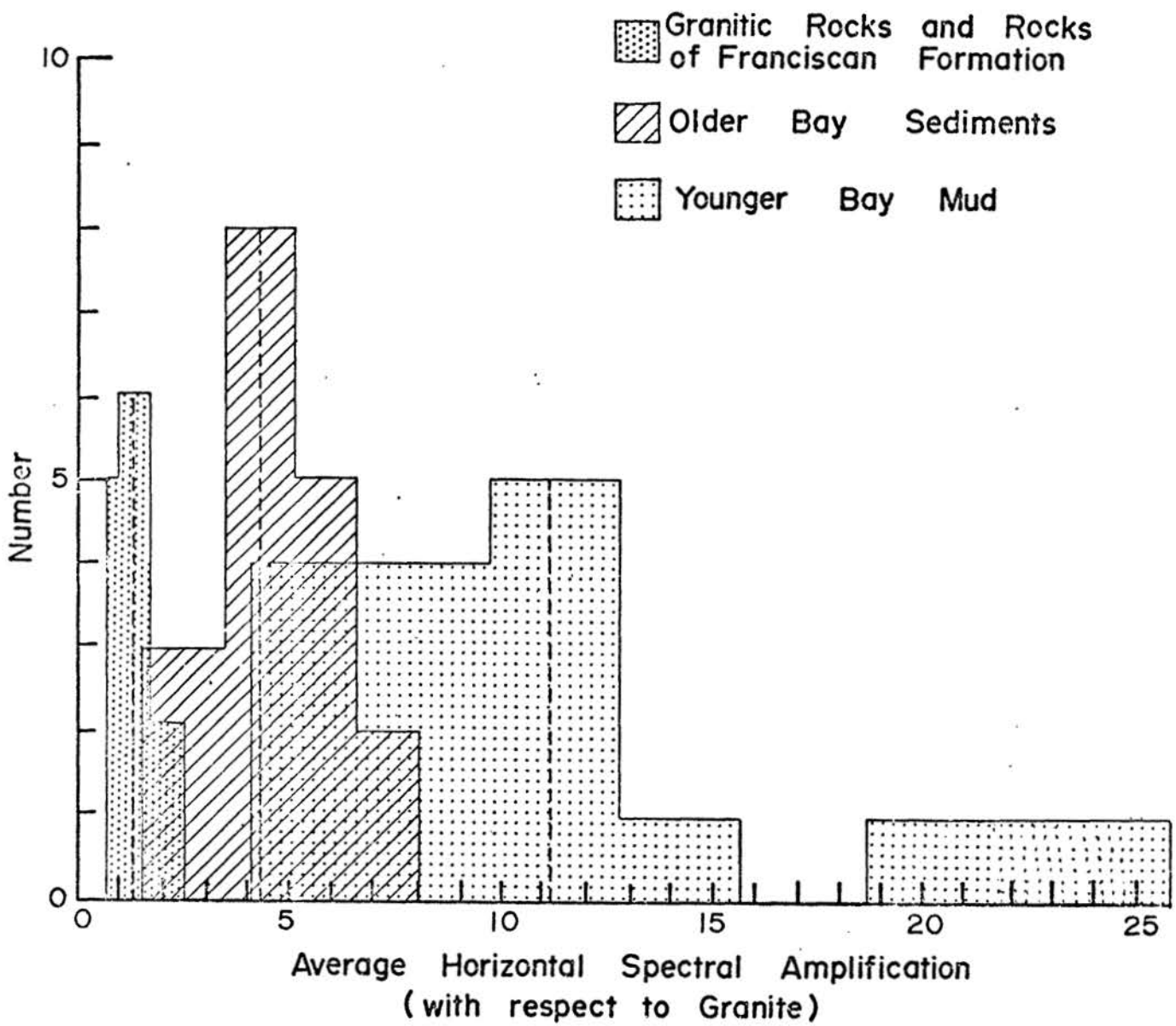
Granitic Rocks and Rocks of Franciscan Formation
Older Bay Sediments
Younger Bay Mud
Number
10
5
0
0
5
10
15
20
25
Average Horizontal Spectral Amplification
(with respect to Granite)

Figure 52

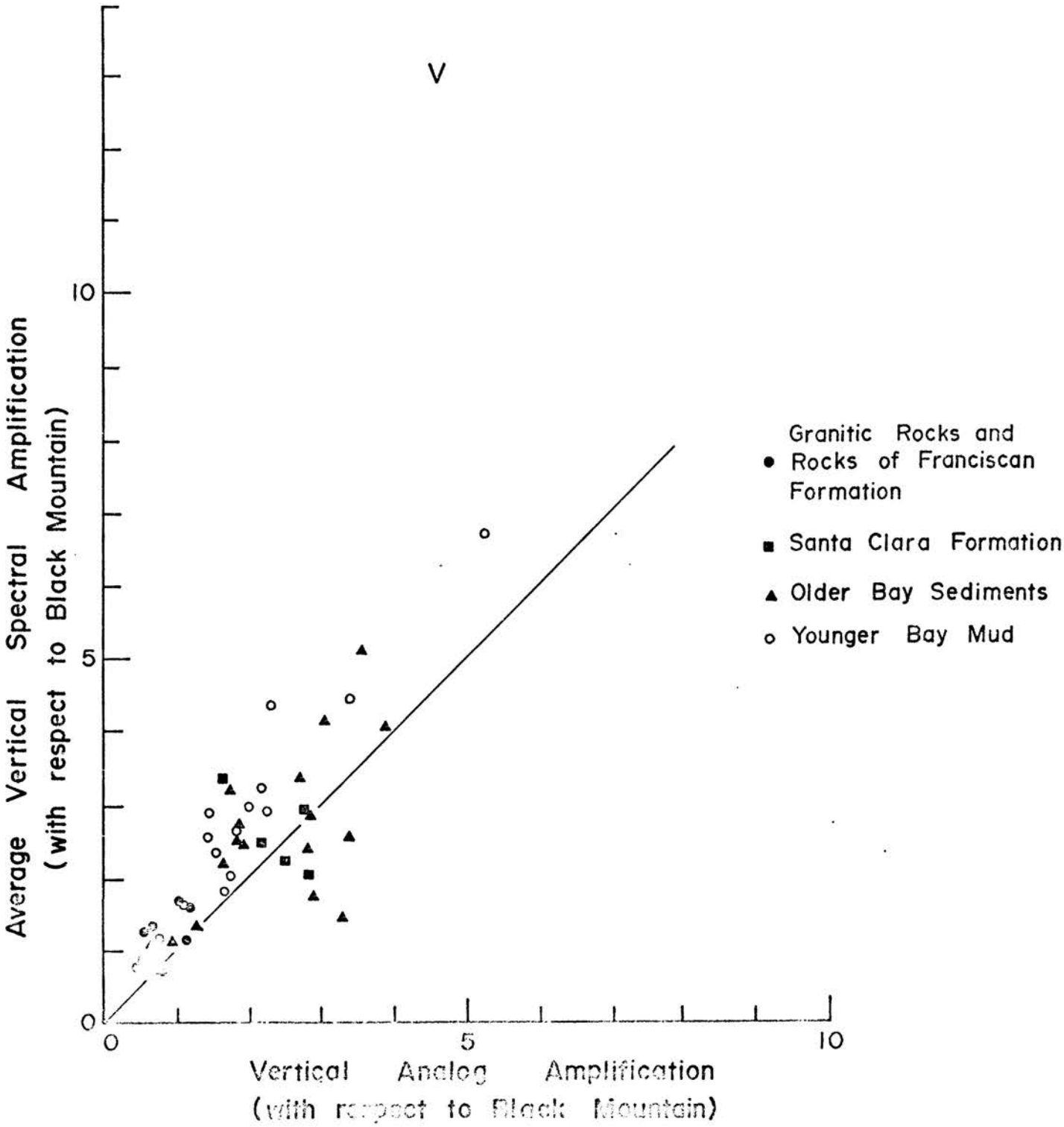
V
10
5
0
0
5
10
Average Vertical Spectral Amplification
(with respect to Black Mountain)
Vertical Analog Amplification
(with respect to Black Mountain)
Granitic Rocks and Rocks of Franciscan Formation
Santa Clara Formation
Older Bay Sediments
Younger Bay Mud

Figure 53

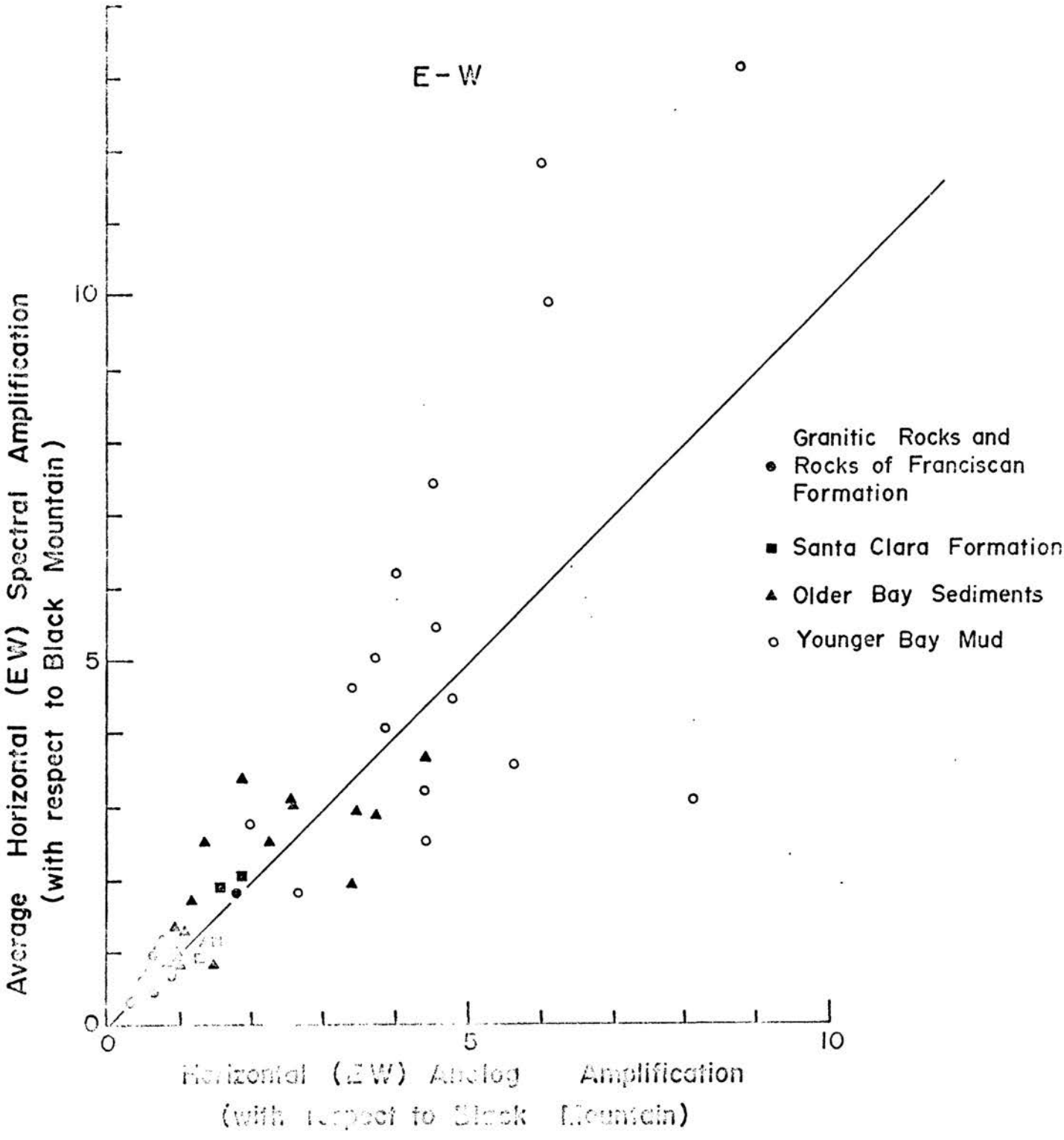
E-W
Average Horizontal (EW) Spectral Amplification
(with respect to Black Mountain)
10
5
0
0
5
10
Horizontal (EW) Analog Amplification
(with respect to Black Mountain)
Granitic Rocks and Rocks of Franciscan Formation
Santa Clara Formation
Older Bay Sediments
Younger Bay Mud

Figure 54

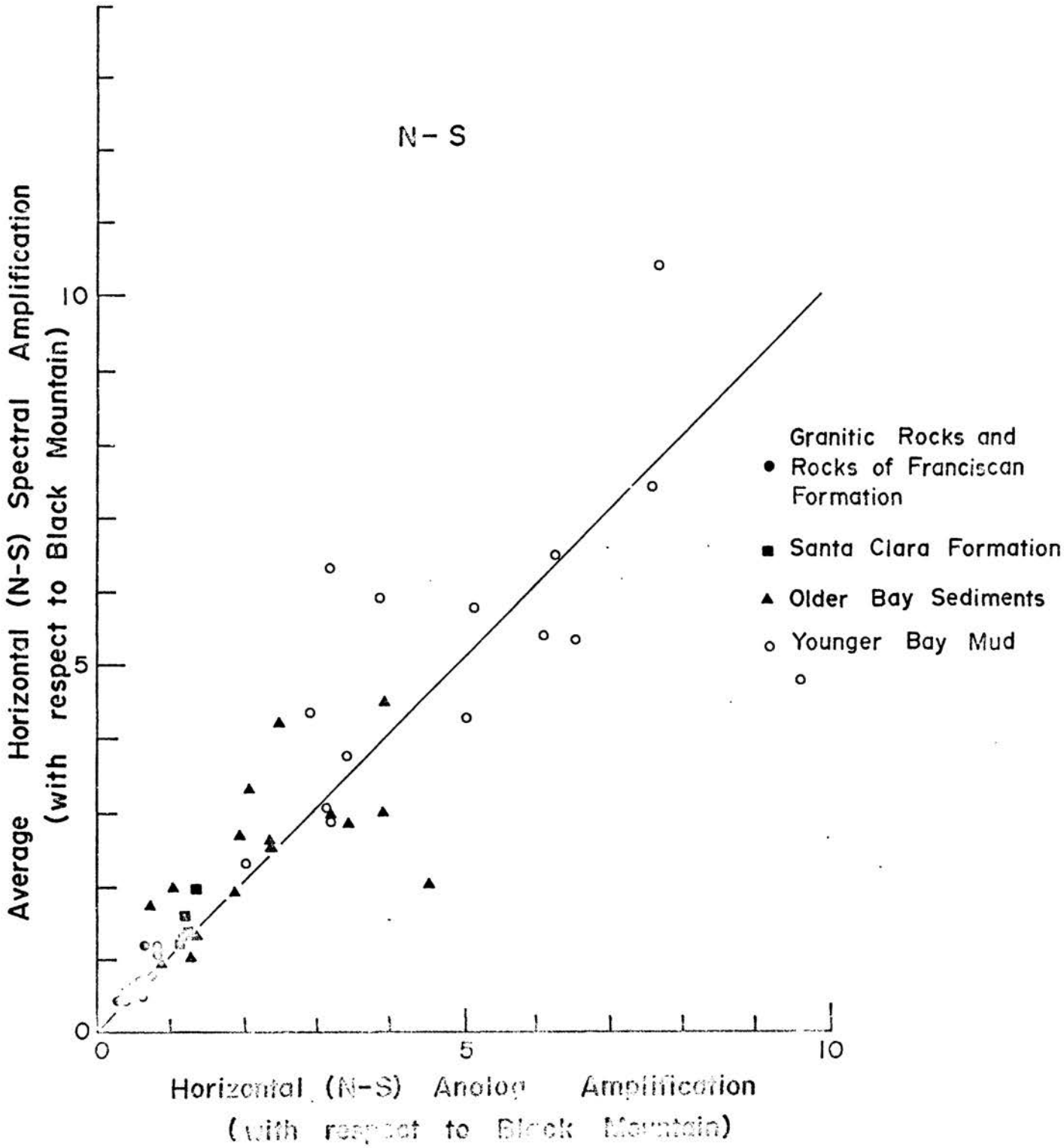
N - S
Average Horizontal (N-S) Spectral Amplification
(with respect to Black Mountain)
0
5
10
Granitic Rocks and
Rocks of Franciscan
Formation
Santa Clara Formation
Older Bay Sediments
Younger Bay Mud
0
5
10
Horizontal (N-S) Analog Amplification
(with respect to Black Mountain)

Figure 55

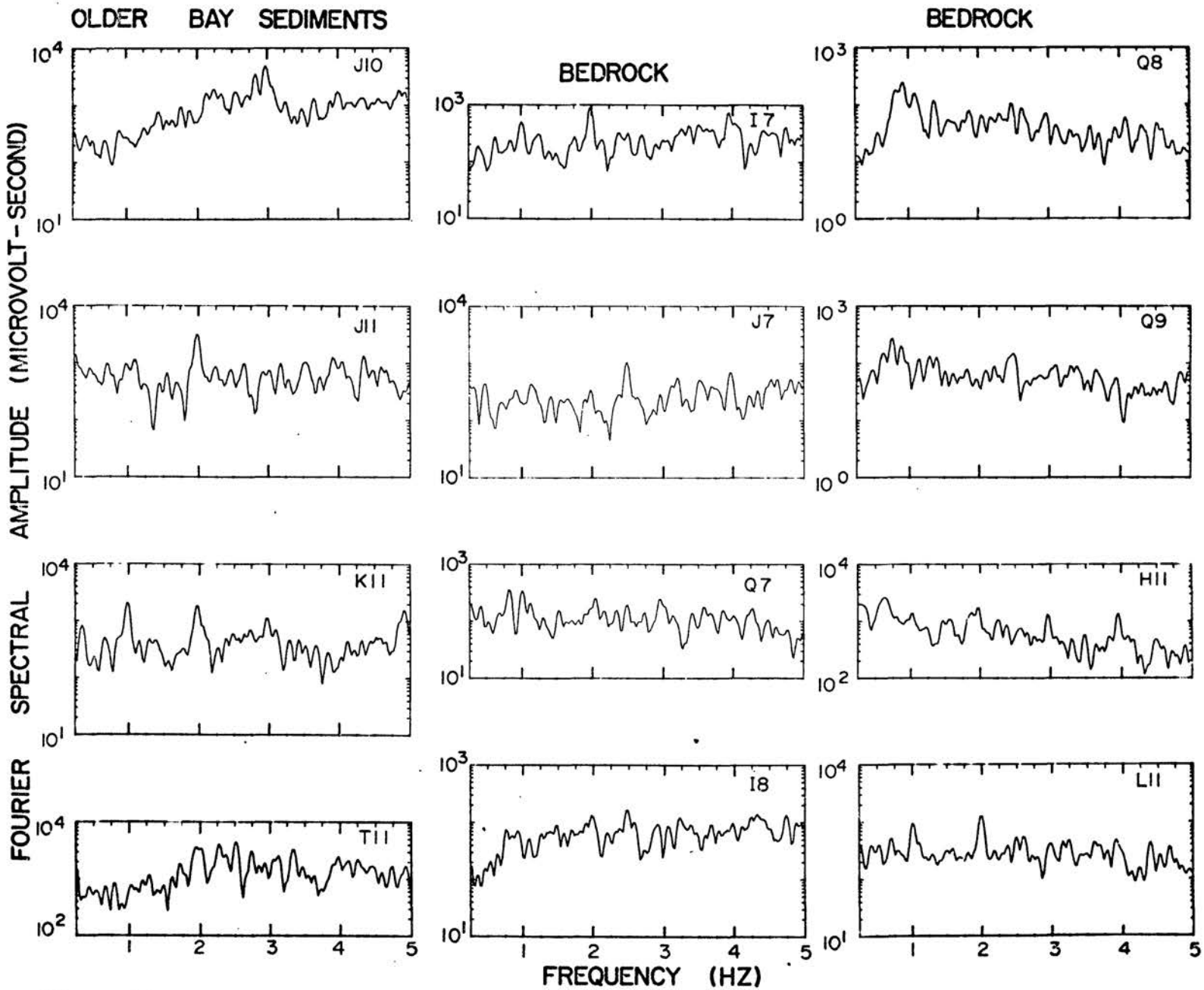
OLDER BAY SEDIMENTS
BEDROCK
BEDROCK
FOURIER SPECTRAL AMPLITUDE (MICROVOLT-SECOND)
FREQUENCY (HZ)
J10
I7
Q8
J11
J7
Q9
K11
Q7
H11
T11
I8
L11

Figure 56

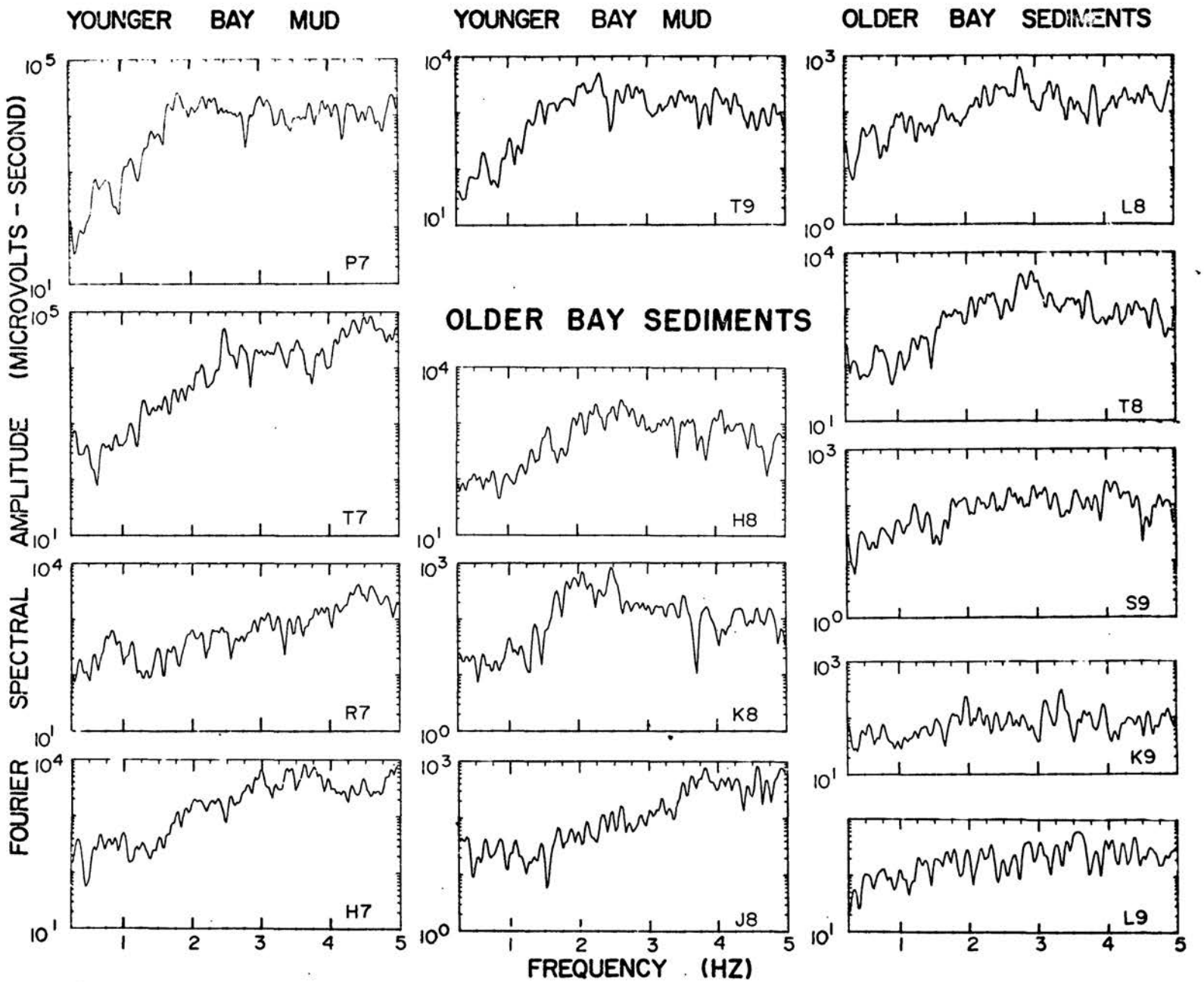
YOUNGER BAY MUD
YOUNGER BAY MUD
OLDER BAY SEDIMENTS
OLDER BAY SEDIMENTS
FOURIER SPECTRAL AMPLITUDE (MICROVOLTS - SECOND)
P7
T7
R7
H7
T9
H8
K8
J8
L8
T8
S9
K9
L9
FREQUENCY (HZ)

Figure 57

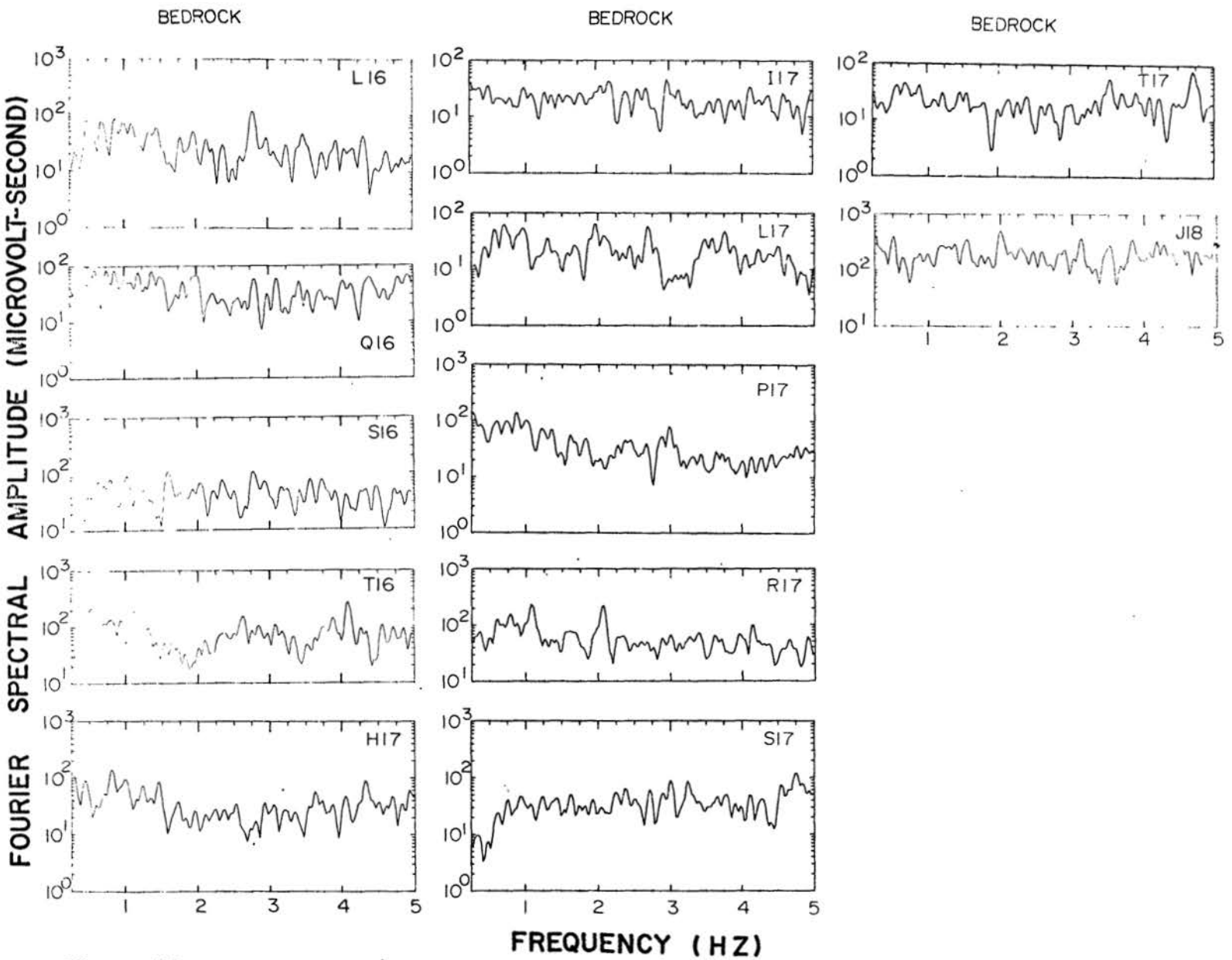
BEDROCK
BEDROCK
BEDROCK
L16
Q16
S16
T16
H17
I17
L17
P17
R17
S17
T17
J18
FOURIER SPECTRAL AMPLITUDE (MICROVOLT-SECOND)
FREQUENCY (HZ)

Figure 58

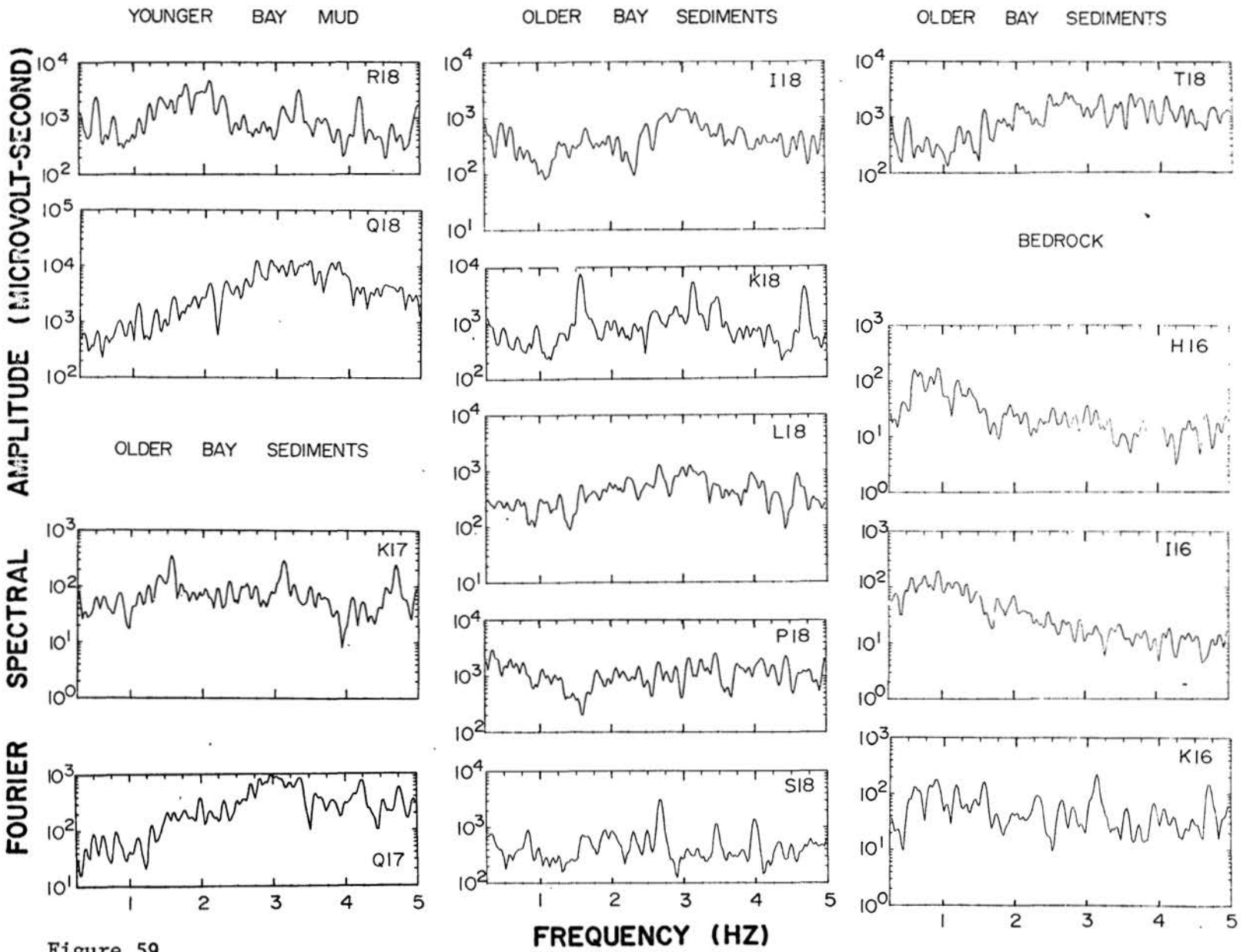
YOUNGER BAY MUD
OLDER BAY SEDIMENTS
OLDER BAY SEDIMENTS
OLDER BAY SEDIMENTS
BEDROCK
FOURIER SPECTRAL AMPLITUDE (MICROVOLT-SECOND)
R18
Q18
K17
Q17
I18
K18
L18
P18
S18
T18
H16
I16
K16
FREQUENCY (HZ)

Figure 59

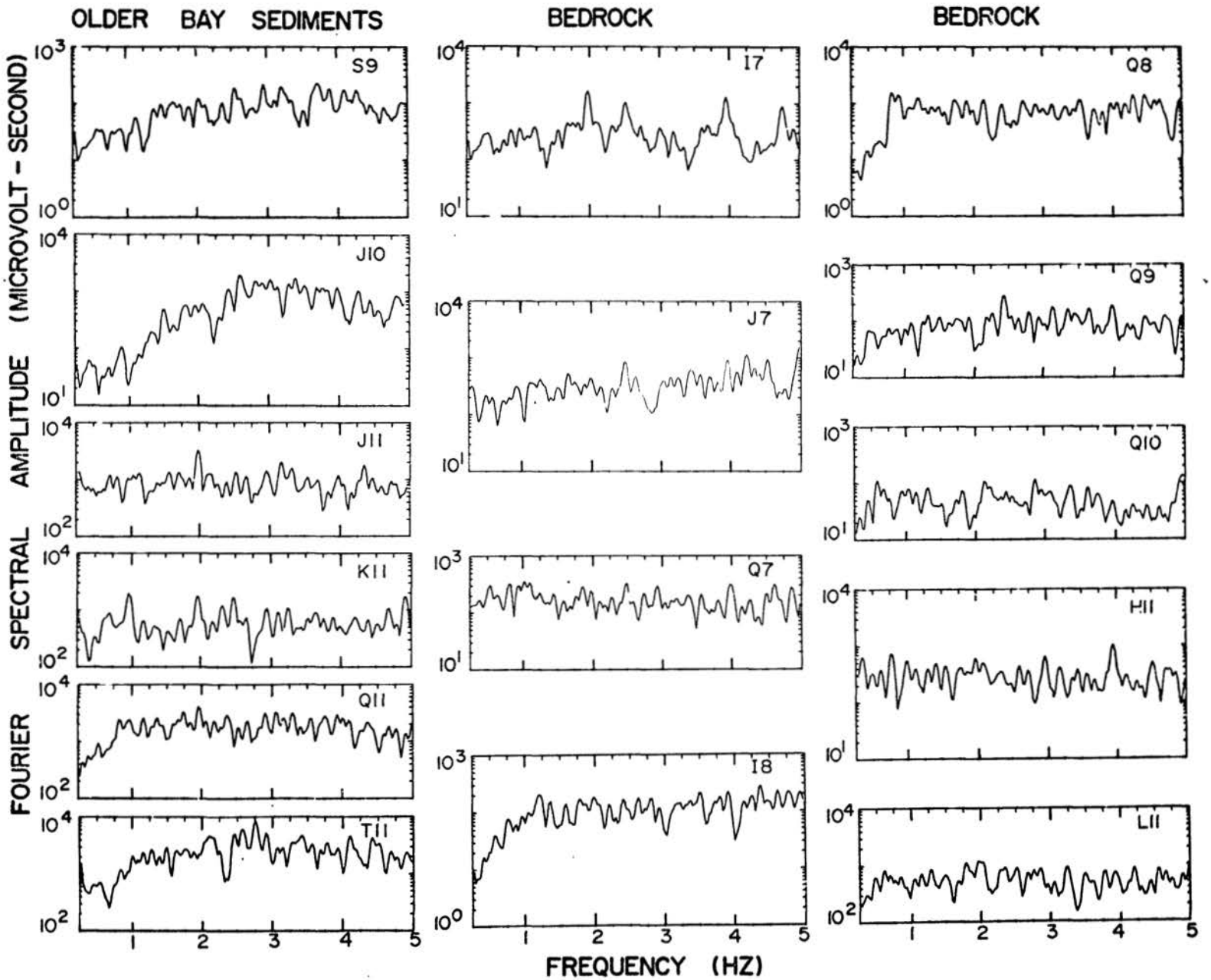
OLDER BAY SEDIMENTS
BEDROCK
BEDROCK
SPECTRAL AMPLITUDE (MICROVOLT - SECOND)
FOURIER
S9
J10
J11
K11
Q11
T11
I7
J7
Q7
I8
Q8
Q9
Q10
H11
L11
FREQUENCY (HZ)

Figure 60

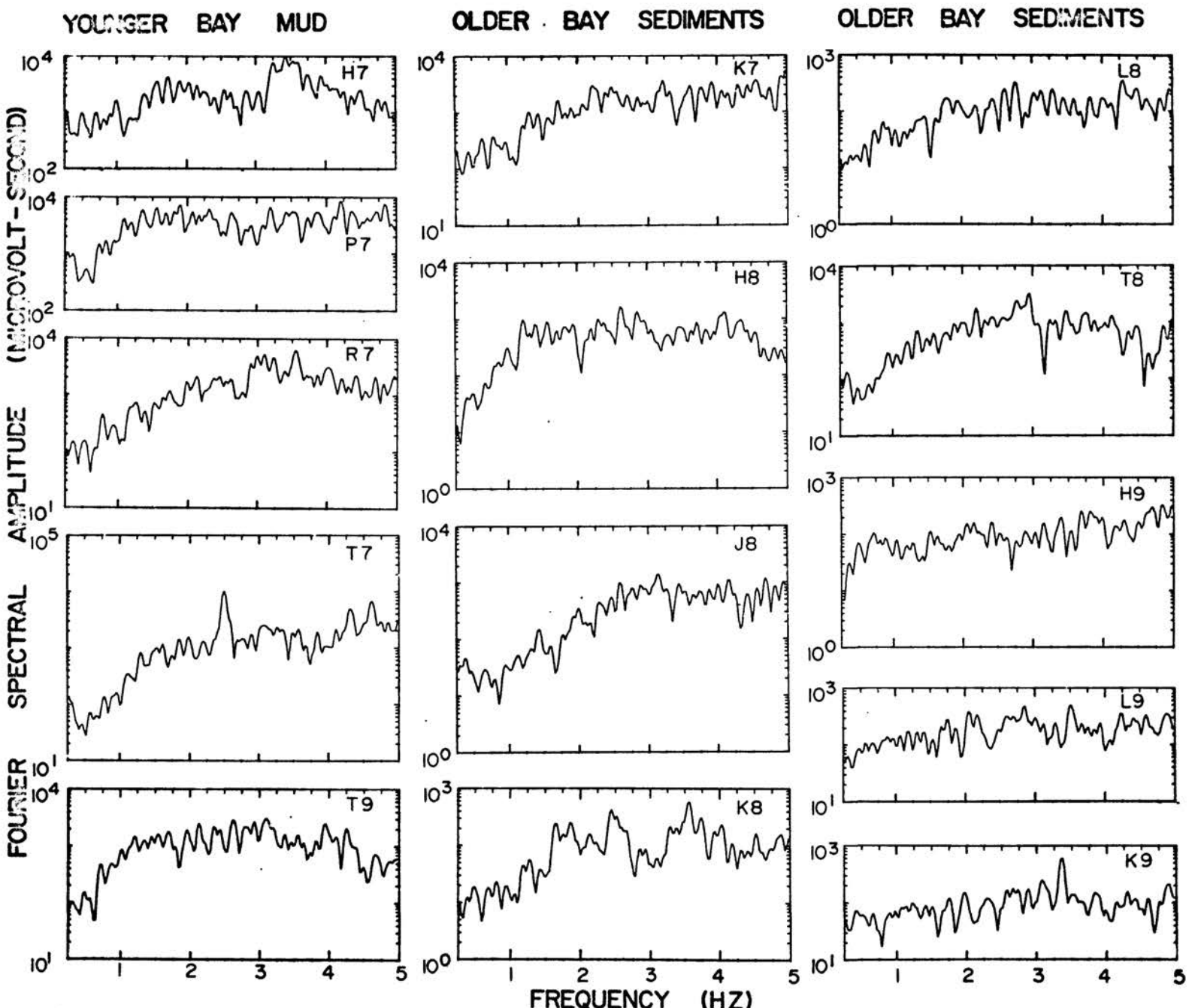
YOUNGER BAY MUD
OLDER BAY SEDIMENTS
OLDER BAY SEDIMENTS
FOURIER SPECTRAL AMPLITUDE (MICROVOLT-SECOND)
H7
P7
R7
T7
T9
K7
H8
J8
K8
L8
T8
H9
L9
K9
FREQUENCY (HZ)

Figure 61

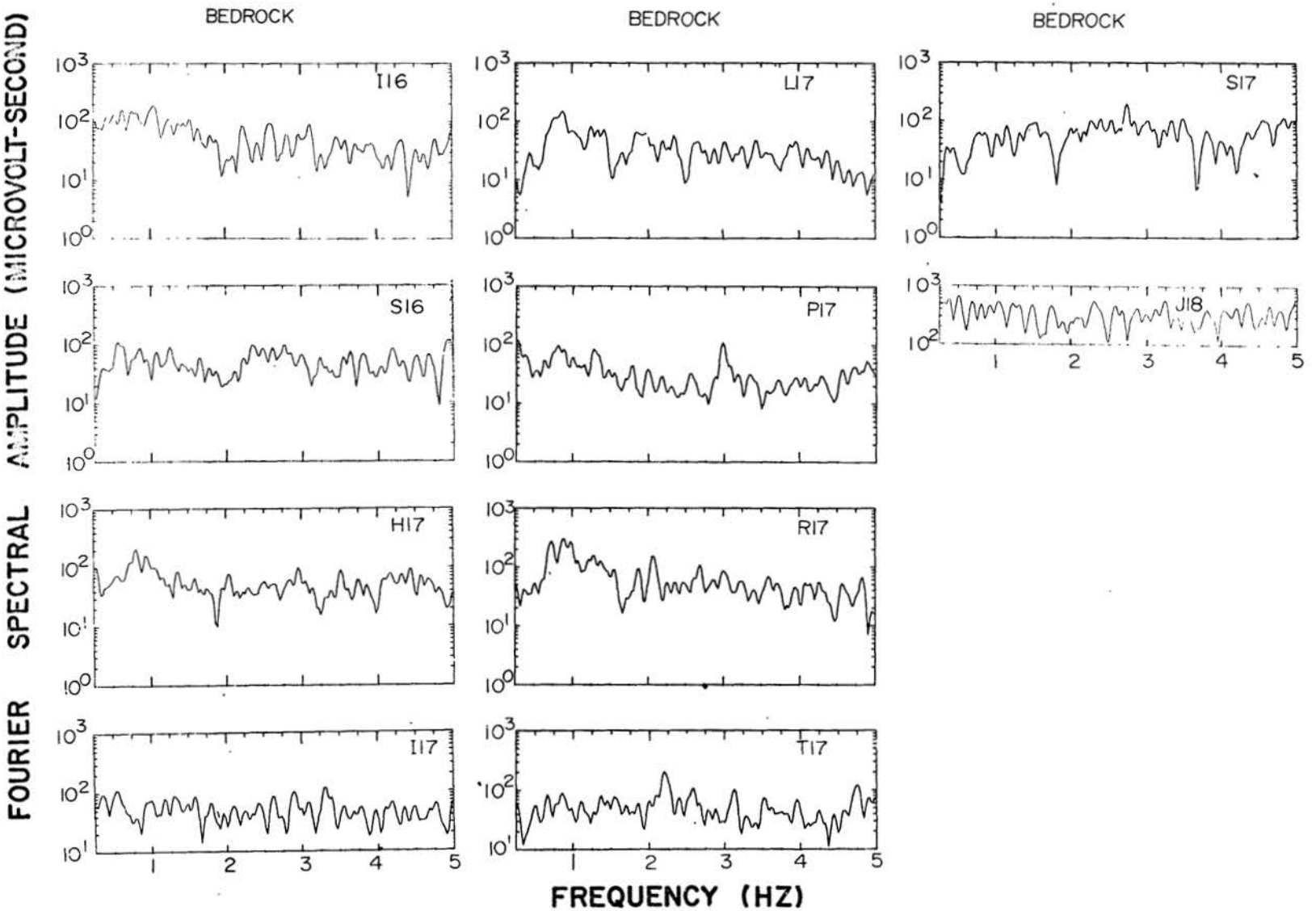
BEDROCK
BEDROCK
BEDROCK
FOURIER SPECTRAL AMPLITUDE (MICROVOLT-SECOND)
I16
L17
S17
S16
P17
J18
H17
R17
I17
T17
FREQUENCY (HZ)

Figure 62

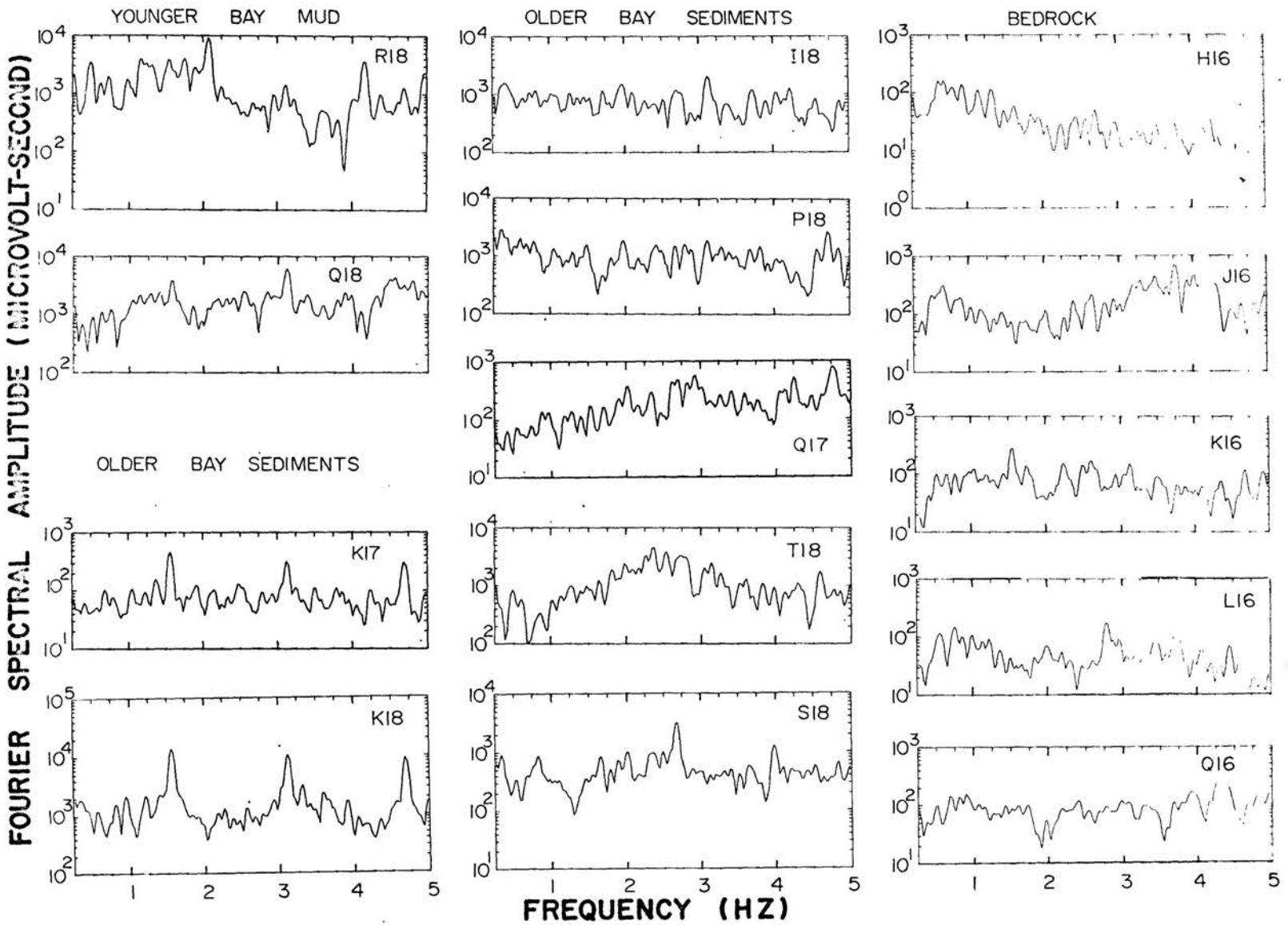
YOUNGER BAY MUD
OLDER BAY SEDIMENTS
BEDROCK
R18
Q18
K17
K18
I18
P18
Q17
T18
S18
H16
J16
K16
L16
Q16
FOURIER SPECTRAL AMPLITUDE (MICROVOLT-SECOND)
FREQUENCY (HZ)

Figure 63

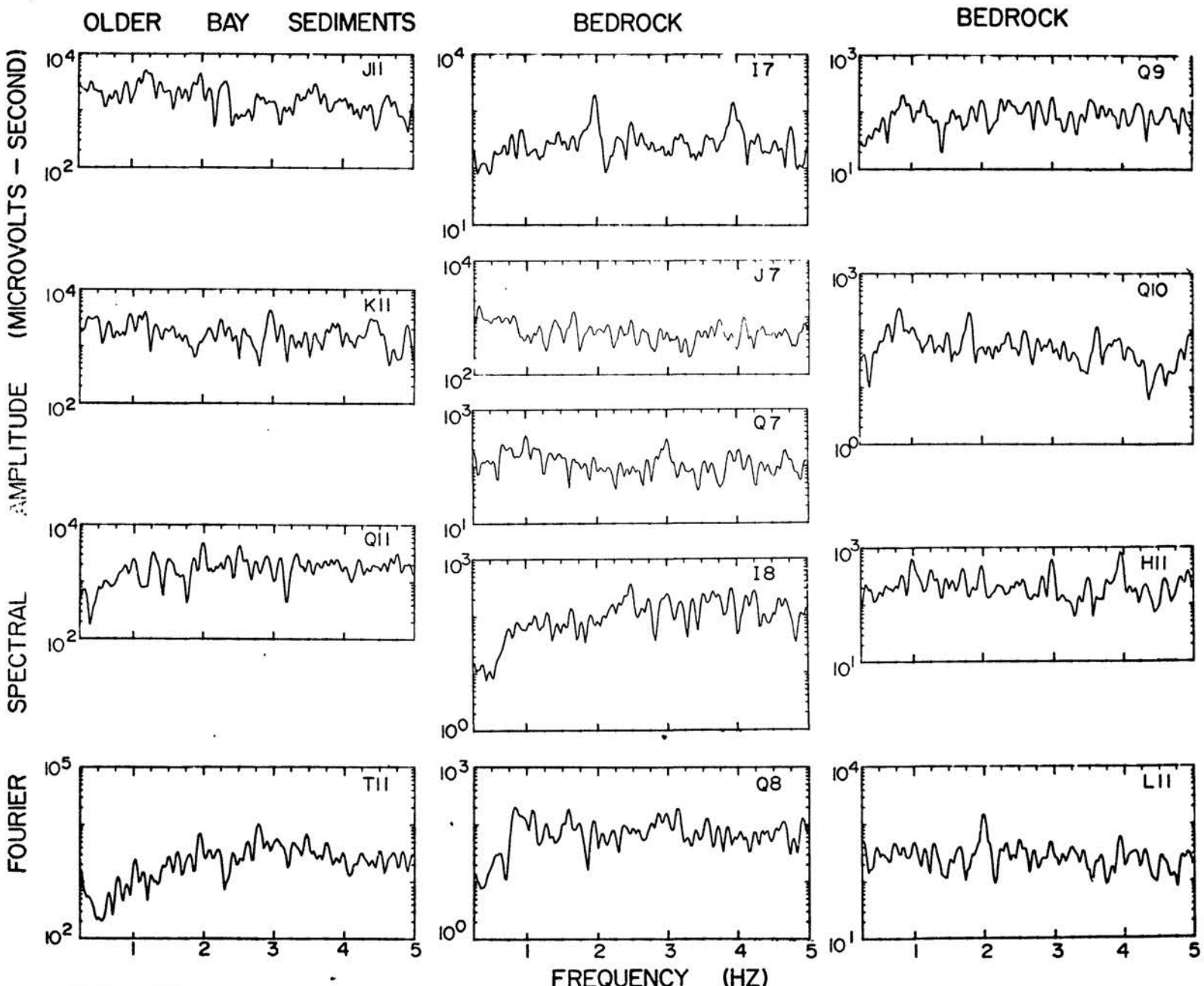
OLDER BAY SEDIMENTS
BEDROCK
BEDROCK
FOURIER SPECTRAL AMPLITUDE (MICROVOLTS – SECOND)
J11
K11
Q11
T11
I7
J7
Q7
I8
Q8
Q9
Q10
H11
L11
FREQUENCY (HZ)

Figure 64

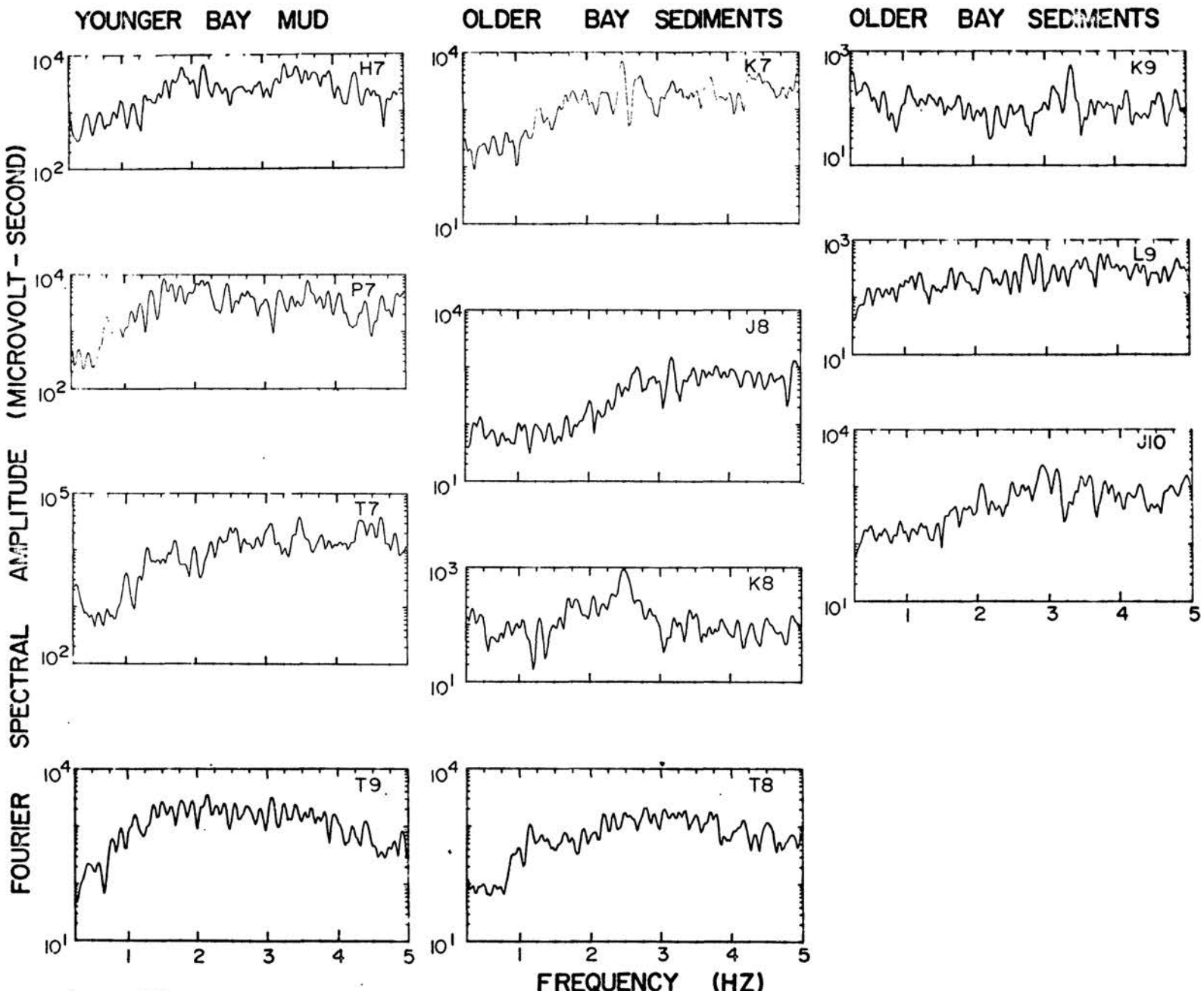
YOUNGER BAY MUD
OLDER BAY SEDIMENTS
OLDER BAY SEDIMENTS
FOURIER SPECTRAL AMPLITUDE (MICROVOLT - SECOND)
H7
P7
T7
T9
K7
J8
K8
T8
K9
L9
J10
FREQUENCY (HZ)

Figure 65

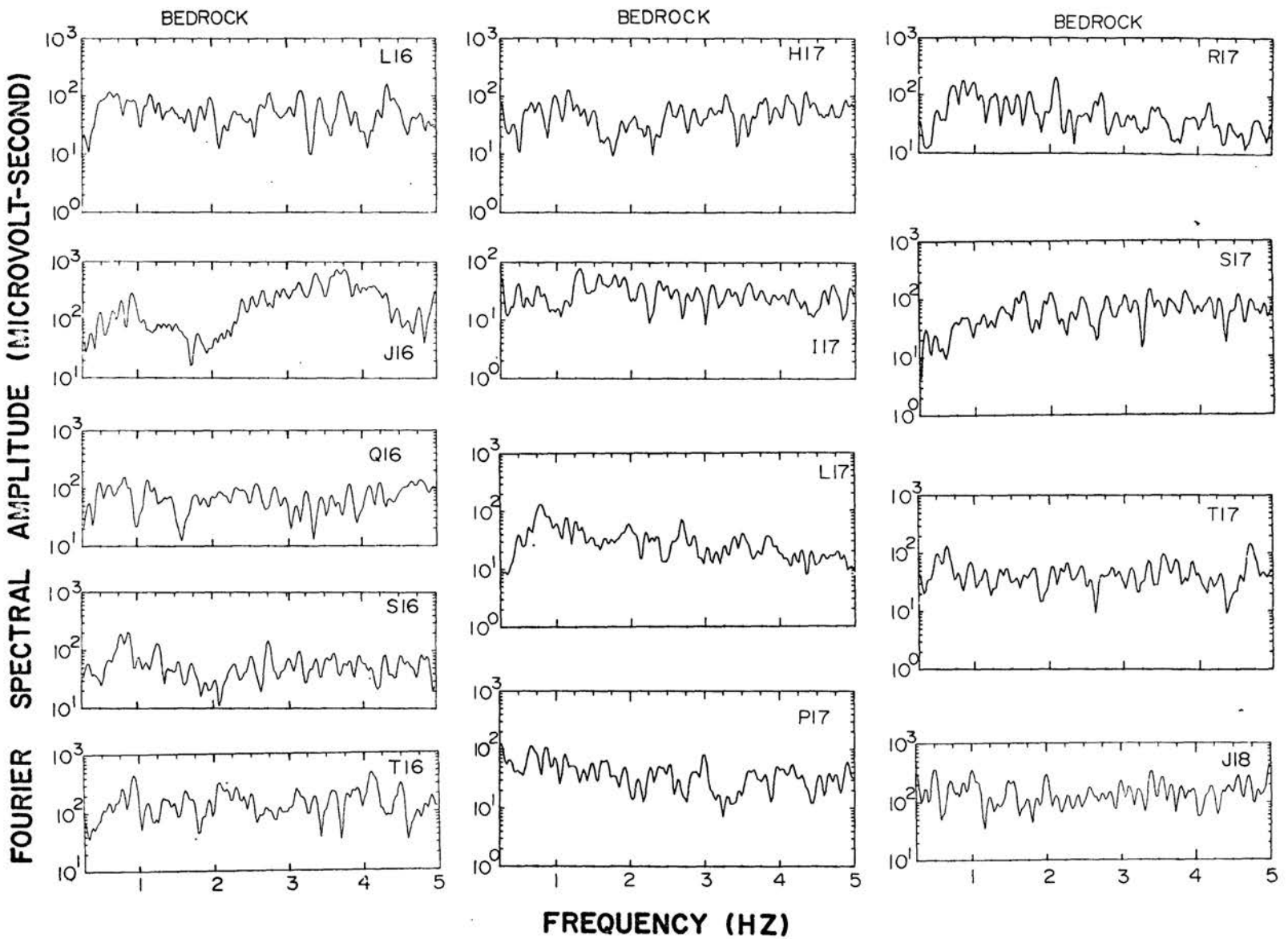
BEDROCK
BEDROCK
BEDROCK
L16
J16
Q16
S16
T16
H17
I17
L17
P17
R17
S17
T17
J18
FOURIER SPECTRAL AMPLITUDE (MICROVOLT-SECOND)
FREQUENCY (HZ)

Figure 66

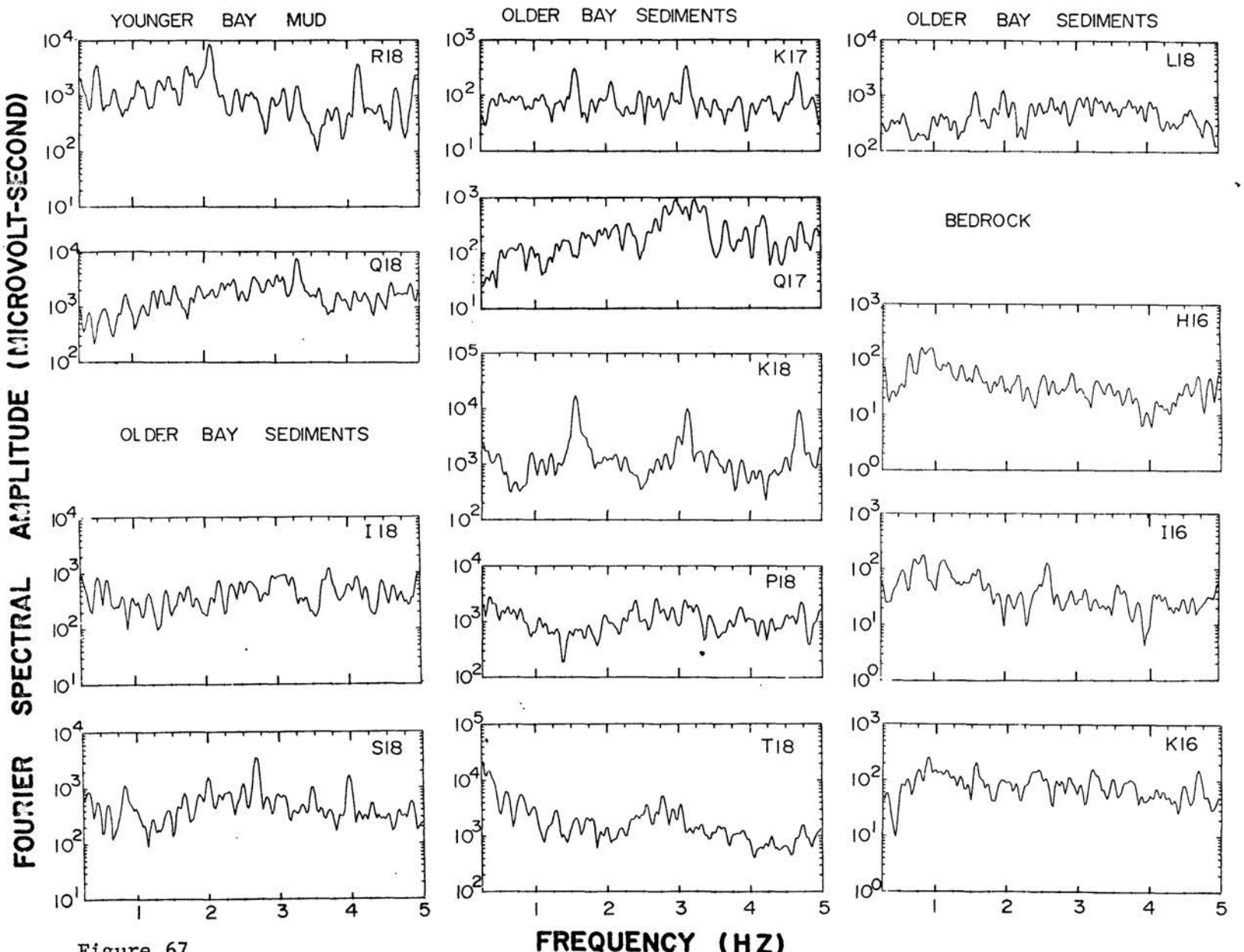
YOUNGER BAY MUD
R18
Q18
OLDER BAY SEDIMENTS
I18
S18
OLDER BAY SEDIMENTS
K17
Q17
K18
P18
T18
OLDER BAY SEDIMENTS
L18
BEDROCK
H16
I16
K16
FOURIER SPECTRAL AMPLITUDE (MICROVOLT-SECOND)
FREQUENCY (HZ)

Figure 67

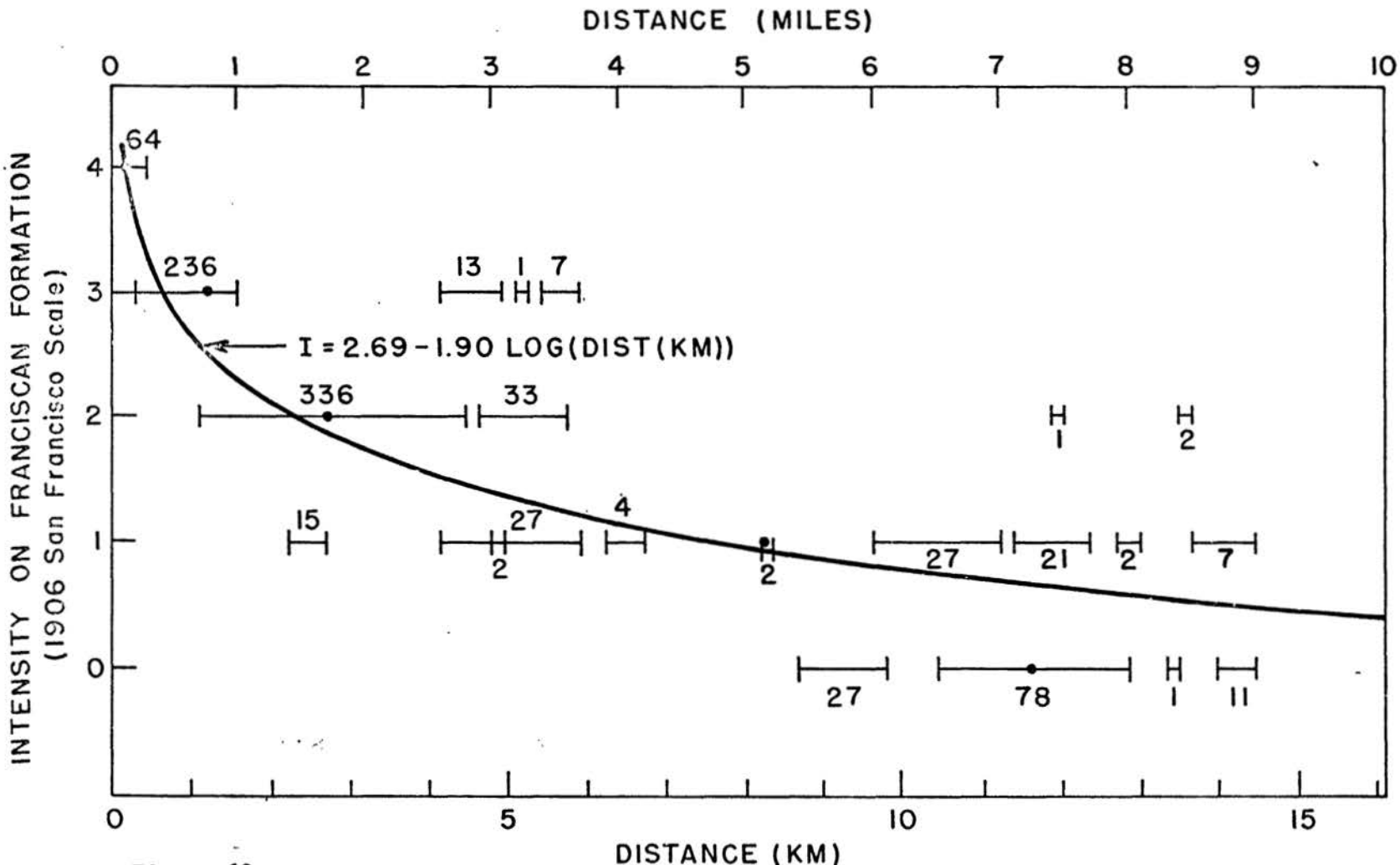
DISTANCE (MILES)
0
1
2
3
4
5
6
7
8
9
10
INTENSITY ON FRANCISCAN FORMATION
(1906 San Francisco Scale)
4
3
2
1
0
64
236
13
1
7
I = 2.69 - 1.90 LOG(DIST(KM))
336
33
H
1
H
2
15
27
4
2
2
27
21
2
7
27
78
H
1
11
0
5
10
15
DISTANCE (KM)

Figure 68

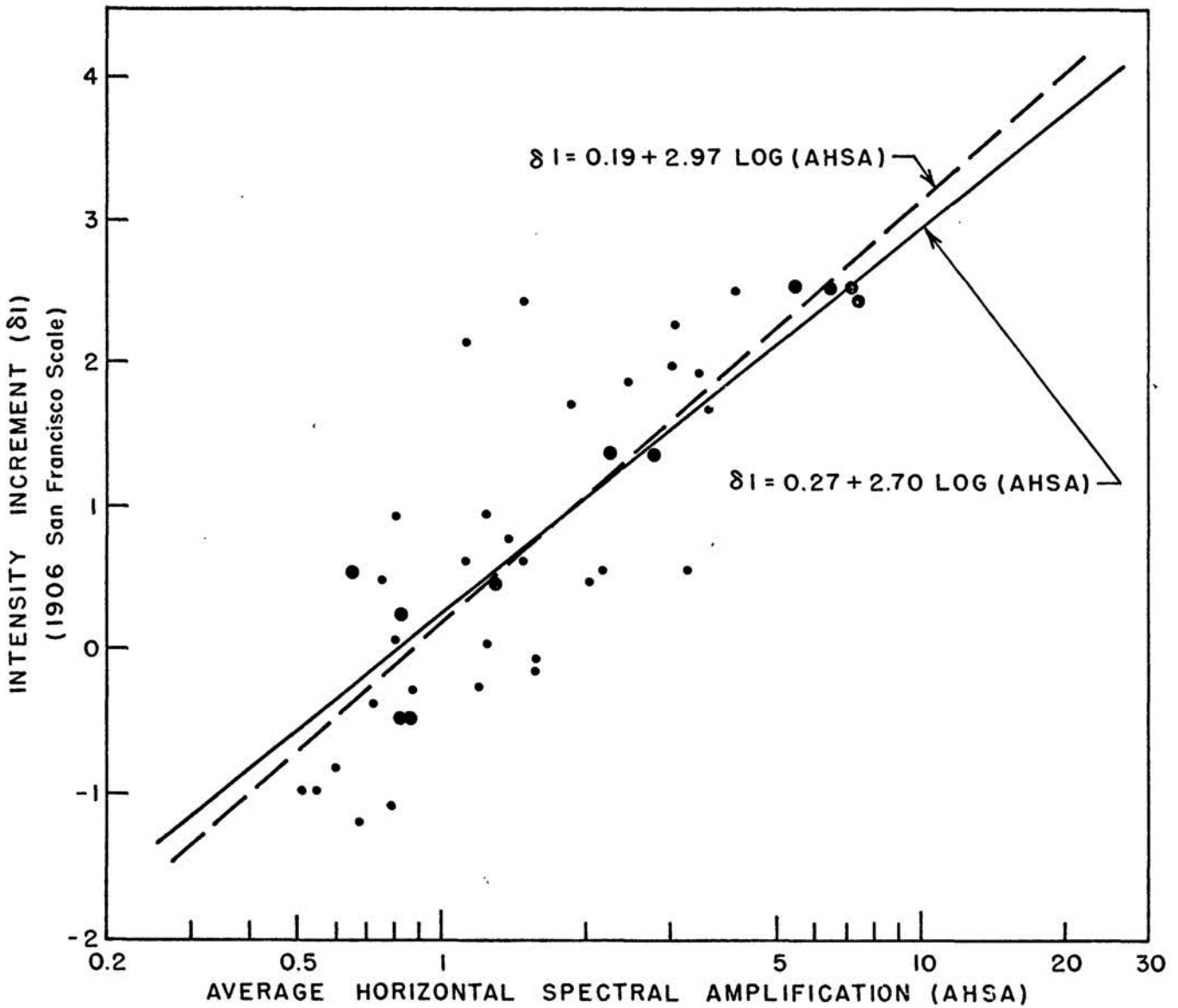
δI = 0.19 + 2.97 LOG (AHSA)
δI = 0.27 + 2.70 LOG (AHSA)
INTENSITY INCREMENT (δI)
(1906 San Francisco Scale)
4
3
2
1
0
-1
-2
0.2
0.5
1
5
10
20
30
AVERAGE HORIZONTAL SPECTRAL AMPLIFICATION (AHSA)

Figure 69